POLITECNICO DI MILANO

School of Industrial and Information Engineering

Department of Chemistry, Materials and Chemical Engineering
"Giulio Natta"

POLITECNICO
MILANO 1863

Master's Degree Thesis in Materials Engineering and Nanotechnology

COLORIMETRIC ASSAY FOR ADVANCED GLYCATION END-PRODUCTS

Nanyang Technological University, Singapore

Advisor: Prof. Guglielmo Lanzani

Co-advisor: Prof. Bo Liedberg

Carla Giorgia Delachi, 899690

Academic Year 2019/2020

Alla mia famiglia

TABLE OF CONTENTS

LIST OF TABLES

LIST OF FIGURES

LIST OF ABBREVIATIONS

Notations	Descriptions
T2D	Type 2 diabetes
WHO	World Health Organization
RCS	Reactive Carbonyl Species
ROS	Reactive Oxygen Species
AGEs	Advanced glycation end-products
POC	Point of Care
POCTs	Point of Care Tests
CPs	Conjugated Polymers
PT	Polythiophenes
ALEs	Advanced lipid end-products
RAGE	Receptor of AGEs
HPLC	High Performance Liquid Chromatography
ELISA	Enzyme-linked immunosorbent assay
LFAs	Lateral Flow Assays
VFAs	Vertical Flow Assays
DNA	Deoxyribonucleic Acid
RNA	Ribonucleic Acid
NPs	Nanoparticles
AuNPs/GNP	Gold Nanoparticles
AgNPs	Silver Nanoparticles
AMI	Acute Myocardial Infarction
LED	Light Emitting Diodes

FET	Field Effect Transistors
FRET	Fluorescence Resonance Energy Transfer
CPEs	Conjugated Polyelectrolytes
CPT	Cationic Polythiophenes
CPB	Cationic Polythiophene Biosensor
FCR	Fluorescence Chain Reaction
PVDF	Polyvinylidene fluoride
NMR	Nuclear Magnetic Resonance
PAGE	Polyacrylamide Gel Electrophoresis
DI	De-Ionized
FR	Fluorescence Recovery
LC/MS	Liquid Chromatography-Mass Spectroscopy
LOD	Limit of Detection
CNTs	Carbon Nanotubes

ABSTRACT

Multiple exogenous and endogenous triggered factors can be the cause of an imbalance in the levels of free radicals and reactive carbonyl and oxygen species in humans. Carbonyl and oxidative stress, which corresponds to high level of, respectively, carbonyl and oxygen reactive species, may lead to damage of significative biological molecules such as proteins, carbohydrates and nucleic acids, which in turn cause cell death and tissue injury. These conditions contribute to various disorders like type 2 diabetes and cardiovascular diseases. An assay for stress related biomarkers can therefore assist in the early diagnosis of the disease and guide the clinical practice of T2D patients. The major methods today available are not always suitable due to sophisticated and bulky laboratory instruments and trained personnel they require; so, a point of care assay for these biomarkers can be conclusive considering its advantages such as low cost, fast response, high sensitivity and selectivity.

The major aim of this project is the development of a colorimetric biosensor for monitoring carbonyl/oxidative stress biomarkers associated to T2D (i.e. advanced glycation end-products), that takes the advantages of the superior properties of cationic polythiophenes and the high selectivity and specificity of aptamers. These conjugated polymers are used as the luminescent reporters for the optical detection of the biomarkers (target molecule) and aptamers are employed as recognition elements.

The sensing strategy is based on the monitoring of changes in optical properties of the polymer and its associated conformational change when interacting with the aptamer in presence or absence of the target biomolecule.

The colorimetric assay is developed employing five different types of carbonyl/oxidative stress biomarkers, four different cytosine-rich aptamers and four different cationic polythiophenes, without requiring tedious sample pre-treatment.

The responses are obtained at clinically relevant concentrations and can find application in practical management of the disease either at clinical settings and at patient's home, thus being an affordable and simple healthcare solution.

SOMMARIO

Molteplici fattori possono essere la causa di uno squilibrio nei livelli di radicali liberi e specie reattive nell'uomo. Stress carbonilici e ossidativi, che corrispondono a un livello elevato, rispettivamente, di specie reattive carboniliche e ossidative, possono danneggiare alcune molecole biologiche come proteine, carboidrati e acidi nucleici, che a loro volta causano disfunzione cellulare e lesioni ai tessuti. Queste condizioni contribuiscono alla nascita di vari disturbi come il diabete di tipo 2 o malattie cardiovascolari. Un test per identificare i biomarcatori può quindi aiutare nella diagnosi precoce della malattia e guidare la pratica clinica dei pazienti. I principali metodi oggi disponibili non sono adatti a causa di strumenti di laboratorio sofisticati, ingombranti e personale addestrato di cui hanno bisogno; quindi, un test point of care per questi biomarcatori può essere conclusivo considerando i suoi vantaggi come basso costo, risposta rapida, sensibilità e selettività. L'obiettivo principale di questo progetto è lo sviluppo di un biosensore colorimetrico per il monitoraggio dei biomarcatori associati a stress carbonilico / ossidativo legati al diabete di tipo 2 (ovvero prodotti finali di glicazione avanzata), che sfrutta i vantaggi delle proprietà dei politiofeni cationici e l'elevata selettività e specificità degli aptameri. Questi polimeri coniugati sono usati come reporter luminescenti per il rilevamento ottico dei biomarcatori, mentre gli aptameri sono impiegati come elementi di riconoscimento. La strategia di sensing si basa sul monitoraggio dei cambiamenti nelle proprietà ottiche del polimero e dei cambiamenti conformazionali ad esso associati quando interagisce con l'aptamero in presenza o in assenza del biomarcatore. Il progetto è stato sviluppato impiegando cinque diversi tipi di biomarcatori, quattro aptameri e quattro politiofeni cationici, senza necessità di pretrattamento del campione. Le risposte sono ottenute a concentrazioni clinicamente rilevanti e possono trovare applicazione nella gestione pratica del disturbo sia in ambito clinico che a casa del paziente, costituendo quindi una soluzione sanitaria semplice e conveniente.

Chapter 1: INTRODUCTION

1.1 BACKGROUND AND SIGNIFICANCE

Metabolic disorders are inclusive of multiple types of pathophysiological conditions caused by energy and redox imbalance in metabolic pathways. These disorders are mainly characterized by some risk factors such as glucose intolerance, defective insulin secretion, hypertension, obesity and chronic inflammation; one or more of these risk factors contribute to cellular disfunction and redox imbalance resulting in the making of damaged and highly reactive biomolecules [1, 2]. The described risk factors are collectively known as metabolic syndrome, which in turn are associated with the development of type 2 diabetes (T2D) and cardiovascular diseases [3, 4]. Diabetes is a chronic metabolic disease featured by progressive loss of glucose homeostasis. According to the World Health Organization (WHO), about 422 million people worldwide have diabetes, particularly in low-and middle-income countries, and 1.6 million deaths are directly attributed to diabetes each year. Both the number of cases and the prevalence of diabetes have been steadily increasing over the past few decades [5].

T2D, as described in Chapter 2, is primarily caused by insulin resistance in target organs, such as liver, skeletal muscles and adipose tissue, with subsequent inability of cells to absorb glucose and causing hyperglycemia [6, 7].

Recent studies indicate a clear correlation between oxidative stresses and metabolic disorders: this may be helpful for the identification of biomarkers, targets and therefore therapies [1].

Carbonyl and oxidative stresses are defined as the condition of imbalance between generation and inactivation of reactive carbonyl species (RCS) and reactive oxygen species (ROS); moreover, recent studies indicate that carbonyl and oxidative stresses play a key role in the condition of insulin resistance and therefore in the initiation of T2D [8, 9]. This imbalance in the regular redox reactions of a cell, indeed, produces in turn free radicals that harm proteins, lipids, carbohydrates and nucleic acids, causing cell deaths, like insulin-producing cell and tissue damage, leading to different and multiple cardiovascular complications and even metabolic diseases like T2D [12-15].

In normal conditions, low values of ROS and RCS are important for cell signal transduction and immune system response. ROS and RCS are chemically reactive molecules produced as by-products in some biochemical processes: high concentrations of ROS and RCS, above acceptable levels, cause, respectively, oxidative and carbonyl stresses which are responsible for cell damage and manipulation of the signal [8, 10, 11]. Furthermore, these two conditions are interrelated: it has been observed, indeed, the increase in RCS levels originates from oxidative stress and vice versa, causing a cyclic reaction [10]. The increase in ROS find its source in both endogenous path and exogenous path. The endogenous sources are triggered from the by-products of metabolic reactions, while exogenous sources embody UV radiation, smoking, alcohol consumption as well as long-term intoxication of aluminium chloride from drinking water.

A healthy lifestyle and good habits like the right diet and steady physical activity can help in the prevention of the disease, or even surgery interventions can lessen the severity of this condition, T2D is still a non-remission and chronic disease (insulin-producing cells are, indeed, low proliferating and once damaged, there is no way they can recover).

The above mentioned oxidative and carbonyl stresses are considered precursors of T2D due to its occurrence before the onset of T2D; this condition is also known as pre-diabetes [14]. Pre-diabetes state, when recognized, puts the patient in an advantageous position because enables the early detection of carbonyl and oxidative stresses, so that full-blown T2D and any other complication is prevented. Hence, the detection of measurable carbonyl/oxidative stress related biomarkers is pivotal for the early diagnosis as well as for the monitoring of T2D.

Advanced glycated end products (AGEs) are formed as a consequence of glycation, that is a non-enzymatic addition of a sugar to a protein or lipid and are considered known biomarkers for carbonyl stress [12, 14, 16]. Once again, it is important, for a proper early diagnosis, to detect these known biomarkers of T2D and eventually develop assays to evaluate them quantitatively and qualitatively. Several assay platforms have been reported for biomarkers detection, but the majority of these methods require complex tools, expensive instrumentation, trained personnel to carry out the analysis and are time consuming.

Diagnostics assays currently used in the developed world are not suitable for resource-constrained settings with limited financial resources, basic health infrastructure, and few trained technicians [17]. Moreover, most of the kits available today in the market are not

specific enough and their impact in clinical research is not yet validated; in this context it has become necessary to develop a point of care (POC) assay for these biomarkers' detection.

Point of care tests (POCTs) are rapid and reliable detection assays. They are cheap, cost-effective and require minimal sample amounts and limited resources; moreover, they show good correlation to laboratory experiments [18-20]. Many and different materials have been studied for POC device manufacture. Some of them are glass, silicon, polymers, plastics and paper. Paper-based tests are devices that exploits only capillary pressure to drive the flow in a porous matrix (i.e. "paper"); they are, most of all, easy to carry out and to employ, they are cost-effective, and they allow an easy diagnostic process, even in resource-limited backgrounds. In this project will be mentioned mainly two different kinds of POC devices: lateral flow assay and vertical flow assay. But there are various, such as dipstick assay, microfluidic analytical devices. The different possible detection mechanisms in paper based POCT devices and the limits of detection strongly rely on the labels that have been used, the target analytes and the fabrication protocols. The sensitivity of POC test devices is confined in the complexity of the clinical samples employed, such as blood, urine and saliva: all complex systems. Therefore, extraction or sample clean-up before testing is usually required. Unfortunately, these mentioned are all expensive techniques, as an alternative of rapid and less expensive extraction process may be filter membranes. Besides, the sensitivity of paper-based POCTs is affected by the intrinsic characteristics of the materials that have been employed in the fabrication such as electrodes, nanoparticles, dyes and also by the recognition molecules: aptamers, antibodies and peptides [21].

Colorimetric assays have been primarily considered in this project because they are, among the various detection methods, preferable due to their quick visual response without any instrument but human eye [22-24].

Conjugated polymers (CPs), together with other optical reporters such as gold nanoparticles, magnetic nanoparticles, carbon nanotubes, dyes, quantum dots, have been considered for POC colorimetric assays [25]. CPs are significantly interesting in biosensing field because of the delocalized π-electrons along their backbone that lead to superior optical and electronic properties, as described in Chapter 2; these features vary with different external stimuli such as temperature, presence of a solvent, pH change, presence of an electric field and interaction with other molecules that in turn may induce modifications the molecular structure, yielding to changes in the conjugation length of the

polymer and, consequently, to a visual output. The optical transitions of CPs are possible thanks to the conformational alterations in the backbone that increase (or reduce) the effective conjugation length leading to red/bathochromic shift (or blue/hyposochromic shift) in the electromagnetic spectrum. Cationic polythiophenes (PT) have been largely employed in biosensing field because of their solubility in water and alcohol solvents, biocompatibility and advanced optical and electronic properties [26].

Today POC assays for T2D are based on antigen-antibody interaction and takes the advantages of analyte specific enzymes for a specific binding but the progress made so far in biosensing field and in nucleic acid engineering, proved to be fundamental in the development of bio recognition elements such as aptamers. Aptamers are oligonucleotides able to fold in a unique 3D conformation in a way that it binds specifically to a target molecule; moreover, are highly stable and selective. Aptamers' synthesis is a chemical process, this means that they are easy to create and also to manipulate, so that a large variety of targets can be detected, unlike antibodies (see Chapter 2). Aptamer-based assays can also overwhelm the washing step and thus they are preferred because they are not time consuming (therefore also cost-effective) [26]. In the last decades, many studies have deepened the role of aptamers and they have been engineered for various T2D biomarkers such as apolipoprotein E, glucagon, 8-hydroxy-2'-dexyguanosine (8-OHdG) and AGEs, as it is of this project interest [27-30].

The overall benefits of both cationic PT and aptamers are the fundamental principles for the development of this thesis, focusing mainly on the colorimetric assays using different cationic polythiophenes for the detection of AGEs associated to T2D.

1.2 HYPOTHESES

Cationic polythiophene is studied mostly for solution-based assays as both colorimetric and fluorometric reporter; the use of these special polymers as optical reporter is favourable compared to the commonly used detection labels such as enzymes, nanoparticles, latex beads or fluorescent tags, in order to have high-performance assays for the detection of carbonyl and oxidative stress biomarkers with only minimal instrumentation.

Cationic polythiophenes with varying pendant groups can be used for the visual detection of oxidative stress biomarkers at clinically relevant concentrations, avoiding tedious standard procedure and instrumentation [31].

Aptamers are single stranded nucleic acid sequences that can change its conformational structure folding in secondary and tertiary structures in order to bind specifically to their ligands.

Furthermore, literature shows that aptamers could be used in solution or paper-based assays [32, 33]. Aptamers, compared to the commonly used antibodies are small size, hence easy to handle and can also be adapted to the specific target [30]; moreover, are way cheaper than antibodies. Aptamers are also more stable on site and specific especially for small molecule targets, making the detection of carbonyl/oxidative stress to be immediate [34].

Thus, the use of different aptamers has been considered for selective detection of biomarkers of carbonyl/oxidative stress at clinically relevant concentrations.

This project aims at development of a colorimetric biosensor that takes the advantages of the superior properties of cationic polythiophenes and the high selectivity and specificity of aptamers to detect one of the carbonyl and oxidative stress biomarkers associated to type 2 diabetes: advanced glycation end-products (AGEs).

The overall sensing mechanism of AGEs is based on the survey of a colour change of the solution samples. The variation in the conformational structure of polythiophenes upon interactions with the aptamers in presence or absence of AGEs results, indeed, in the diversification of its optical properties.

The sensing strategy is explained in Chapter 4.

1.3 OBJECTIVE

Hyperglycemia is a condition in which high levels of circulating glucose are registered. This generates, within the circulatory system, reactive oxygen species (ROS) and reactive carbonyl species (RCS) that in turn damage those cells that secrete insulin and/or induce insulin resistance in peripheral tissues [8, 9].

The overall objective of this thesis is to develop a diagnostic assay that can assist in clinical decision making (i.e. diagnostics) and guide the clinical practice of T2D patients through the development of a simple and handy diagnostic assay (or technological tool) aimed at detecting with high sensitivity and specificity, oxidative and carbonyl stresses biomarkers levels for the early detection of the disease.

In this particular context the aim is to develop an assay for these oxidative and carbonyl stresses biomarkers associated to T2D using different cationic polythiophenes and aptamers: advanced glycation end-products (AGEs), that are elevated in concentration under oxidative stress in plasma and serum and associated to insulin resistance, endothelial dysfunction and vascular inflammation.

The detection of AGEs, as well as other factors, can yield vital information on the progression of chronic complications associated to pre-diabetes or undiagnosed T2D. Clinically relevant concentrations of the target biomarkers (AGEs) is about 10µg/ml [35-37].

There is no gold standard technique for the detection of AGEs and the methods such as liquid chromatography tandem mass spectroscopy (LC-MS) is time consuming, requires multiple steps (several injections per sample) and is expensive [35-37]. No electronic tool exploiting flow assay has been developed in this project; it remains an objective of the future perspectives.

1.4 SCOPE

This project is aimed at the development of a colorimetric assay that can detect the carbonyl and oxidative stresses biomarkers above mentioned, AGEs, associated to T2D.

This system not only is ideal for point-of-care applications, but it also allows an immediate detection of AGEs in clinical samples without requiring expensive instrumentation; this is essential for the early diagnosis of Type 2 Diabetes and its possible complications.

Chapter 2: LITERATURE REVIEW

2.1 TYPE 2 DIABETES

Type 2 diabetes, also known as adult-onset diabetes, is a disease characterized by high blood glucose concentration, insulin resistance and relative lack of insulin [38]. Long-term complications from high blood glucose concentration include heart disease, strokes, diabetic retinopathy (which can result in blindness), kidney failure and poor blood flow in the limbs which may lead to amputations. Type 2 diabetes may occur as a result of obesity and poor active lifestyle. Even if sometimes bariatric surgery and lifestyle intervention may help mitigate the severity of the disease for those suffering obesities, T2D is, indeed, a chronic and non-remission disease and it is associated with a ten-year-shorter life expectancy [39-41]. The main reason why T2D is a non-remission disease is the loss of insulin-producing cells in the pancreas, which are in turn low proliferating cells. The progress of type 2 diabetes is due to a combination of lifestyle and genetic factors; some of the triggering causes are under personal control (such as diet and obesity), other factors are not (such as aging and genetics) [42, 43].

While type 1 diabetes is characterized by insufficient insulin production (related to definitive beta cell disfunction), type 2 diabetes is featured mainly by insulin resistance.

Insulin is a peptide hormone that regulates the metabolism of carbohydrates, fats and protein by promoting the absorption of glucose from the blood into liver, fat and skeletal muscle cells.

Although T2D is triggered by insulin resistance, the disease might be due to both insufficient insulin production from beta cells, that are type of cell found in pancreatic islets (i.e. islets of Langerhans) that synthesize and secrete insulin, and insulin resistance [44]. Insulin resistance is the typical state of type 2 diabetes and is the condition for which cells of peripheral tissue are unable to respond adequately to normal levels of insulin and occurs first within muscles, liver and fat tissue [45]. This in turn leads to the inability of cells to absorb glucose from the blood. In normal conditions in the liver, insulin restrain glucose release but in case of insulin resistance the liver inappropriately releases glucose into the

blood causing hyperglycemia [46]. The proportion of insulin resistance versus beta cell dysfunction differs among individuals suffering T2D [44].

In 2015 it was estimated that there were 392 million people with type 2 diabetes in the whole world, making up about 90% of diabetes cases (while the other 10% is relative to type 1 diabetes): this is equivalent to about 6% of the world's population [46, 47]. Diabetes is a widespread disease both in the developed and the developing world; nevertheless, it remains uncommon in the least developed countries [44, 46]. Rate of diabetes, both type 1 and type 2, in 1985, was estimated at 30 million, then increased to 135 million in 1995 and 217 million in 2005: this rise is most probably due to the global population aging and some other factors [48]. As shown in Figure 2.1, the five countries with the greatest number of people suffering diabetes in 2000 are India (31.7 million), China (20.8 million), the United States (17.7 million), Indonesia (8.4 million) and Japan (6.8 million) [49].

T2D is identified as a global epidemic by the World Health Organization (WHO).

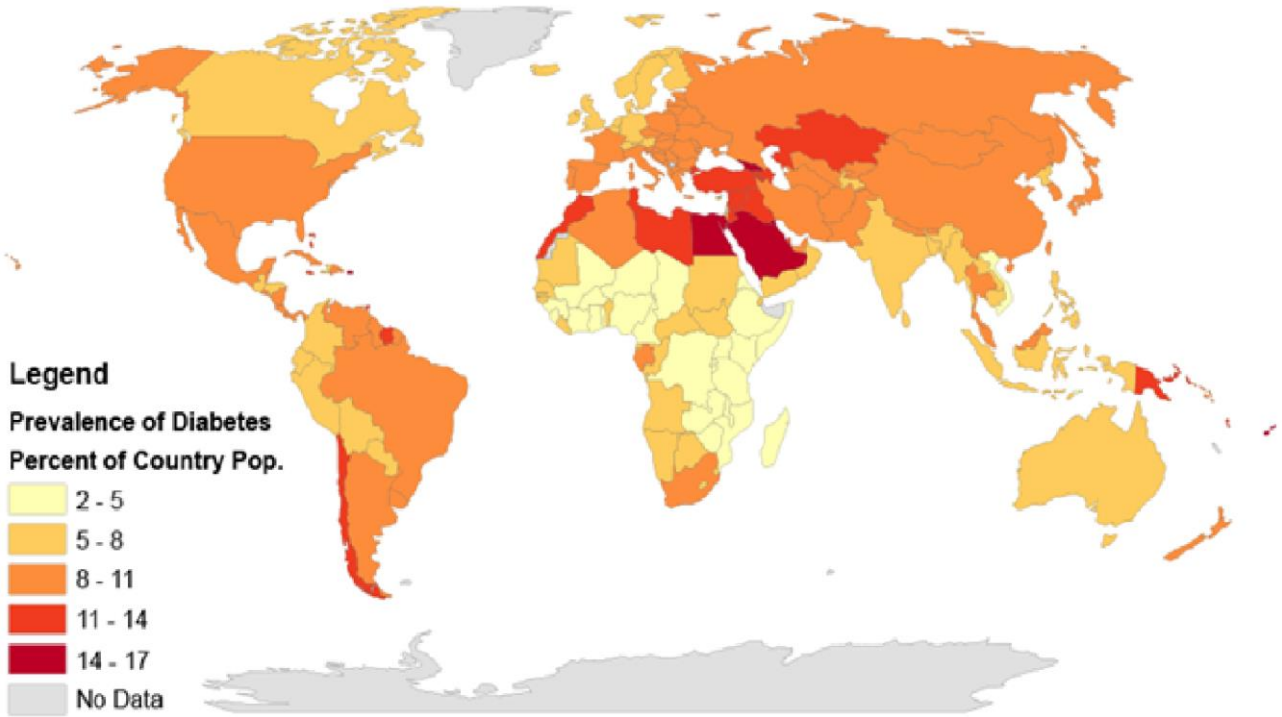

Figure 2.1 - Regional rates of diabetes using data from 195 countries in 2014 [50]

2.2 BIOMARKERS

As already mentioned, ROS and RCS are chemically reactive molecules produced as by-products in some biochemical processes. However, in healthy conditions, low values of reactive oxygen species (ROS) and reactive carbonyl species (RCS) are important for cell signal transduction and immune system response.

People suffering from hyperglycemia generates harmful ROS and RCS in the circulatory system that may cause damage to some biomolecules and, in particular, to the beta cells that produce insulin or to the cells of peripheral tissue causing insulin resistance [8, 9].

The accumulation of reactive oxygen species may have both endogenous source (from by-products of metabolic reactions or, in general, genetics) and exogenous source (smoke, pollution, UV radiation, alcohol consumption, intoxication of aluminium chloride, etc.) and is known as Oxidative stress [51, 52]. Oxidative stress is in turn responsible for cell damage and manipulation of cell signal transduction.

In reference to Figure 2.2, ROS as superoxide, hydrogen peroxide and hydroxyl radicals may lead to tissue damage through oxidation process and consequently formation carbonyl stress. In this scenario carbonyl and oxidative stresses are interrelated and are correlated to some conditions such as defective insulin secretion, hypertension and obesity that are, in turn, linked to some diseases such as T2D [53, 54].

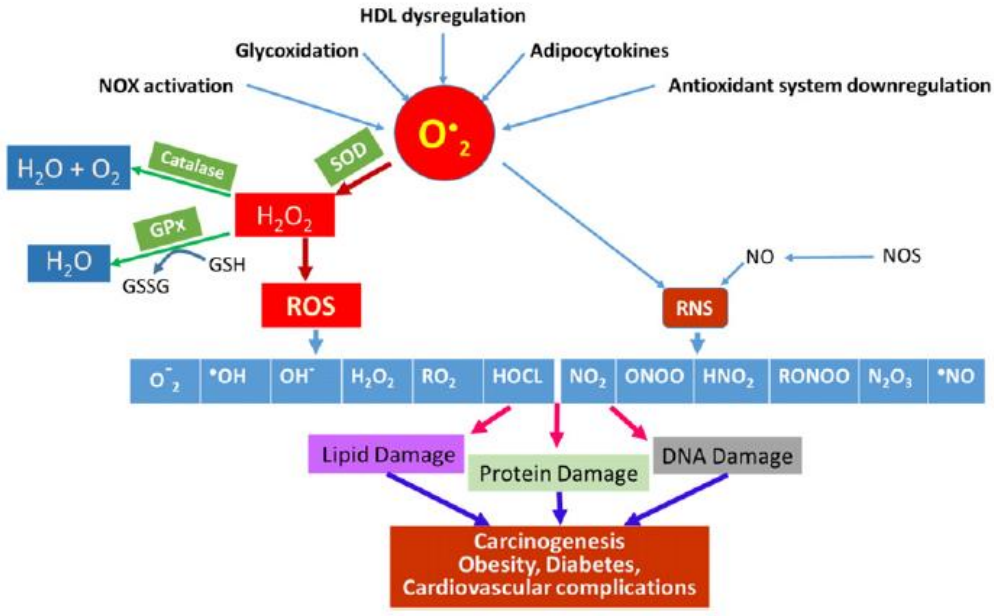

Figure 2.2 - Schematic mechanism of sources of ROS leading to macro-biomolecular damage [1]

So, an increase in carbonyl and oxidative stresses biomarkers is also registered in patients who suffer type 2 diabetes. The above-mentioned carbonyl/oxidative stress biomarkers are inclusive of all the damaged biomolecules related to the progression of the disease, and in this project mainly focused on advanced glycation end-products (AGEs).

2.2.1 ADVANCED GLYCATION END-PRODUCTS (AGEs)

Advanced glycation end-products (AGEs) can be formed by non-enzymatic glycosylation (i.e. a covalent attachment between a sugar and a protein or lipid) or by oxidative reactions to form stable structures accumulating on proteins with small turnover and most probably are involved in the process of aging [55, 56].

Advanced glycation end-products (AGEs) include a heterogeneous group of molecules and are formed by a combination of glycation (also known as non-enzymatic glycosylation), oxidation and/or carbonylation, which can be divided into three distinct pathways as shown in Figure 2.3 [55].

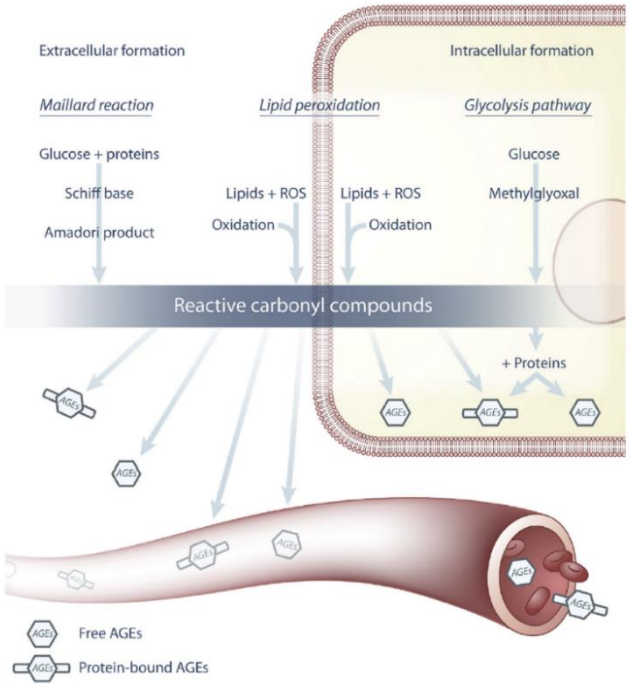

Figure 2.3 - Formation of AGEs [55]

The first pathway is glycoxidation in which it is pointed out AGEs formation from Maillard reaction between glucose or reducing sugars and proteins, as describes in Appendix II; this reaction is responsible of a distinctive flavour in browned food. Carbonyl groups, indeed, present in the reducing sugars, reacts with the amino group of the proteins and this results in the formation of a Schiff base in a limited time. This Schiff base undergoes intramolecular rearrangement, resulting in a stable Amadori product or early glycation end-product. Its subsequent oxidation lead to the formation of reactive carbonyl compounds and eventually to AGEs [55]. The most important AGEs derived from this process of are pentosidine, Nε-carboxymethyl-lysine (CML) and glucosepane [55, 57].

The second pathway may take place both intracellularly and extracellularly: lipid peroxidation, in which lipids become reactive carbonyl compounds in presence of reactive oxygen species (ROS) and after oxidation; this results in the formation of AGEs or advanced lipid end-products (ALEs). This is a faster process with respect to the first one. An example of ALE is malondialdehyde [55, 58].

Third and last is glycolysis pathway, again a faster process with respect to glycoxidation and it occurs only intracellularly. In this case glucose turns into reactive carbonyl compounds and its chemical interaction with proteins results in AGEs formation. The most known reactive carbonyl compound is methylglyoxal and subsequent AGEs formation by this pathway is methylglyoxal-derived hydroimidazolone (MG-H1).

Considering these different pathways, it's clear that there are several chemically distinct classes for AGEs derived from glucose, fructose, di-carbonyl compounds and α-hydroxyaldehydes.

These above described mechanisms are all endogenous source formation of AGEs, but also exogenous source formation may occur. All above, accumulation of AGEs results from inhalation of tobacco smoke because it contains highly reactive glycation products which forms, almost instantly, AGEs [55, 59]. Another important source of AGEs is high-AGE food products and, in particular, temperature at which food is prepared plays a crucial role in the resulting amount of AGEs. Oven frying is the most severe inducer of AGEs [55, 60]. For this reason, good habits in food education and a healthy lifestyle is an important therapy for people suffering from T2D. Clearance of the kidney and metabolism by the liver are conditions that may also affect the exposure to AGEs: high levels of AGEs have been found in patients with renal or liver failure [55, 61, 62].

Formation and accumulation of AGEs is normal with aging but is considerably enhanced under carbonyl and oxidative stresses or in case of hyperglycemia. Pathogenic level of AGEs in presence of oxidative stress, during ageing and in case of cardiovascular disease may be the precursors of insulin resistance condition, vascular inflammation, micro- and macro vascular diabetic complications, atherosclerosis, sarcopenia and neurodegenerative disorders such as Alzheimer's and Parkinson's disease.

AGEs can be found in some biological sample including blood, urine, tissue and plasma (see Figure 2.4) [55]. Currently, several techniques are available to measure AGEs; an overview is given below.

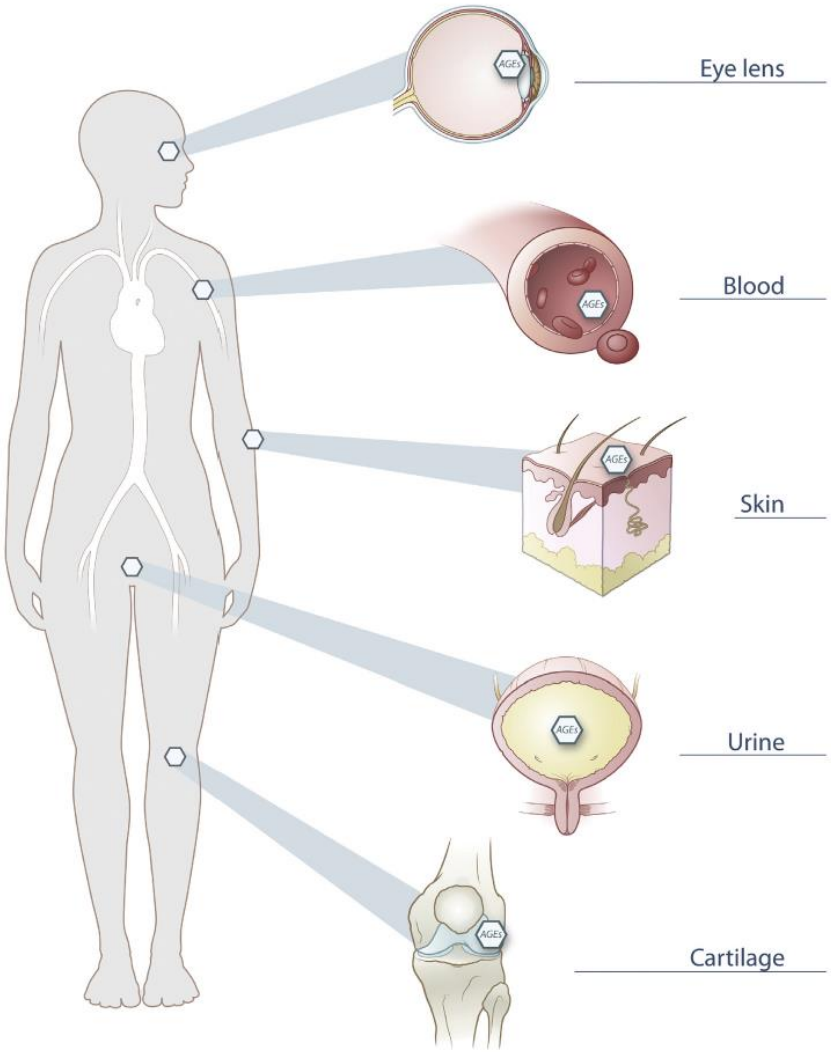

Figure 2.4 - Measurements of advanced glycation end-products (AGEs) [55]

Circulating AGEs can be due not only to the biochemical reactions described in the previous chapters, but also through ingestion of high AGEs content foods, such as red meat, certain cheeses, oils, fried eggs, butter, cream cheese, margarine, mayonnaise and nuts.

So, AGEs assay must be elaborated on with food samples due to the varied presence of these biomarkers in daily consumed foods and drinks; it would be interesting to find the various levels and concentrations of AGEs in the above-mentioned specimens. It is indeed pivotal for those suffering type 2 diabetes, the determination of the amount of AGEs in food intake in such a way that a low AGEs diet can be established. The control of food intake through a dietary intervention is a simple way of prevention against premature aging and diseases such as diabetes.

Glyceraldehyde, a triose monosaccharide, is a reducing sugar molecule that reacts with the amino group of a protein forming glyceraldehyde derived AGEs (Gly-AGEs) and has a strong binding affinity to the receptor of AGEs (RAGE) [63-66]. For this reason, it has been considered to be one of the biomarkers in this study. From literature, another four different types of advanced glycation end-products (AGEs) have been used as target biomolecules in order to determine the specificity of the assay; they are described in Chapter 3.

2.3 CURRENT STATUS OF ANALYTICAL TECHNIQUES

The detection of carbonyl and oxidative stresses have been studied in several analytical methods, such as spectrophotometry, chromatography, electrophoresis and immunoassays. All these analytical techniques can detect and quantify oxidative damage to some biomolecules; general drawbacks lie in the need of expensive instruments, time and trained personnel to carry out the analysis.

These classic techniques are described below.

2.3.1 SPECTROPHOTOMETRIC ASSAY

The first classical approach described is spectrophotometric assay and is a highly sensitive assay for the detection of protein carbonyls, that involve the derivatisation of the carbonyl group with 2,4-dinitrophenylhydrazine (DNPH) and lead, as shown in the Figure 2.5, to the formation of 2,4-dinitrophenyl (DNP) hydrazine, a stable product [67, 68].

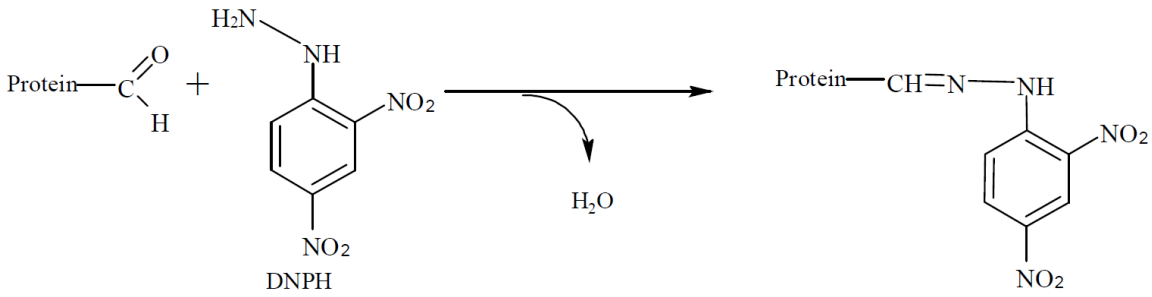

Figure 2.5 - Derivatization of carbonyl group with DNPH [68]

This covalent reaction is the most widely used measure of protein oxidation in several disease. Stable DNP group itself absorb UV light (maximum absorption at 370 nm), so the carbonyl content of proteins can be quantified by a spectrophotometric assay [67, 69].

Spectrophotometric DNPH method is easily used in various biological samples such as plasma, tissue homogenates, cellular extracts or isolated proteins and is useful to quantify the carbonyl content, as a marker or oxidative damage.

This method has provided much information on the correlation of carbonyl formation with oxidative stress and it does not require any expensive equipment.

Some disadvantages are no information of the extent of oxidative damage to a particular protein (i.e. no selectivity) in a complex system like plasma, requirement of high amount of protein, interference with compounds that absorb in the same region and need to remove nucleic acids as they react with DNPH [67, 68, 70, 71].

2.3.2 CHROMATOGRAPHY

The analytical technique that exploit the separation of molecules through differences in their structure and/or composition is known as chromatography. Having a sample moving through a system over a stationary phase, the molecules of the sample will be separated due to the affinities with the stationary support. This method can be used to separate different compounds through a column and takes the advantage of the strong interactions that bind a component of the sample with the stationary phase; in particular, at stronger interactions corresponds lower travel speed through the column so that the target molecule is soon highlighted [72].

Materials used in chromatography for the stationary state are immobilized silica on glass plates (thin-layer chromatography), volatile gases (gas chromatography), paper (paper chromatography) and liquids (liquid chromatography).

Derivatization of the sample can be carried out: usually is a non-necessary procedure but it is useful to improve the detection. Derivatization results in the alteration of the molecular structure of the analyte through a chemical reaction.

In order to quantify the amount of a specific compounds that has been separated (and dissolved in solution), high performance liquid chromatography (HPLC) is carried out. HPLC may be associated to an electrochemical detection (HPLC-ECD) or to a diode array detector (at 370nm after an initial separation of the protein fractions by gel filtration) to emphasize its performance [68]. Gas chromatography-mass spectroscopy (GC-MS) and high-performance liquid chromatography mass spectrometry (HPLC-MS) are able to analyse carbonyl proteins and carbonyl compounds [73, 74].

Drawbacks of this technique are solubilization and assessment of proteins, high pH requirement for derivatization process, time-consuming technique and requirement of expensive instruments [68].

2.3.3 ELECTROPHORESIS

Electrophoresis is the motion of particles of a fluid resulting from the application of an electric field. This technique is used to separate macromolecules based on size: because of the application of a negative charge, proteins move towards a positive charge. Today there are several types of electrophoresis, such as capillary electrophoresis, gel electrophoresis and isotachophoresis. A study showed how, in order to be quantified, carbonyl groups can be reduced with sodium tritiated borohydride then treated with gel electrophoresis [75]. Disadvantages lies mainly in the poor selectivity.

Capillary electrophoresis is used for determination and separation of several proteins and it turns out to be extremely versatile.

Some of the advantages of capillary electrophoresis are high sensitivity, accuracy, requirement of small volume of the sample and qualitative characterization of protein carbonyls [68].

2.3.4 IMMUNOASSAYS

Immunoassays exploit the selectivity and specificity of generated antibody reagents or immunoglobin in order to quantify biomolecules: antibodies are, indeed, able to selectively bind to a target molecule [76]. Carbonyls proteins can be quantified using immunoblotting assays (i.e. immunoassays), for which commercial kits are available [68].

Enzyme-linked immunosorbent assay (ELISA) is a sensitive method based on formation of 2,4-dinitrophenylhydrazone (DNPH derivatization) with subsequent non-specific adsorption of hydrazine to ELISA plate, dying with biotinylated anti-dinitrophenyl (DNP) antibody. It results interference at 450 nm of free DNPH and other non-protein constituents. So, the accuracy and sensitivity of this method is higher compared to the spectrophotometric assay. Positive aspects of ELISA are requirement of small amounts of proteins and that there are already commercial kits available on the market and for this reason is an extremely widely used test for the measurement of protein carbonyls in biological fluids such as plasma and serum [68, 77]. Drawback of this technique lies in the interference of DNA (i.e. Deoxyribonucleic Acid) and small molecules that lead to an underestimation of the total carbonyl protein content. Moreover, it does not provide any data on the molecular nature of the carbonyl protein or on the extent of carbonylation of a specific biomolecule in a complex system [68].

Another immunochemical dot blot method (i.e. an immunoassay in which proteins that must be detected are not separated by electrophoresis before treatment) for the detection and quantitation of protein carbonylation has been developed. This technique is widely used in purified proteins or homogenates [68, 78].

2.4 INTRODUCTION TO POINT OF CARE DIAGNOSTICS

Today, in the developed world, health care can provide everyone appropriate and timely care to patients. This includes, for instance, water, safe blood banking and diagnostics. The developed technologies meet the needs of developed world's medical community which comprises well-founded laboratories in a quality-assessed environment. However, a great amount of population, the majority of whom live in the developing world, has no access to this high standard medical care due to low-resource settings such as lack of essential equipment and trained personnel in laboratories. For this reason, scientists all over the world are trying to engineer point of care (POC) diagnostics. Recent studies on

microfluidics and nanotechnology undertake good solutions for sample processing, assay performance and analyte detection; these solutions can bring to the POC accurate and sensitive diagnostic tests both in the developed world and in the developing world [79].
In the developing aeras POC diagnostic tests can substitute laboratory analysis and represent the most cost-efficient solution for health care.
An example of utility of POC diagnostics also in the developed world is the military environment or in a site of outbreak or a rural centre far from a clinic or hospital [79, 80].
POC diagnostic tests can be used by health care professionals to help in the diagnostic procedure or as an alternative to clinical analysis but can also be used by patients directly, thanks to their ease of use and the speed at which the result is shown; for this reason they are also known as one-step assays or one-handling step assays. Some other positive aspects of POC diagnostic tests are small sample volumes, rapid outcome, portability, cheapness and versatility. POC diagnostics are used to detect disease markers as well as monitor therapies avoiding worsening of health conditions [81]. An example of successful point-of-care diagnostics devices, already available in the market, is the pregnancy test that involves the use lateral flow assay, in which an antigen concentration, above a fixed threshold, is detected [81]. Or, again, HIV detection is now possible through a POC lateral flow test [82]. In this context POC tests enable patients to monitor their health conditions remotely and to become more closely involved in their own disease management [80].
This may happen in the developed world, while in the developing world POC diagnostics plays a stronger role: it can, indeed, deliver appropriate and consistent medical intervention [83, 84]. The above-mentioned lateral flow assays (LFAs) run the liquid sample laterally along the surface of the sample pad simply exploiting capillary forces and are engineered for specific binding reactions of the analyte achieved on a nitrocellulose paper with high sensitivity. They consist of four parts: sample pad, conjugate pad, detection pad and absorbent pad. LFAs major disadvantage is that it cannot reach equal distribution of the sample and for this reason vertical flow assays (VFAs) or flow-through assays are carried out. VFAs systems require the vertical application of the sample using a syringe pump in a way that the speed can be adjusted. In this case the analyte pass through a membrane [85].
Illustrated in Table 2.1 a comparison between LFAs and VFAs.

Table 2.1 - Comparison between LFAs and VFAs [85]

LFAs	VFAs
Limited multiplexing (1 to 4)	No limit in multiplexing
Possibility of having non-specific binding (analyte in a sample are exposed to all reagents at the same time)	Unique reagents are employed for each test zone
Moderate speed	Fast speed
Easy to use	Easy to use
Require co-formulation of reagents for storage	Can integrate assays easily from individual to multiplex
Used mainly for immunoassays	Can perform different types of assays on the same device
No wash steps required	Wash steps are sometimes required
No need of syringe pump	Syringe pump employed

The World Health Organization (WHO) declared that a POC test must observe some criteria, exemplified in: 'ASSURED' (Affordable, Sensitive, Specific, User-friendly, Rapid and robust, Equipment-free or minimal equipment and Deliverable to end-users).

Unfortunately, there still exists financial difficulties in translating promising technologies to the market for global health disease. However, according to WHO, an intervention with POC diagnostic tests is deemed very cost-effective.

Design of a POC diagnostics device is full of challenges, primarily in low-resources settings, ruled by the need of extreme low-cost resources, low power consumption, poor infrastructures and challenging environmental conditions for transport and storage.

On the technical side, the development of a device count on the design choices that depend on precise end-use settings: there are specific design features that need to be observed on a common set of technical challenges, considering the type of diagnostic marker [82].

In Figure 2.6 is shown an ideal POC device, complete with all its functions in order to detect quantitatively several analytes within minutes in a selective way [86].

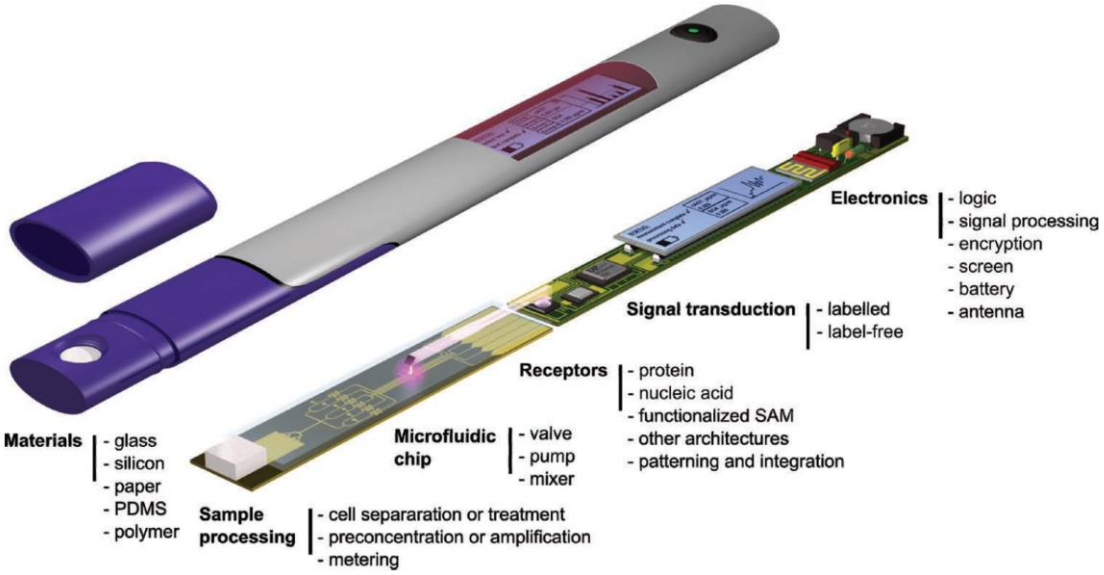

Figure 2.6 - Ideal POC device [86]

It's pivotal the ability of the device to not only analyse the sample but also calibrate the results, record and transmit encrypted data wirelessly to an electronic health record in order to be easily used by everyone, even not trained people.

The properties of the microfluidic flow path, such as capillary pressure, flow rate, wettability, optical properties, adhesion of biomolecules and disposable income rule the material used. The first devices were made in silicon and glass; today chip devices are engineered using a variety of materials and techniques. Some examples are shown in Figure 2.7: (a) a capillary electrophoresis chip in glass, (b) a POC immunoassay chip in silicon, (c) channels in paper, (d) 3D flow path in poly(dimethyl siloxane) (PDMS), (e) micromixers of porous patterned methacrylate in microchannels [86].

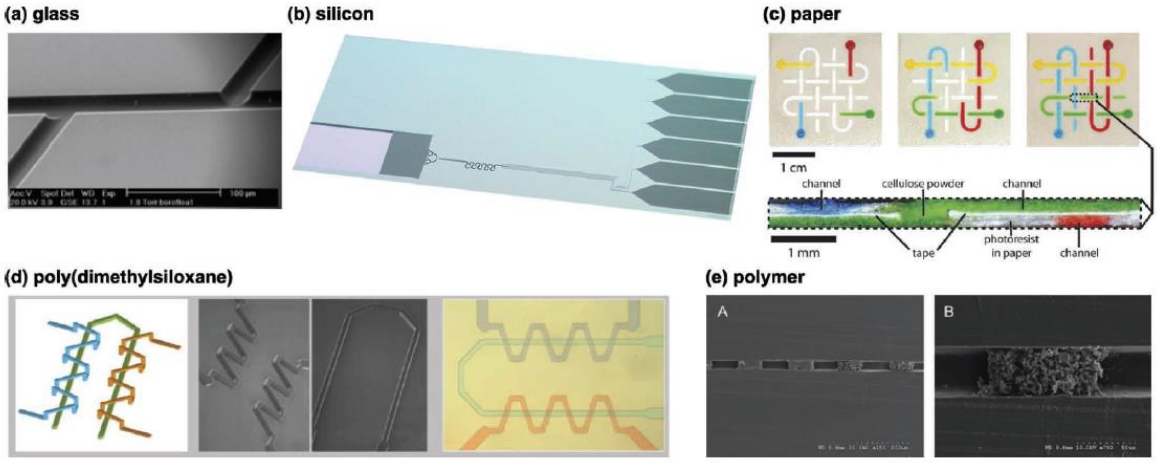

Figure 2.7 - Microfluidic flow paths [86]

The so-called paper-based assays are the ones described above: devices consisting of a porous network that takes the advantage of capillary pressure mechanism to drive the flow in a porous matrix, so that the tool is completely automatic in pumping the fluid along the device [1].

Paper-based microfluids hold good potential to deliver POC diagnostics due to their versatility, abundance, biodegradability, hydrophilicity and biocompatibility and they are of great interest in this project, even though it was not investigated further.

Paper-based devices are, indeed, robust, cheap, easy to use and it requires no external driving force. A comparison between chip-based devices and paper-based devices is displayed in Table 2.2 [86].

Table 2.2 - Comparison between chip-based and paper-based devices [87]

Comparison	Chip-based device	Paper-based device
Material	Glass, silicon, polymer, etc.	Paper and membrane
Manufacture	Channel fabrication and surface modification	Hydrophilic channels and hydrophobic barriers
Driving force	Pump	Capillary force and evaporation
Result analysis	Reader	Reader or visual detection

2.5 BIOSENSOR/DETECTION

Biosensors are analytical devices able to detect in a selective way a chemical substance and, in particular, when a biochemical interaction is involved, a biological component. Biosensors employ a biorecognition element, uniquely specific to the target analyte (or a group of analytes); the biorecognition element is then linked to the transducer, giving a sensitive read-out signal that coincide with the analyte concentration [88].

It is possible to distinguish catalytic mechanism biosensors and affinity-based biosensors. While the first uses enzymes as biorecognition elements, the latter make use of antibodies or aptamers as biorecognition molecule.

The ideal biosensor should be extremely sensitive and selective as well as specific. Moreover, it would be preferable to make it easy to perform and quick in giving a response. An ideal biosensor, working by the principle of affinity, is shown in Figure 2.8.

Within the analyte and the receptor, a highly selective and stable complex is created, and a measurable signal is revealed [88].

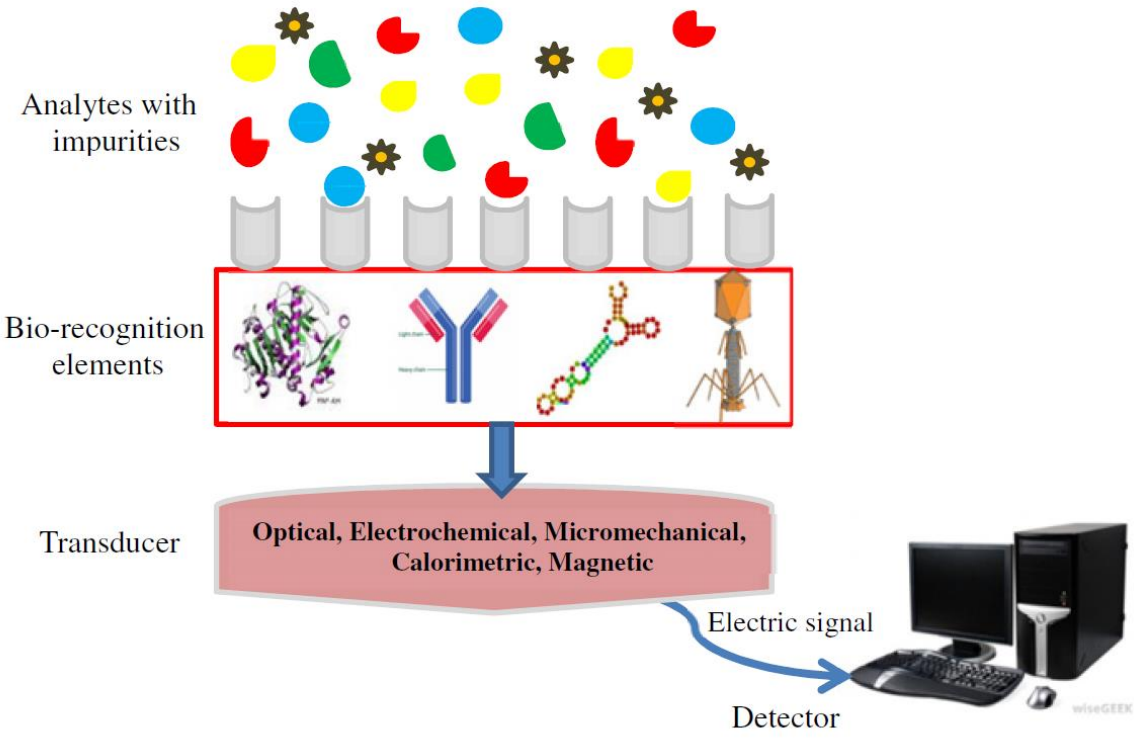

Figure 2.8 – Schematic principle of affinity-based biosensor [88]

The different possible categories of biosensors are distinguished according to the settings of biorecognition elements, such as catalytic or affinity mechanism, or to the physical and chemical transducer that can be electrochemical, piezoelectric, microgravimetric, magnetic, mass sensitive, thermal and optical. Among these, optical biosensors are of great interest in this project due to their high sensitivity, fast response and adaptability to different conditions [88].

2.5.1 COLORIMETRIC SENSOR

Colorimetric detection takes the advantage of the colour change of the detection system after the occurrence of a chemical or biochemical reaction between the target analyte (e.g. protein, nucleic acids and organic solvents) and the colorimetric probe, that in turn measure the concentration of the analyte [88, 89].

The unique advantage of this assay is that it allows the naked-eye detection, therefore no advanced instrumentation is required and for this reason is of great interest particularly in the biomedical field and in point of care (POC) diagnostics. Other benefits of the colorimetric sensor are ease of use, low costs, high portability and disposability [89].

Today for this sensing there are different colorimetric probes and reporters such as enzymes, noble metals and luminescent polymers that are discussed below.

2.5.1.1 Enzyme Based Detection

Enzymes are proteins specifically acting like biological catalysts. Catalysts can considerably accelerate the chemical reactions occurring in a system without being consumed, therefore they repeatedly work.

In clinical diagnosis, glucose is significant because its role as an analyte in pointing out diabetes. Glucose oxidase (GOx) (or GOx combined with enzymes such as horseradish peroxidase (HRP)), has been studied for a long time to detect glucose through colorimetric technique. Glucose oxidase generates hydrogen peroxide (H_2O_2), in presence of which GOx, combined with the enzyme HRP, alter 3,3',5,5'-tetramethylbenzidine (TMB), a chromogenic compound, into a blue product [90, 91].

Besides glucose detection, also albumin, uric acid and alanine aminotransferase (ALT) are good examples of enzyme-based detection. Total protein, for instance, is measured as a

result of the colorimetric reaction between albumin and tetrabromophenol blue, a colour marker. ALT and uric acid are detected using an enzymatic assay kit, already on the market [91]. However, enzymes at room temperature are less stable and thus less active; this results in poor sensitivity of the enzyme-based detection method.

2.5.1.2 Nanoparticle Based Detection

Today nanoparticles (NPs) are widely used in bio-analysis due to their higher stability and higher extinction coefficient (i.e. how strongly NPs absorb light at a given wavelength), with respect to organic molecules; moreover, besides optical features, they have unique electronic properties. These features make NPs the best in sensitivity for target analytes. High molar absorptivity of NPs is exploited to achieve low detection limits and high sensitivities. Nanoparticles are generally used to detect cancer biomarkers and antigens, antibodies, bacteria, proteins and infectious diseases. The most important advantage for POC applications, in the use of NPs, is that in most of the cases detection is performed visually. Colorimetric detection with NPs is also possible because of their high surface area and catalytic functionality [91].

Gold nanoparticles (AuNPs), silver nanoparticles (AgNPs) and ceria nanoparticles are widely used in biosensing field today, even though AuNPs are preferred due to their features: they can be easily functionalised, they show different colours at different size, shape and state of aggregation. Moreover, they are almost non-toxic, biocompatible and stable [92].

In recent studies it was shown that it is also possible to change size and concentration of AuNPs in order to have high performance assays in terms of sensitivity and limit of detection. Peptides are short chains of amino acids that can act as antibodies in molecular affinity recognition but, with respect to antibodies, are easier to be produced at high purity level and are more robust. Peptide-functionalized AuNPs are used in this colorimetric assay to detect cardiac troponin I (cTnl), one of the biomarkers of acute myocardial infarction (AMI). In particular, as shown in Figure 2.9, if cTnl is absent, AuNPs will remain dispersed and red in colour; on the opposite side, if cTnl is present, there will be aggregation of AuNPs, resulting in a shift in colour (from red to purple) depending on the concentration of the biomarker [93].

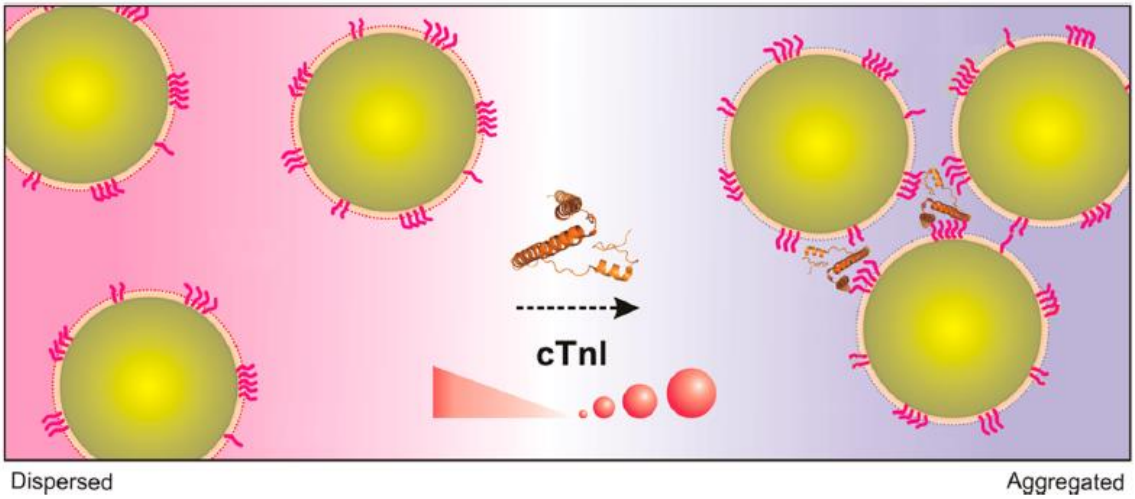

Figure 2.9 - Schematic illustration of the AuNPs assay for the detection of cTnI [93]

Another practical example of nanoparticle-based detection method is using ceria nanoparticles as quantitative chromogenic probes, replacing organic dyes for the detection of H_2O_2 and glucose. The colorimetric response is given thanks to ceria nanoparticles variation in its physiochemical and optical properties in presence of the analyte, thus avoiding other instruments. Ceria nanoparticles and glucose oxidase (GOx) are co-immobilized on a bioactive sensing paper. As shown in the picture below (Figure 2.10), if glucose is present, a shift in colour from white-yellowish to dark orange of the ceria nanoparticles present onto the paper is registered, triggered from hydrogen peroxide generated by glucose oxidase [94].

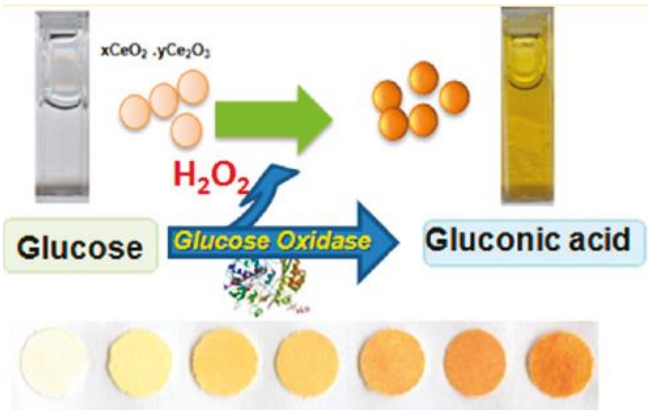

Figure 2.10 - Representation of the detection of glucose using ceria nanoparticles [94]

The use of NPs has the high risk of uncontrolled aggregation of the particles, that results in a change in colour of the product, thus giving non-reliable outcome. This unsolicited aggregation is caused by poor stability of the nanoparticle suspension and can be solved by strict control of buffer composition, presence of contaminants and ionic strength and acidity [95].

2.5.1.3 Polymer Based Detection

Conjugated polymers (CPs) are organic macromolecules having the particular structure of saturated single bonds and unsaturated double bonds in alternation. CPs have unique and useful optical and electronic properties due to the system of delocalized π- electrons created by overlapping p-orbitals between two subsequent monomers along the chain direction. According to the different backbone structures, it is possible to differentiate among some CPs, as shown in Figure 2.11 [96-100].

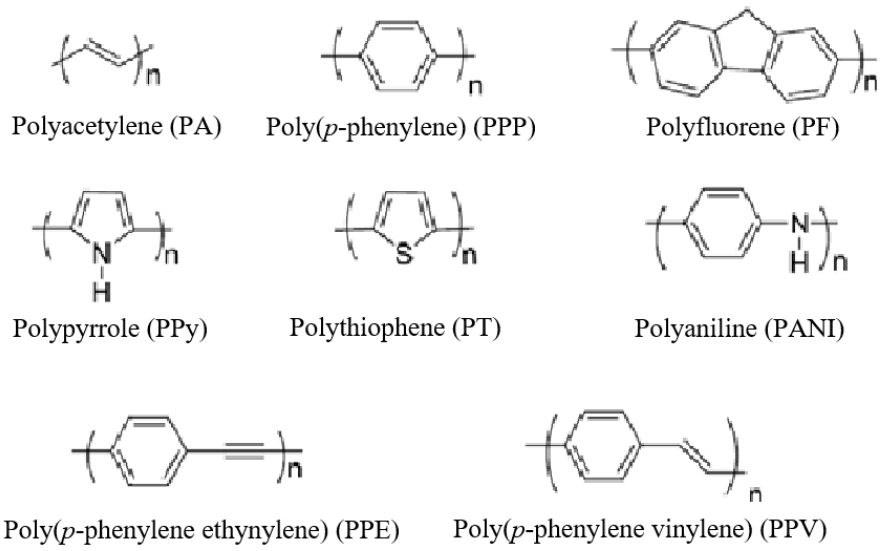

Figure 2.11 - Structures of some CPs [96]

Considering the above-mentioned properties, there are many applications in which CPs are employed, such as light-emitting diodes (LED), solar cells, field-effect transistors (FET), sensors and biosensors [100-103]. In biological sciences CPs, that are the base of CP-based sensors, can specifically detect different and various chemical and biological molecules (i.e. targets) and, thanks to the extreme sensitivity of these polymers to minor perturbations,

it results a highly sensitive and observable diagnostic, simply exploiting these polymers' opto-electronic characteristics, mostly CP's transport properties and electrical conductivity [98, 100]. CPs properties vary depending on the temperature, pH and presence of an electric field. Moreover, if a conjugated polymer binds to other molecules, it will eventually form a supramolecular structure [104-106]. Electroluminescent conjugated polymers are also well known; here fluorescent polymers emit light when excited by an electric current [102]. Fluorescence generally is defined as the emission of radiation from the lowest vibrational level of the excited state (S_1) to any of the vibrational levels of the ground state (S_0).
Conjugated polymers are appreciated due to their versatility; some photophysical properties, indeed, such as colour, absorption and emission efficiency, can be optimized according to the application, through the manipulation of the CPs chemical structure, in particular: type of substituent -R, effective conjugation length, intermolecular packing and intramolecular conformational change (Figure 2.12) [107, 108].

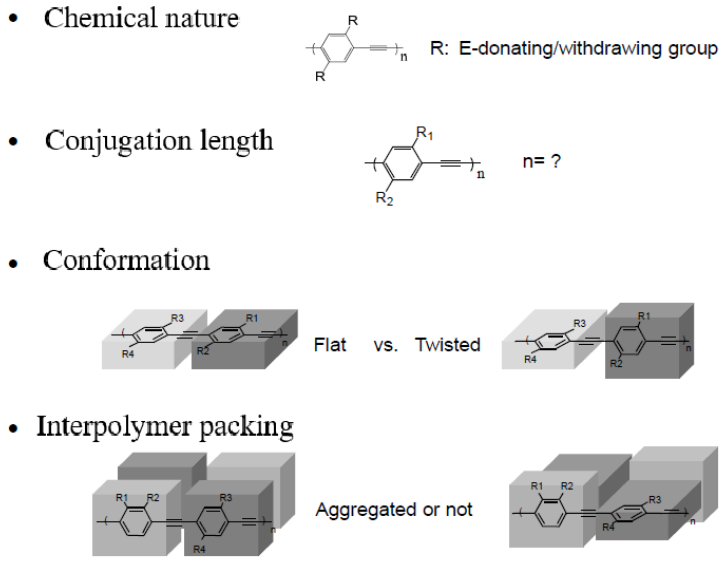

Figure 2.12 - Factors governing properties of CPs [107]

Emission wavelength can be tuned with the charge density of the CP backbone by replacing the side chain moiety: if an electron-donating group is linked to the backbone, the emission of the polymer will undergo a bathochromic shift (i.e. red-shift) and vice versa (hyposochromic, or blueshift). Moreover, also at longer chain length of the CP corresponds longer emission wavelength and consequent redshift. Equally also conformational changes and intermolecular packing have an influence in the final emission [107].

Usually for colorimetric detection organic dyes are employed as sensors but in this project the aim was to use conjugated polymers because, as opposite to dyes, they can enhance the signal from a recognition event, and this is extremely important when the analyte concentration is low. CPs electronic properties are indeed affected by the presence of the analyte that binds locally to a functional receptor. The consequent amplification or quenching of fluorescence is a unique feature of CPs; while for conjugated polymers the binding event affects the entire molecule of chromophores, binding event on small molecules (i.e. dyes) results in the fluorescence variation of a single chromophore. Small fluorescent dyes also show poor photostability in long-term applications [109, 110].
The possible detection modes developed for the sensing of biomolecules are turn-on or enhancing, turn off or quenching, fluorescence colour chance and visible colour change, as outlined in Figure 2.13.

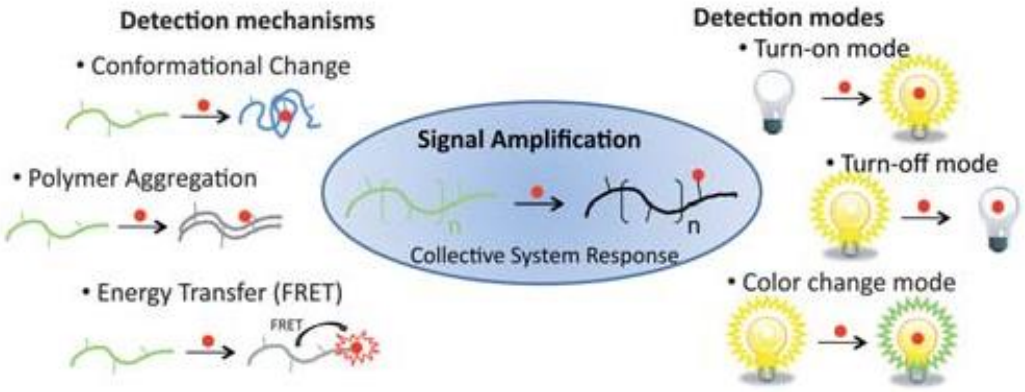

Figure 2.13 - Detection mechanisms for CPs biosensors [109]

When turn-on mechanism is triggered, target binding perturbs the electron density around the backbone and variations in the conformation of the CP chain is expected; this results in polymer fluorescence. In turn-off mode the target binding is responsible for the quenching of the CP caused by non-radiative relaxation mechanisms or intermolecular aggregation of the chain. Colour change mode is caused by a variation in the electron density of the backbone or by electron energy transfer due to the target binding event. In all these modes the signal can then be amplified through fluorescence resonance energy transfer (FRET), a mechanism that exploits the transfer in energy between two light-sensitive molecules (i.e. chromophores). The major advantage of CPs is that they are visible colorimetric sensors:

the final outcome (i.e. change in colour) is immediately visualized with naked eye. This makes them particularly suitable for clinical diagnostics purposes. Colour change mode is triggered when the binding event results in a variation of the conjugation length of the polymer chain, eventually leading to changes in light wavelengths absorbed [109, 110].

CPs are today used as colorimetric and fluorometric sensors with specific biological receptors for DNA and proteins (and others) detection [109].

Conjugated polyelectrolytes (CPEs) are typically used in the sensing field and are characterized by an ionic pendant group which makes the overall polymer exhibit optical and electronic properties as well as solubility in highly polar media, such as alcohol and water. Therefore, CPEs are water-soluble conjugated polymers.

Among all the conjugated polymers and conjugated polyelectrolytes, polythiophenes (PTs) are preferred thanks to their superior optical and electronic properties; moreover, they are eligible for biosensing. Even in the case of PTs, its optical transitions are caused by conformational changes of the chain that lead to bathochromic or hyposochromic shift [111-113].

Examples

It is been considered the use of water-soluble cationic PT to detect single stranded DNA (ssDNA). At first the polythiophene is in form of random coil and for this reason the colour of the solution is yellow; in presence of the target molecule (i.e. ssDNA), PT conformation undergoes a variation. The occurring electrostatic interactions makes the polymer structure appear planar, resulting in the formation of a duplex. Following this conformational change, polymer also shifted in colour, from yellow to red; moreover, it is noticed a quenching in the fluorescence intensity. In presence of a complementary ssDNA sequence, fluorescence intensity is restored and the solution shifted back to yellow colour; this means that the conjugation length of PT is decreased (blueshift) due to the formation of a triplex, that include conformational changes or aggregation between PT and hybridized nucleic acid sequences, which are double stranded DNA (dsDNA). This method, showed in Figure 2.14, is used to detect DNA hybridization and, in a wider context, fluorescence can be considered the mean by which the recognition event is transduced into a physically measurable value without requiring additional instrumentation [114, 115].

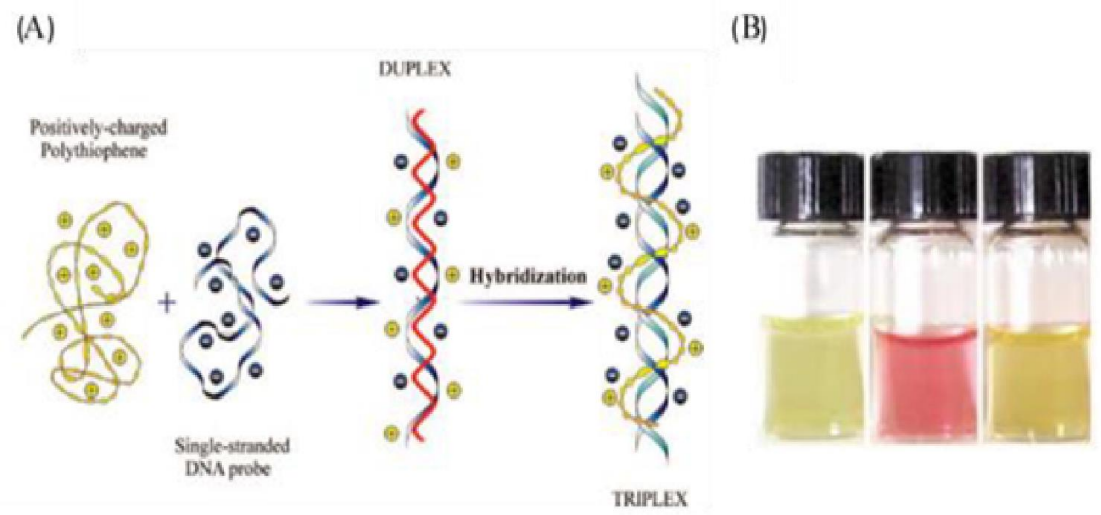

Figure 2.14 - DNA hybridization. (A) Detection mechanism (B) Matching pictures [114]

Of course, colour change is possible only if the duplex is formed due to the electrostatic interactions. If the ssDNA analyte is fragmented by S1 nuclease, a specific enzyme, duplex formation is prevented, PT remains in the form of random coil and, as depicted in Figure 2.15, no colour change of the polymer is detected [115].

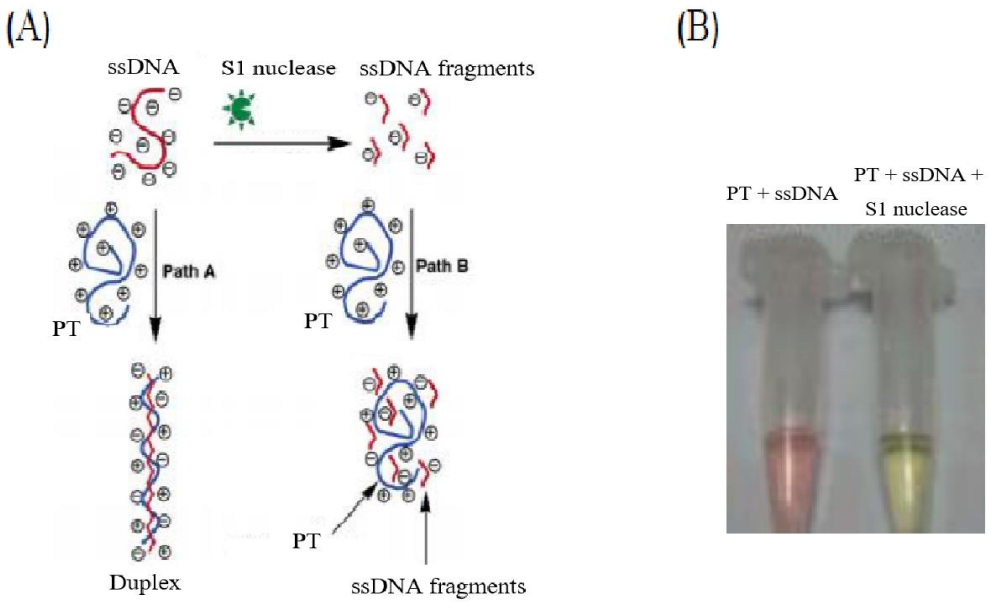

Figure 2.15 - (A) Mechanism in presence of S1 nuclease (B) Matching pictures [115]

Water-soluble cationic PTs are also used in combination to aptamers, that are, as already mentioned, artificial nucleic acid ligands and act as molecular recognition elements.

Aptamers are able to bind different molecules and biomolecules, such as proteins, with high affinity and specificity. After the occurrence of the binding event between an aptamer and its target, water-soluble PT will transduce the signal into a clear optical visualization, both in colorimetric and fluorometric terms [116].

So, aptamers are used as a specific molecular recognition element for the detection of monovalent potassium cation; moreover, K^+ has folding-inducing properties for several nucleic acids. The aptamer, indeed, after binding, undergoes a conformational change resulting in the formation of a G-quadruplex structure. The difference from free structure of the aptamer and G-quadruplex structure is pointed out by the water-soluble cationic PT. The solution turns from yellow (PT is in the form of random coil) to red due to the duplex structure formed by the electrostatic interactions between free aptamer and cationic PT; if the binding event between aptamer and potassium cation takes place and there's the formation of G-quadruplex, PT will wrap around the structure and the solution becomes orange. This mechanism is shown in Figure 2.16 [116].

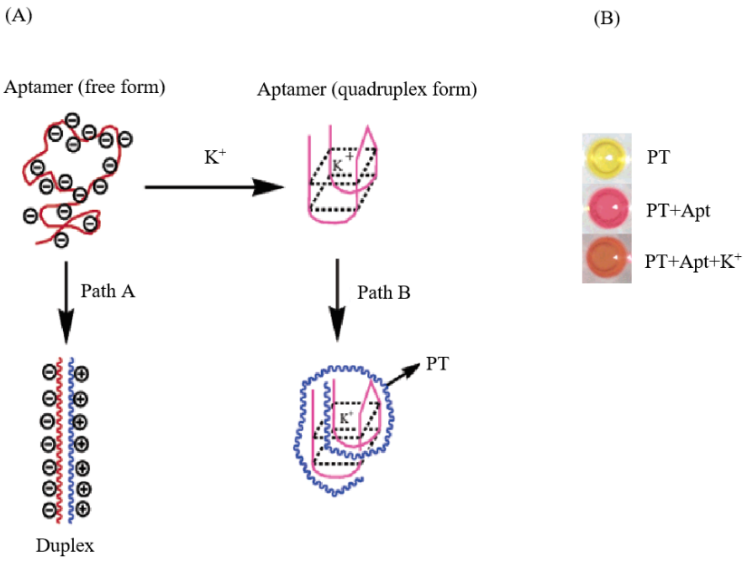

Figure 2.16 - (A) Detection of potassium ion (B) Matching pictures [116]

It's easy to understand that some biomacromolecules like DNA or proteins and PT are able to bind in a strong way, thus providing a significant colorimetric and fluorescent output; at

the opposite, analytes, that are small molecules, bind so weakly that no conformational changes are expected, thus producing no optical outputs [117].

Cationic polythiophene (CPT) derivative with anthracene side group is used as a dual-modal probe (both colorimetric and fluorescent) for adenosine triphosphate (ATP) detection. Due to electrostatic interactions, ATP and CTP bind together, forcing the formation of planar configuration of CPT resulting in the aggregation of PT backbones. Anthracene groups (side groups) will promote PT aggregation and $\pi - \pi$ stacking, allowing ATP detection. Of course, this stacking results in a colour change (redshift). A schematic illustration is provided in Figure 2.17 [117].

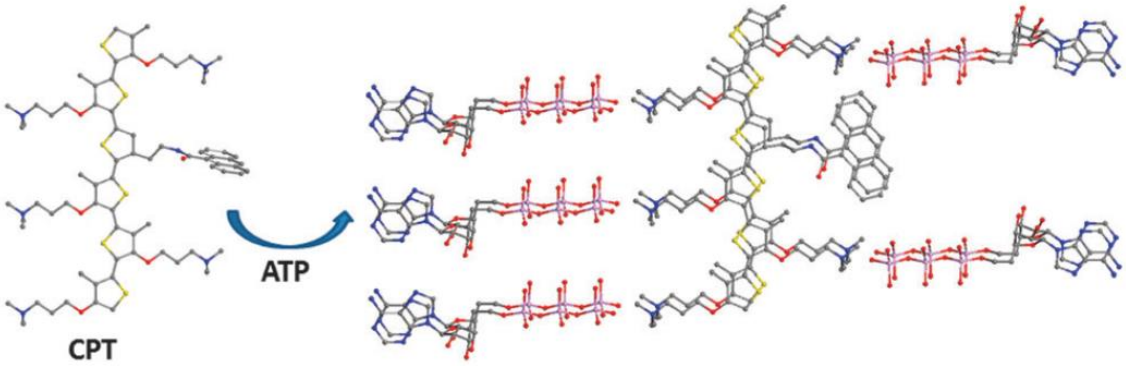

Figure 2.17 - Schematic illustration of the detection of ATP [117]

Water-soluble cationic polythiophene biosensors (CPB) are also used for direct and easy assessment of the microbiological quality of drinking water, offering a valid cost- and time-effective alternative to already existing methods, especially because some indicators are today still inadequate. It is exploited the ability of cationic polythiophenes, therefore positively charged, to rearrange in a more organized state after binding to a positive-charged molecule such as microbes, leading to an optical transition in terms of colour (when the structure changes from non-planar to planar conformation) and fluorescence intensity. Escherichia Coli (E. coli) is used as the target molecule. After the addition of E. coli to the polymer solution, a decrease in the fluorescence intensity is observed but no wavelength shift. Therefore, sensing is revealed by quenching but no colour shift, as depicted in Figure 2.18 [118].

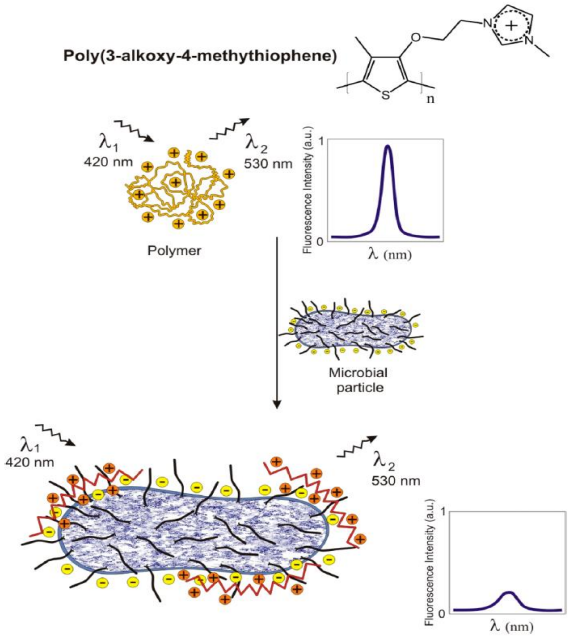

Figure 2.18 - Detection mechanism of microbial particle [118]

Polythiophenes in combination with aptamers can be used also to detect thrombin protein in solution and on a solid support. Fluorescence chain reaction (FCR) is a new method of amplification of the signal used in this study, that takes the advantages of different electrostatic and chromic interactions and fluorescence resonance energy transfer (FRET). The aptamer has been labelled with cyanine dye (Cy3), which excitation wavelength fitted the emission wavelength of the polymer in order to have optimal FRET, and with an amine group. Polymer and aptamer solution are then laid on a surface-treated glass with which it forms covalent bonds (through amine group). As shown below (Figure 2.19), as soon as thrombin analyte is added, the solution immediately appeared fluorescent. Other molecules, such as immunoglobulin (IgE) and bovine serum albumin (BSA) are used to test the selectivity in detecting only thrombin protein [119].

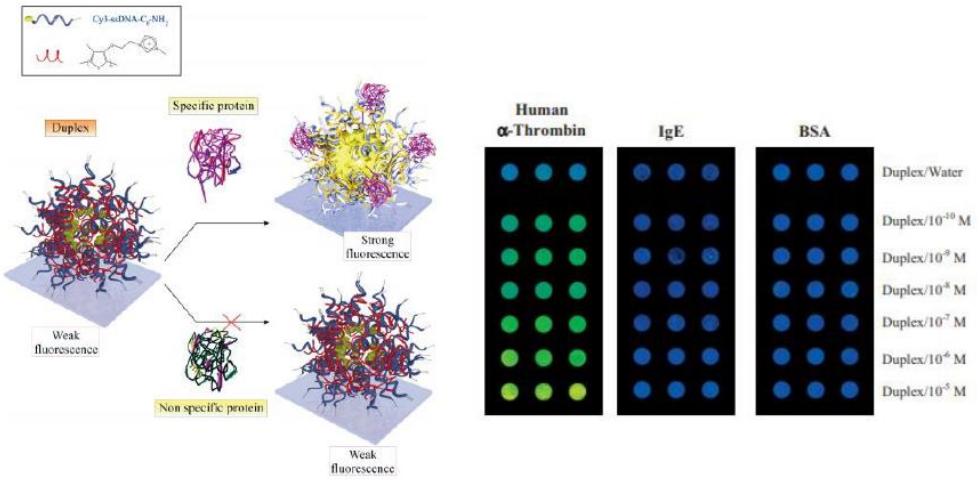

Figure 2.19 - Detection mechanism of thrombin and specificity, as a function of concentration of analyte [119]

The major drawback of using polythiophenes solutions is that there is high amount of non-specific interactions. PT is also used on a paper-based platform for miRNA (micro ribonucleic acid, i.e. sequence associated to lung cancer) naked eye detection. The thin paper of poly(vinylidene fluoride) (PVDF) is impregnated with cationic PT and it plays the role of luminescent reporter, while peptide nucleic acid (PNA) is the receptor.

As depicted in Figure 2.20, the non-complementary output will undergo a change in colour due to duplex formation, becoming purple; on the other hand, complementary sequence or "Target" miRNA forms a triplet and no change in colour is detected. This is due to the efficient hybridization with the peptide nucleic acid (PNA) [120].

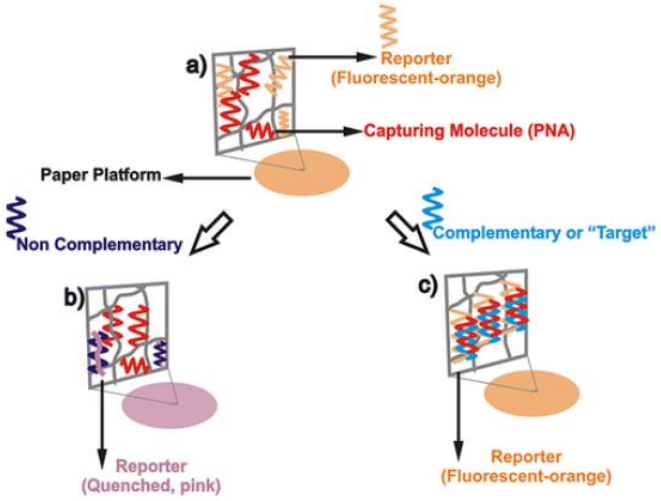

Figure 2.20 - Detection mechanism of miRNA analyte [120]

In this project, different cationic polythiophenes, as described in Chapter 3, have been engineered with different pendant groups in order to modify and vary hydrophobicity of the whole conjugated polymer. The pendant groups lead to tuning of the response to polar and non-polar molecules.

2.5.2 APTAMERS

The name "aptamer" originates in the Latin expression *aptus*, "to fit" and in the Greek word *meros*, "part", and it was used for the first time in 1990; from that time on, any short strand of DNA or RNA of 10 to 100 nucleotides, able either to set a specific 3D conformation and to bind to different target molecules, are named nucleic acid aptamers. Aptamers are one of the major components of the biosensing assay. They are, indeed, the recognition element, employed to detect the target analyte in a specific way, replacing antibodies and peptides [121]. A schematic comparison, enhancing aptamers advantages, between aptamers and antibodies is offered in Table 2.3.

Table 2.3 - Comparison between aptamers and antibodies [121, 122, 126]

Aptamers	Antibodies
In-vitro production (chemical synthesis)	In-vivo production (cell culture)
Simple and cheap production process	Difficult and expensive production process
Synthetized in a challenging environment, even with toxic and non-immunogenic compounds	No detection of toxic targets, only common proteins
Easy to handle and store thanks to their small size	Difficult to handle and store, due to their large size
Almost no variation from batch to batch	Common variations occurring from batch to batch
Long shelf life	Short shelf life
Stable also to change in temperature and pH; easily restored if damaged	Not stable and sensitive to changes in temperature and pH; no possibility of restoration if damaged
Tunable with other molecules	No possibility of modification

Nucleic acid aptamers are short and single-stranded DNA or RNA oligonucleotides extremely stable due to their 3D structure, which is also responsible of their intrinsic functionality. Aptamers' conformation relies on the primary sequence, the length of the nucleic acid molecules and the environmental conditions. These molecules are able to link to molecular targets of different type and size, ranging from small ions to protein, to large molecules and complex systems. When the aptamer recognizes the target molecule, it will fold its conformational structure leading to the formation of a specific binding site for the target. The binding mechanisms rely on the components' intermolecular interactions and, in particular, since the structures are complementary in shape, stacking interactions ($\pi - \pi$ stacking), electrostatic interactions and hydrogen bonds are considered [121, 122].

The production of aptamers is based on chemical synthesis and particularly through a process called SELEX, Systematic Evolution of Ligands by Exponential enrichment. SELEX method is introduced with a random sequence library of 20 to 100 nucleotides in length of ssDNA or ssRNA. The random nucleic acids sequence causes a differentiation of 4^n, where *n* is the number of randomized bases; this leads to about 10^{16} different aptamers. To each random sequence is attached a constant sequence in order to be captured. All these aptamers are then exposed to a target molecule: some of them undergo conformational change, folding as soon as the analyte is bonded, meaning that the aptamer is able to bind specifically to that target molecule, while some others are not and will be washed away. Those aptamers with high affinity to that target are amplified, enriched and then re-exposed to the same target molecule; at this point the process starts again from the beginning, with the possibility of adding to the new library any modification, chemical or functional, in order to increase the possibilities of molecule interaction. This is an iterative mechanism which ensures, after several rounds, an increased aptamers affinity to the target molecules and, consequently a final specific sequence (at the end there will be a pool filled only with clones). As depicted in Figure 2.21, it is possible to simplify the SELEX procedure into four simple steps: binding, partition, elution and amplification [122, 123].

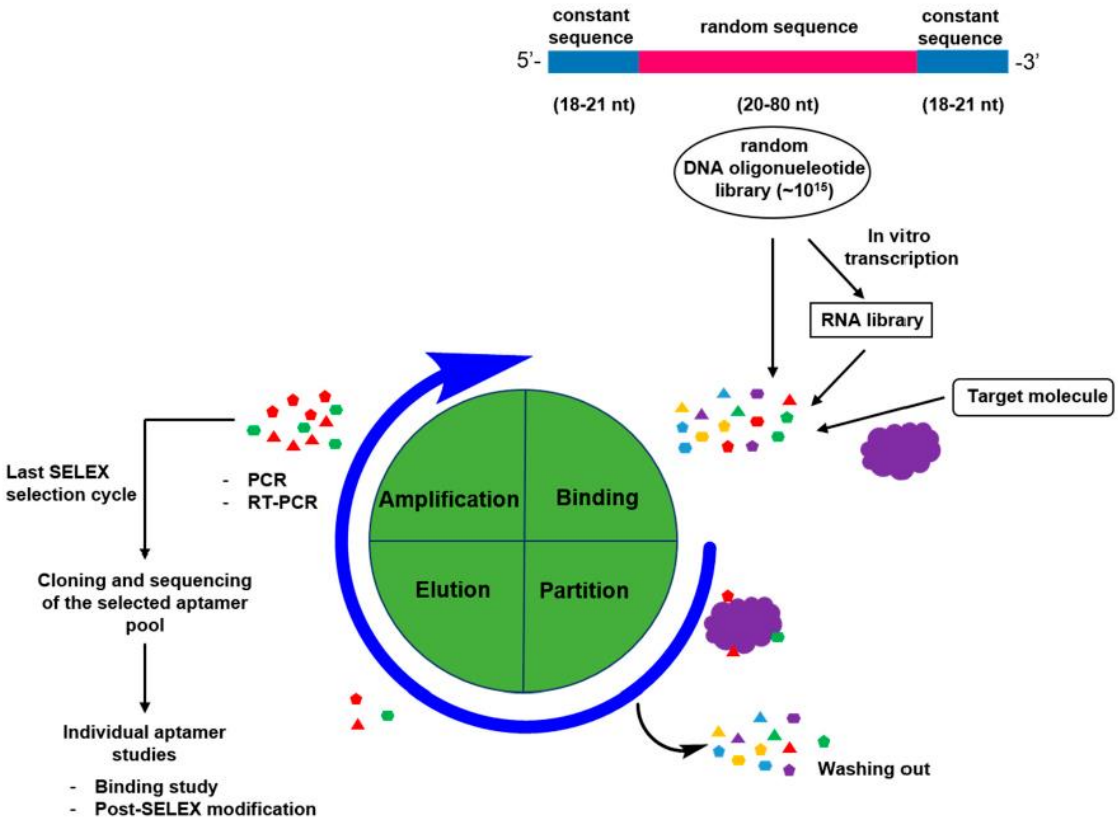

Figure 2.21 - SELEX process [123]

As already mentioned, aptamers are single or double strands of DNA or RNA, usually illustrated as double strand of a helical molecule, linked together by hydrogen bonds that binds the bases (adenine with thymine and guanine and cytosine). Actually, aptamers can fold in several complex and stable 3D structures that depends on the sequence of the nucleotides, thus allowing the binding event. Some of them as shown in Figure 2.22, are hairpin, pseudoknot and G-quadruplex. Hairpin structure is formed when the bases are complementary to each other, while G-quadruplex is usually created due to an excess of guanine basis (guanine is linked together by hydrogen bonds) [121, 125].

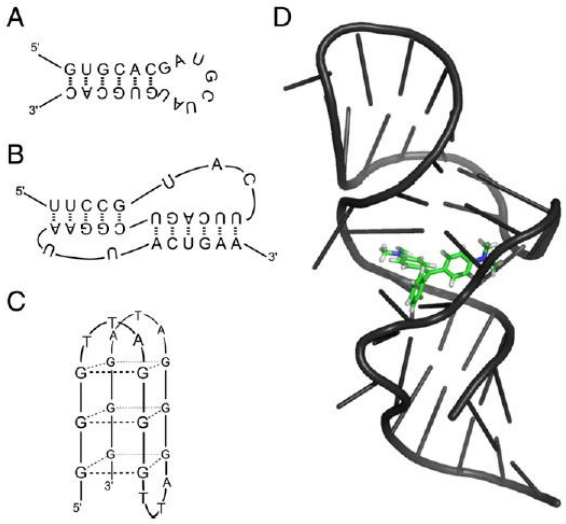

Figure 2.22 - Aptamer structures (A) Hairpin (B) Pseudoknot (C) G-quadruplex (D) Green aptamer in complex with its ligand [125]

There are several techniques for the determination of the structure of a complex comprehending an aptamer. Nuclear magnetic resonance (NMR) spectroscopy and X-ray crystallography are employed for structure inspection of high resolution [124, 125].

Optical probes such as gold nanoparticles (AuNP or GNPs), quantum dots and dyes are employed for paper-based assays that also takes the advantages of aptamers.
GNPs and aptamers are used on a paper chip for the detection of kanamycin, an aminoglycoside antibiotic. Gold nanoparticles are first synthetized, characterized and coated with citrate, then added to an aptamer; the overall solution is then laid on the paper chip and allowed to dry. As depicted in Figure 2.23, if the target analyte is absent and after salt addition, no colour change is depicted, so no aggregation of nanoparticles occurred because of the aptamer presence that prevented it; generally citrate-coated GNPs, indeed, aggregate and change colour from red to blue in high concentration NaCl solution.
On the opposite, in presence of kanamycin, the aptamer specifically binds with the analyte, its conformational structure changes allowing the GNPs to aggregate, thus revealing a change in colour [127].

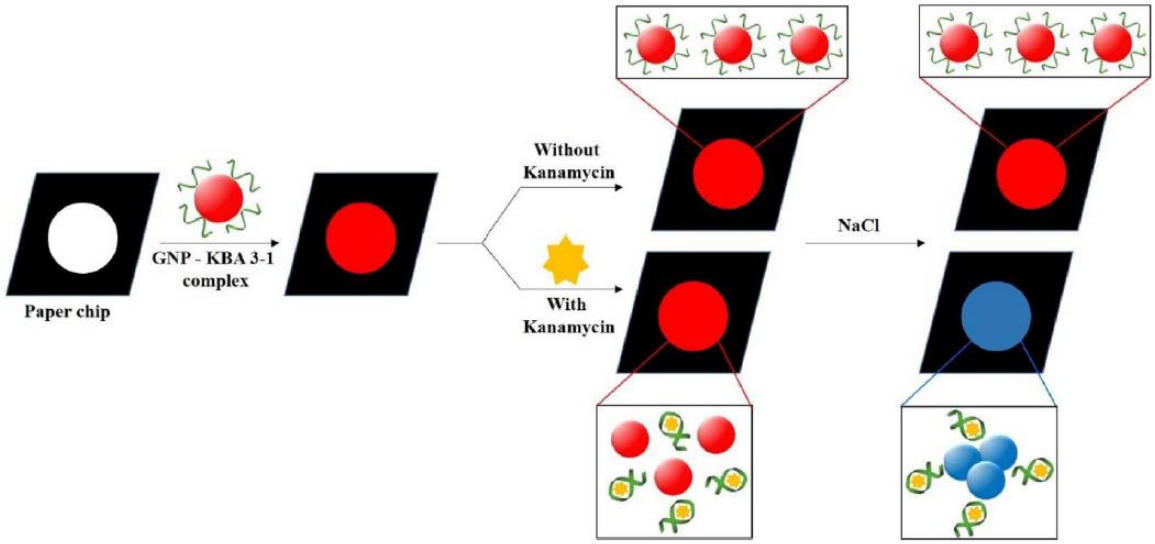

Figure 2.23 - Kanamycin detection [127]

Lateral flow assays (LFAs) are comprehended in POC devices field and can detect a high number of analytes, such as proteins, toxins, hormones, ions and viruses. Their major drawback is that they can give a false positive, due to non-specific binding, or false negative outputs, due to the hook effect (i.e. the analyte concentration is so high that any output is prevented); moreover, sometimes also non-equal distribution of the sample is experienced. Tests made by LFA run the liquid sample laterally along the surface of a pad, made of capillary beds such as porous paper, micro structured polymers etc. able to filter specifically some components and transport fluid towards a conjugation pad where the solution encounters a detection label made of recognition element attached to a reporter molecule like AuNPs. Aptamers (i.e. the recognition element) in the test zone, bind with the target, if present, so that it remains fixed. The presence of the reporter molecule gives a signal that can be directly seen. There are two types of LFAs: sandwich and competitive formats. In reference to Figure 2.24, in the sandwich assay two aptamers are employed: the first one is conjugated with the detection label and the other is fixed at the test zone. The target will bind with both aptamers one after the other creating an output. In the competitive assay when the target is absent AuNPs-aptamer conjugate of the detection label binds with the complementary DNA sequence of the aptamer present in the test line, forming a duplex and therefore giving an output; while if the target analyte is present, the conjugate AuNPs-aptamer will bind preferentially to it giving no signal output (or a reduction of it). Depending on the target concentration the intensity of the colour will change; this provides

a semi-quantitative analyte detection. Control line validates an appropriate fluid flow, giving a qualitative assessment [32, 128, 129].

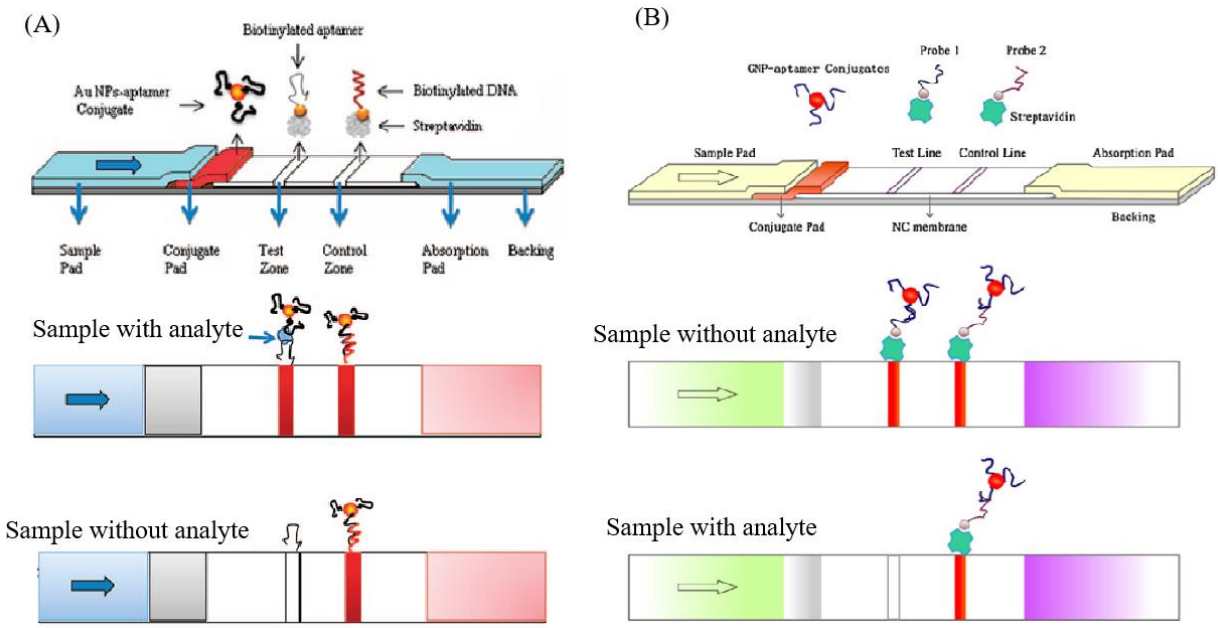

Figure 2.24 - LFA biosensor (A) Sandwich format [32] (B) Competitive format [129]

A classification of various biosensors exploiting aptamers' properties for the investigation of different targets and their limit of detection, is listed below in Table 2.4.

Table 2.4 - Aptamer- and paper-based optical biosensors

Target	Optical Probe	Limit of Detection	Ref.
Thrombin	AuNPs	2.5nM; 4.9pM	[32, 134]
Ramos cells	AuNPs	4000 Ramos cells, 800 Ramos cells (with reader)	[33]
Adenosine	AuNPs	20μM	[130]
Cocaine	AuNPs	10μM	[130]
Ochratoxin A	AuNPs; Cy5-labeled aptamer	1ng/ml, 0.18ng/ml (with reader); 0.4 ng/ml	[131, 132, 138]
Vaspin	AuNPs	0.105nM	[136]
E. coli	AuNPs; TMB/H_2O_2	10CFU/ml; [-]	[133, 139]

HCV core antigen	AuNPs	100pg/ml, 10pg/ml (with reader)	[135]
Beta-conglutin	AuNPs	9fM	[137]
Aflatoxin B1	Cy5-labeled aptamer	0.1ng/ml	[138]
Cancer cells	Quantum dots with graphene oxide	65cells/ml	[140]
Adenosine	Iodine-starch	0.16μM	[141]
Pb^{2+}	Dye with hydrogel	200nM	[142]

These kinds of paper-based biosensors employ mostly gold nanoparticles, as in the examples above, but also dyes, as detection element; while as recognition element have been used, besides aptamers, antibodies.

This project aims at development of a colorimetric biosensor that takes the advantages of the superior properties of cationic polythiophenes and the high selectivity and specificity of aptamers to detect one of the carbonyl and oxidative stress biomarkers associated to type 2 diabetes: advanced glycation end-products (AGEs).
In this thesis, as shown in Chapter 3, five different types of advanced glycation end-products (AGEs) have been used as target biomolecules and four different cytosine-rich aptamers, suitable for binding with AGEs due to their high affinity, are employed as the recognition element.

Chapter 3: EXPERIMENTAL METHODS

3.1 MATERIALS AND INSTRUMENTS

In this chapter, the development of a novel solution-based bio sensing platform for both colorimetric and fluorometric detection of five types of AGEs using different cationic polythiophenes and various aptamers is described. As explained in Chapter 4, selectivity studies are also carried out for each cationic polymer used. The validity of the solution-based assay for the detection of one of the biomarkers (Gly-AGEs) is also demonstrated at different biomarker concentrations and in plasma. One biomarker (CML-AGEs) it has been studied on a polyvinylidene difluoride (PVDF) membrane. Detailed studies in plasma and on membranes are interesting to further explore and are left to future laboratory activities. To ensure reproducibility, every analysis is repeated in three independent trials.

For experiments carried out in buffer, the solution of Phosphate-buffered saline (PBS) of composition: sodium chloride [NaCl]: 1.37 M, potassium chloride [KCl]: 27 mM, disodium phosphate [Na_2HPO_4]: 100 mM, potassium dihydrogen phosphate [KH_2PO_4]: 18 mM is diluted 10-fold in DI water, resulting in 10xPBS solution. PBS have pH 7.2 and is employed in many uses in biological research because in non-toxic to most cells and it helps maintaining a constant pH. All reagents and solvents included PBS, are purchased from Sigma-Aldrich and used without any further purification.

From literature, five different types of advanced glycation end-products (AGEs) have been used as target biomolecules. Every AGE has initial (stock) concentration of 1mg/ml and are presented in PBS solution. Some AGEs may have intrinsic fluorescence; a high peak at very low wavelengths is indeed detected when the fluorescence intensity measure is carried out (see graphs in Chapter 4). However, these peaks are not of this project interest since the red-shift is considered between polymer solution and polymer-aptamer solution. AGEs are stored at -20°C. Listed below AGEs are provided by BML (Japan) [143-148].

- **AGE1**: Glyceraldehyde derived AGEs (Gly-AGEs)
- **AGE2**: Glycolaldehyde derived AGEs (Glyco-AGEs)
- **AGE3**: Glucose derived AGEs (Glu-AGEs)
- **AGE4**: Methylglyoxal derived AGEs (Met-AGEs)
- **AGE5**: Carboxymethyl lysine AGEs (CML-AGEs)

From literature, four different cytosine-rich aptamers, suitable for binding with AGEs due to their high affinity, are employed as the recognition element. By the analyzation of the aptamers structures, it is possible to notice that Apt1 and Apt4 sequences are similar to each other, and same for Apt2 and Apt3 sequences; this results in same (paired, respectively) molar concentration in most of the trials. Aptamers are usually stable for years, depending on how many times they undergo freezing and de-freezing processes.

All four aptamers are synthesized by IDT (Singapore) followed by polyacrylamide gel electrophoresis (PAGE) purification. The stock solution of 100µM aptamer is prepared with DNase free de-ionized (DI) water, upon 20 seconds centrifuging, and stored at -20°C. Sequences are listed below [30, 149, 150].

- **Apt1**- 5'- TGT AGC CCG AGT ATC ATT CTC CAT CGC CCC CAG ATA CAA G -3'
- **Apt2**- 5'- TAA CTC ACT CCA TAC TCA CTT GCT GAT TCG CCA ACA ACA CAC CCT TAA ACA GTC CC -3'
- **Apt3**- 5'- CCG AAA CCA GAC CAC CCC ACC AAG GCC ACT CGG TCG AAC CGC CAA CAC TCA CCC CA -3'
- **Apt4**- 5'- TG*T* AGC CCG* AG*T* A*TC* A*T*T C*TC C*A*T CGC CCC C*AG* A*T*A C*A*A G- 3'

  ***** representing phosphonothioate bond (PTO bond)

PTO bonds can prevent from aptamer degradation after its exposure to some enzyme present in air or blood. By doing so, a better interaction with the polymer and AGEs is guaranteed.

From literature, four different cationic polythiophenes (PTs) have been synthesized at the Centre for Biomimetic Sensor Science (CBSS) laboratories, as described in Appendix I, through oxidative polymerization of their corresponding monomers [151-160].

Polythiophenes show good thermal stability and processability.

Different cationic polythiophenes have been engineered with different pendant groups in order to modify and vary hydrophobicity of the whole conjugated polymer. The pendant groups lead to tuning of the response to polar and non-polar molecules [155]. The synthetized cationic polythiophenes are water soluble with stock concentration of 1mg/10ml which corresponds to about 300μM. Polymer batches are stored on a stirrer plate, covered with aluminium foil, in order to prevent from aggregates formation and UV light damage. Before being used, polymers are typically subjected to ultrasonication process at 40°C for about 20 minutes, so that no aggregates are present and reliable and reproducible outcomes are guaranteed. PTsyn showed very good responses in PBS solution due to its particular structure that yield to highly fluorescent and therefore distinguishable outcomes.

- **PT1**: poly(3-(4-Methyl-3'-thienyl oxy) propyl triethylammonium bromide)

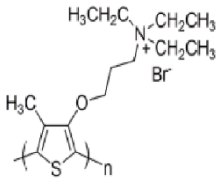

- **PTsyn**: poly(1,4-dimethyl-1-(3-((4-methylthiophen-3-yl) oxy) propyl) piperazin-1-ium bromide)

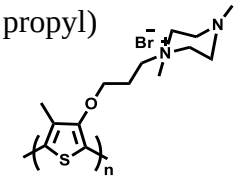

- **PTG**: poly(1-(3-((4-methylthiophen-3-yl) oxy) propyl)-1,4-diazabicyclooctan-1-ium bromide)

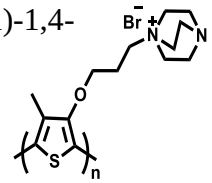

- **PT5**: poly(N-allyl-N-methyl-N-(3-((4-methylthiophen-3-yl) oxy) propyl) prop-2-en-1-aminum bromide)

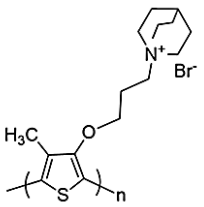

For the AGEs assay, here listed the different optimized concentrations of PTs-Apt-AGEs combinations. To visualize the colour change, the samples are placed under UV

illumination zone (portable UV lamp, at 365nm, 8W) and digital images were captured using a SONY camera (model ILCE-7R, F-stop f/2.8, exposition time 2.5s, ISO sensitivity 250) positioned at a fixed distance from the vials. Afterwards, the digital images are transferred to the computer as jpeg files for editing on software SONY camera Edit (settings: preset +0K, colour temperature 9900K) and then the centroids of vials (100x100 pixel) are used to create a digital array. RGB analysis is further carried out using ImageJ image processing software in order to assess a colorimetric response. The colour is expressed as a triplet of interrelated variables: red, green and blue and each of these components can vary from zero to 255 (maximum value). Delta E values are ranging between 0-100 and represents a metric for human eye perception of colour differences; they are calculated from the software Delta-E Calculator-ColorMine.org exploiting the International Commission of Illumination 1976 (CIE76) algorithm [161, 162]:

$\Delta E_{ab}{}^{*} = \sqrt{(L_2^* - L_1^*)^2 + (a_2^* - a_1^*)^2 + (b_2^* - b_1^*)^2}$ where (L_1^*, a_1^*, b_1^*) and (L_2^*, a_2^*, b_2^*) are coordinates corresponding to two colours in CIELAB colour space. An outcome of about 2.3 corresponds to just noticeable difference.

Finally, steady state fluorescence intensity of the samples is measured using an Infinite M200Pro Tecan plate reader. Fluorescence spectra is obtained with different excitation wavelengths, depending upon the cationic polythiophene used. Every measure is taken with the following settings: emission wavelength range of 450nm-750nm and a step of 2nm. The plate used to run the fluorescence intensity test is a 384 Corning Flat Black.

Every PTs-Apt-AGE combination is the result of an optimization.

- 15µL of 150µg/ml (3µl) of the five different **AGEs** in 10xPBS, pH 7.2 was added to 5µL (10µM) **Apt1** and incubated for 30 minutes followed by the addition of 30µL of 116.67µM **PT1** solution to these samples. Excitation wavelength: 400nm
- 15µL of 150µg/ml (3µl) of the five different **AGEs** in 10xPBS, pH 7.2 was added to 2.5µL (5µM) **Apt2** and incubated for 30 minutes followed by the addition of 30µL of 116.67µM **PT1** solution to these samples. Excitation wavelength: 400nm
- 15µL of 150µg/ml (3µl) of the five different **AGEs** in 10xPBS, pH 7.2 was added to 5µL (10µM) **Apt3** and incubated for 30 minutes followed by the addition of 30µL of 116.67µM **PT1** solution to these samples. Excitation wavelength: 400nm

- 15µL of 150µg/ml (3µl) of the five different **AGEs** in 10xPBS, pH 7.2 was added to 5µL (10µM) **Apt4** and incubated for 30 minutes followed by the addition of 30µL of 116.67µM **PT1** solution to these samples. Excitation wavelength: 400nm
- 15µL of 150µg/ml (3µl) of the five different **AGEs** in DI, pH 7.2 was added to 5µL (10µM) **Apt1** and incubated for 30 minutes followed by the addition of 30µL of 300µM (stock concentration) **PTsyn** solution to these samples. Excitation wavelength: 400nm
- 15µL of 150µg/ml (3µl) of the five different **AGEs** in DI, pH 7.2 was added to 2.5µL (5µM) **Apt2** and incubated for 30 minutes followed by the addition of 30µL of 300µM (stock concentration) **PTsyn** solution to these samples. Excitation wavelength: 400nm
- 15µL of 150µg/ml (3µl) of the five different **AGEs** in DI, pH 7.2 was added to 2.5µL (5µM) **Apt3** and incubated for 30 minutes followed by the addition of 30µL of 300µM (stock concentration) **PTsyn** solution to these samples. Excitation wavelength: 400nm
- 15µL of 150µg/ml (3µl) of the five different **AGEs** in DI, pH 7.2 was added to 5µL (10µM) **Apt4** and incubated for 30 minutes followed by the addition of 30µL of 300µM (stock concentration) **PTsyn** solution to these samples. Excitation wavelength: 400nm
- 15µL of 150µg/ml (3µl) of the five different **AGEs** in DI water was added to 5µL (10µM) **Apt1** and incubated for 30 minutes followed by the addition of 30µL of 50µM **PTG** solution to these samples. Excitation wavelength: 420nm
- 15µL of 150µg/ml (3µl) of the five different **AGEs** in DI water was added to 2.5µL (5µM) **Apt2** and incubated for 30 minutes followed by the addition of 30µL of 50µM **PTG** solution to these samples. Excitation wavelength: 420nm
- 15µL of 150µg/ml (3µl) of the five different **AGEs** in DI water was added to 2.5µL (5µM) **Apt3** and incubated for 30 minutes followed by the addition of 30µL of 50µM **PTG** solution to these samples. Excitation wavelength: 420nm
- 15µL of 150µg/ml (3µl) of the five different **AGEs** in DI water was added to 5µL (10µM) **Apt4** and incubated for 30 minutes followed by the addition of 30µL of 50µM **PTG** solution to these samples. Excitation wavelength: 420nm
- 15µL of 150µg/ml (3µl) of the five different **AGEs** in DI, pH 7.2 was added to 10µL (20µM) **Apt1** and incubated for 30 minutes followed by the addition of 30µL of

300µM (stock concentration) **PT5** solution to these samples. Excitation wavelength: 400nm

- 15µL of 150µg/ml (3µl) of the five different **AGEs** in DI, pH 7.2 was added to 7.5µL (15µM) **Apt2** and incubated for 30 minutes followed by the addition of 30µL of 300µM (stock concentration) **PT5** solution to these samples. Excitation wavelength: 400nm
- 15µL of 150µg/ml (3µl) of the five different **AGEs** in DI, pH 7.2 was added to 7.5µL (15µM) **Apt3** and incubated for 30 minutes followed by the addition of 30µL of 300µM (stock concentration) **PT5** solution to these samples. Excitation wavelength: 400nm
- 15µL of 150µg/ml (3µl) of the five different **AGEs** in DI, pH 7.2 was added to 10µL (20µM) **Apt4** and incubated for 30 minutes followed by the addition of 30µL of 300µM (stock concentration) **PT5** solution to these samples. Excitation wavelength: 400nm

Concerning **PT1**, further insights are described in Chapter 4 and, in particular, different **AGE1** concentrations have been studied both in buffer (10xPBS) and in plasma; moreover, **AGE4** has been examined in a merely colour-based study (i.e. a preliminary study) on polyvinylidene difluoride (PVDF) membrane.
AGEs assay in plasma is carried out in the same way as in PBS, simply replacing the plasma solution to the PBS. Plasma is provided by GeneTex, Taiwan.

PT1 coating on membrane: 200µl of 2µM PT1-0.01%Tween (6µl tween stock + 5994 µl 10XPBS) is centrifuged using PVDF centrifugal tubes at 8000rpm for 3 minutes. The addition of Tween as surfactant, helps in the differentiation of colours and deceasing non-specific binding. In order to obtain a homogeneous coating of PT on PVDF membranes, the above-mentioned step was repeated four times, followed by washing with DI water twice under the same centrifugation conditions. These PT coated membranes are them stored at room temperature overnight for drying. Then, 5µl of solution of 5µM Apt1 (2.5µl in PBS) mixed with 150µg/ml (3µl in PBS) AGE4 and incubated for 30 minutes, is added to the membrane and allowed to dry. Then the process for colour change visualization is carried out in the same way as of the initial study. PVDF membranes are provided by Merk (Singapore).

3.2 ADVANCED GLYCATION END-PRODUCTS DETECTION

As mentioned in Chapter 2, the heterogeneous compounds formed as a consequence of the non-enzymatic reaction between a protein and a sugar, are collectively known as advanced glycation end-products. Glycation, or Maillard reaction, alters the structure and function of a proteins, rendering it dysfunctional. Glycation, described in Appendix II, is a multi-step process in which rearrangements and cyclization reactions are included. As shown in Figure 3.1, the free amino groups of the amino acids of a protein bind with the carbonyl group of a sugar, leading to the formation of a Schiff base, that in turn, being a very unstable product, undergoes rearrangements and an Amadori product is created. The Amadori product itself may undergo rearrangements, degradation or any other spontaneous reaction, forming AGEs. In conclusion, AGEs can be detected in order to prevent any complication of various pathophysiological conditions such as diabetes, to which these biomarkers are associated [144, 163, 164].

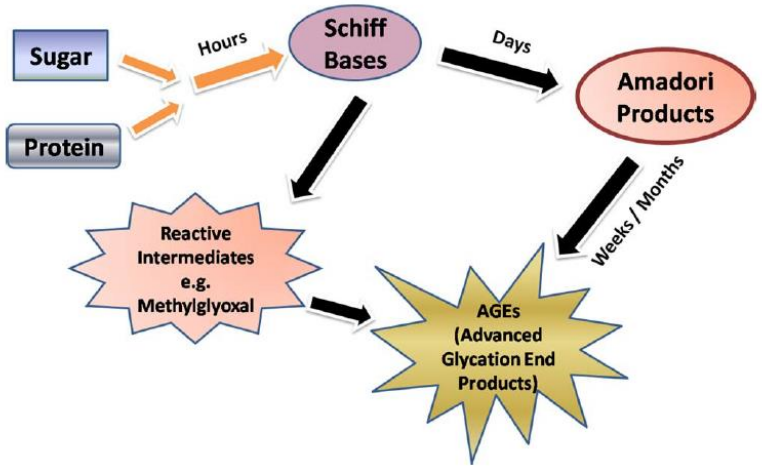

Figure 3.1 - Schematic mechanism of AGEs formation [144]

AGEs can be either cross-linking AGEs which are fluorescent, non-crosslinking AGEs and nonfluorescent cross-linking AGEs. AGEs can alter the structural characteristics of a protein through the formation of cross-links, can interact with their receptor RAGEs which are immunoglobin found on the macrophages surface and other types of cells, and can undergo intracellular accumulation [144]. AGEs play a key role not only, as already described, in several cardiovascular diseases through the modification of structure, function

and the mechanical properties of tissues, but also in the neurodegenerative disorders such as Alzheimer's and Parkinson's diseases [144, 163, 164].

CML-AGEs can be significantly higher in patients having both diabetes and coronary heart disease (8.1U/ml) with respect to patients suffering diabetes only (7.1U/ml). Some AGEs can also be found in the atheromatous lesions in the coronary arteries, proving the harmful role of AGEs in the atherosclerosis evolution. High levels of AGEs enhance the development of heart failure both through coronary dysfunction and damage of the myocardium, in which the binding mechanism of these molecules with their receptors, RAGEs, triggers multiple signal pathways leading to inflammation and development of several diseases [144].

It is clear the importance in reduction of AGEs formation in order to predict (or identify) the severity of a multitude of conditions, and this is best done in a point of care management involving the control of food intake when an increase of level is detected; hence, an assay development for AGEs is required. Figure 3.2 shows how AGEs detection and measurement can be useful at several levels of a disease development.

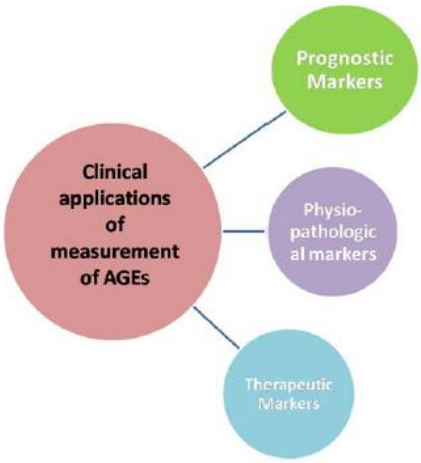

Figure 3.2 - Clinical application of AGEs detection [144]

As mentioned, circulating AGEs can be due not only to the biochemical reactions already described, but also through ingestion of high AGEs content foods, such as red meat, certain cheeses, oils, fried eggs, butter, cream cheese, margarine, mayonnaise and nuts.

It is indeed pivotal for those suffering type 2 diabetes, the determination of the amount of AGEs in food intake in such a way that a low AGEs diet can be established. The control of

food intake through a dietary intervention is a simple way of prevention against premature aging and diseases such as diabetes.

The majority of the methods today available, as discussed in section 4.6, are not suitable in developing world because they require sophisticated and bulky laboratory instruments and trained personnel who carry out the analysis. Therefore, it is highly necessary to develop a point of care assay for AGEs detection. AGEs are heterogeneous molecules with complex structures and, as diagnostic markers, require extremely specific recognition elements (Aptamers) and optical reporters (cationic polythiophenes). This new and highly specific method will assist in the early diagnosis of glycation-associated diseases.

Chapter 4: RESULTS AND DISCUSSION

4.1 INTERACTION OF PT WITH APTAMER AND AGEs

The overall sensing mechanism of AGEs is based, as depicted in Figure 4.1, on the survey of a colour change of the solution samples. The variation in the conformational structure of polythiophenes upon interactions with the aptamers in presence or absence of AGEs results, indeed, in the diversification of its optical properties.

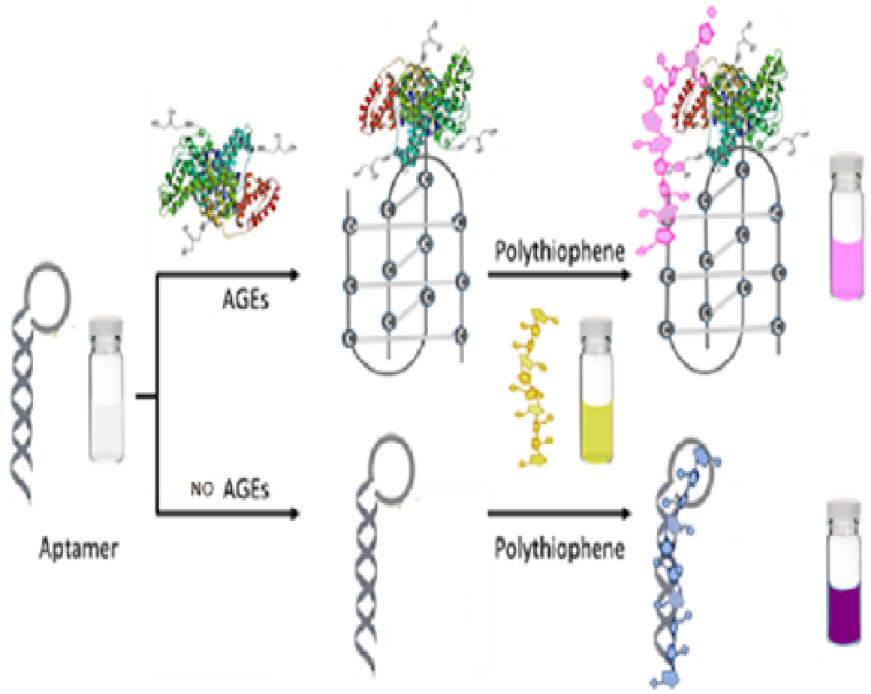

Figure 4.1 - Schematic assay for AGEs detection

The four different aptamers, each one at its fixed molar concentration, are incubated with the five different AGEs at fixed concentration of 150µg/ml in PBS, pH 7.2 for 30 minutes in order to form Apt-AGEs complex, called i-motif complex, a four-stranded quadruplex structure established in presence of cytosine-rich DNA [274]. PT is then added to both samples: aptamer only and Apt-AGEs complex. When PT combines with Apt, so in absence of the molecular target, a duplex configuration is formed, due to the electrostatic interactions between the positively charged PT and the negatively charged Apt; this leads to a variation in the morphology of the polymer, that turns from random-coil to a planar π-

stacking configuration. It results a significant colour change from yellow, corresponding to the random-coil morphology, to red, in agreement with the planar configuration of a conjugated polymer: the typical structure of CPs is indeed given by the alternation of single and double bond, so that electrons along the chain are delocalized and free to move. Consequently, the energy gap between valence band and conduction band, defined as $E_{gap} = \omega * \frac{h}{2\pi}$ where ω is the frequency and h is Planck constant, is reduced, so low frequencies ω are involved, visually corresponding to the red colour. Moreover, a quench in the fluorescence intensity is observed (Fluorescence is defined as the emission of radiation from the lowest vibrational level of the excited state (S_1) to any of the vibrational levels of the ground state (S_0)). Both fluorescence intensity of the polythiophene and the visualized red shift, upon addition of aptamer, are unique values that depends on the intrinsic properties, structures and interaction mode of the molecules involved.

In presence of AGEs, the single stranded Apt undergoes a conformational change creating the i-motif complex, a rigid structure that leads to the reduction of electrostatic interactions between polymer and aptamer, so to a reduced fluorescence quenching (i.e. fluorescence recovery) and reduced colour modification resulting in a transition from yellow to red. So, the addition of AGEs promotes the formation of i-motif complexes, hindering the planarization of PT. Different intermediate colorimetric responses are detected depending on the type and concentration of AGE, aptamer and polythiophene.

In conclusion, a distinguishable naked eye colorimetric response in presence (corresponding to pink/purple colour) or in absence (corresponding to red colour) of AGEs is detected and exploited for the assay.

Every combination PT-Apt is been studied; the first cationic polythiophene considered is **116.67µM PT1**, paired with **10µM Apt1**. **AGEs** fixed concentration of **150µg/ml** in PBS is the result of the optimization in order to have a clear visual outcome (see section 4.3) and for clinical relevance. To ensure reproducibility, every analysis is repeated in three independent trials; then, every bar graph is a mean of the values and standard deviation of the results is included.

Figure 4.2 (A) illustrates the samples with different colours corresponding to the five different AGEs (vials from 3 to 7). These samples are first incubated for 30 minutes allowing the i-motif configuration to establish between Apt1 and AGEs, then PT1 is added to every vial. The first vial contains only PT1, while in vial 2 Apt1 is been added to PT1. Two significantly different optical signals (PT1-Apt1 and PT1-Apt1-AGE1) are subsequently analysed and correlated to the presence of the biomarker.

To validate the assay, fluorescence spectra for the samples is recorded using an Infinite M200Pro Tecan plate reader. Every measure is taken with the following settings: emission wavelength range of 450nm-750nm and a step of 2nm. The plate used to run the fluorescence intensity test is a 384 Corning Flat Black.

PT1 requires an excitation wavelength of 400nm.

The fluorescence intensity spectra of PT1, having its maximum peak at 556nm for PT1 in random-coil morphology, is shown in Figure 4.2 (B) and, upon addition of Apt1, a substantial quenching and red shift (of about 38nm) is revealed: this means that the duplex is formed between PT1 and Apt1. As observed from the graph of Figure 4.2 (C), at different AGEs corresponds different recoveries, depending on the Apt1-AGE interaction: the more Apt1 is specific for the molecular target (AGE), with which it forms the i-motif complex, the more reduced are the electrostatic interactions between PT1 and Apt1. Therefore, fluorescence intensity is proportional to the ability of Apt1 of AGEs interaction: high fluorescence recovery corresponds to highly detected AGE. Fluorescence recovery (F.R.) is calculated as follows: $F.R. = \left(\frac{I - I_{Apt}}{I_{PT} - I_{Apt}}\right) \bullet 100$ where I, I_{Apt}, I_{PT} are, respectively, the maximum intensities of the single AGE, of Apt1 and PT1. In this assay a significant recovery is considered whenever F.R. value is higher than 5%.

Further evidence of complex formation is obtained from RGB analysis of the vials, via ImageJ processing software, as showed in Figure 4.2 (D), upon capture of the samples under UV portable lamp (365nm, 8W) with SONY camera (model ILCE-7R, F-stop f/2.8,

exposition time 2.5s, ISO sensitivity 250) positioned at a fixed distance from the vials. The blue tone of the lamp is affecting the final colour output in such a way that the red colour is perceived as purple. Moreover, Delta-E values in Figure 4.2 (E), ranging between 0-100, that is a metric for human eye perception of colour differences, is measured using the International Commission of Illumination (CIE) 1976 algorithm [225, 226]. Delta-E values indicates that the colour difference between the different vials can be visually distinguished. In this specific case, all five AGEs can be distinguished with respect to vial 2 (PT1+Apt1), indicating that nearly all AGEs can be detected from a colorimetric point of view. However, from fluorescence recovery analysis is clear that AGE1, AGE4 and AGE5 are best detected by PT1 and Apt1.

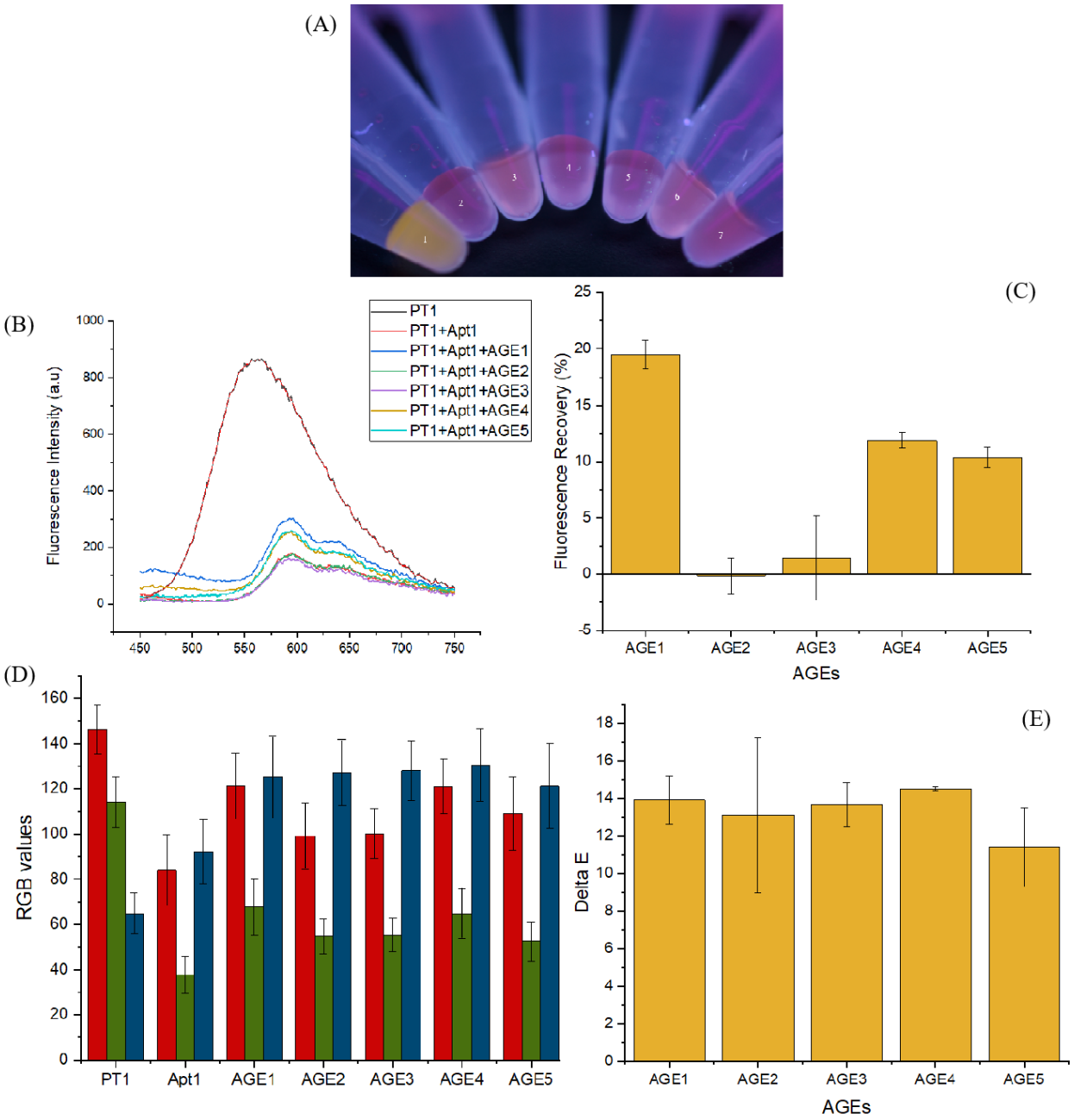

Figure 4.2 - 150µg/ml AGEs detection in 116.67µM PT1 and in presence of 10µM Apt1 (A) Vials (B) Fluorescence Intensity spectra (C) Fluoresce Recovery mean values and standard deviation (D) RGB mean values and standard deviation (E) Delta-E mean values and standard deviation

A similar assay is carried out also for **5µM Apt2** in presence of **116.67µM PT1**. **AGEs** fixed concentration of **150µg/ml** in PBS is the result of an optimization in order to have a clear visual output. To ensure reproducibility, every analysis is repeated in three independent trials; then, every bar graph is a mean of the values and standard deviation of the results is included. Results are shown in Figure 4.3. AGE1, AGE4 and AGE5 are best detected; RGB analysis and Delta-E values are further evidences of this result.

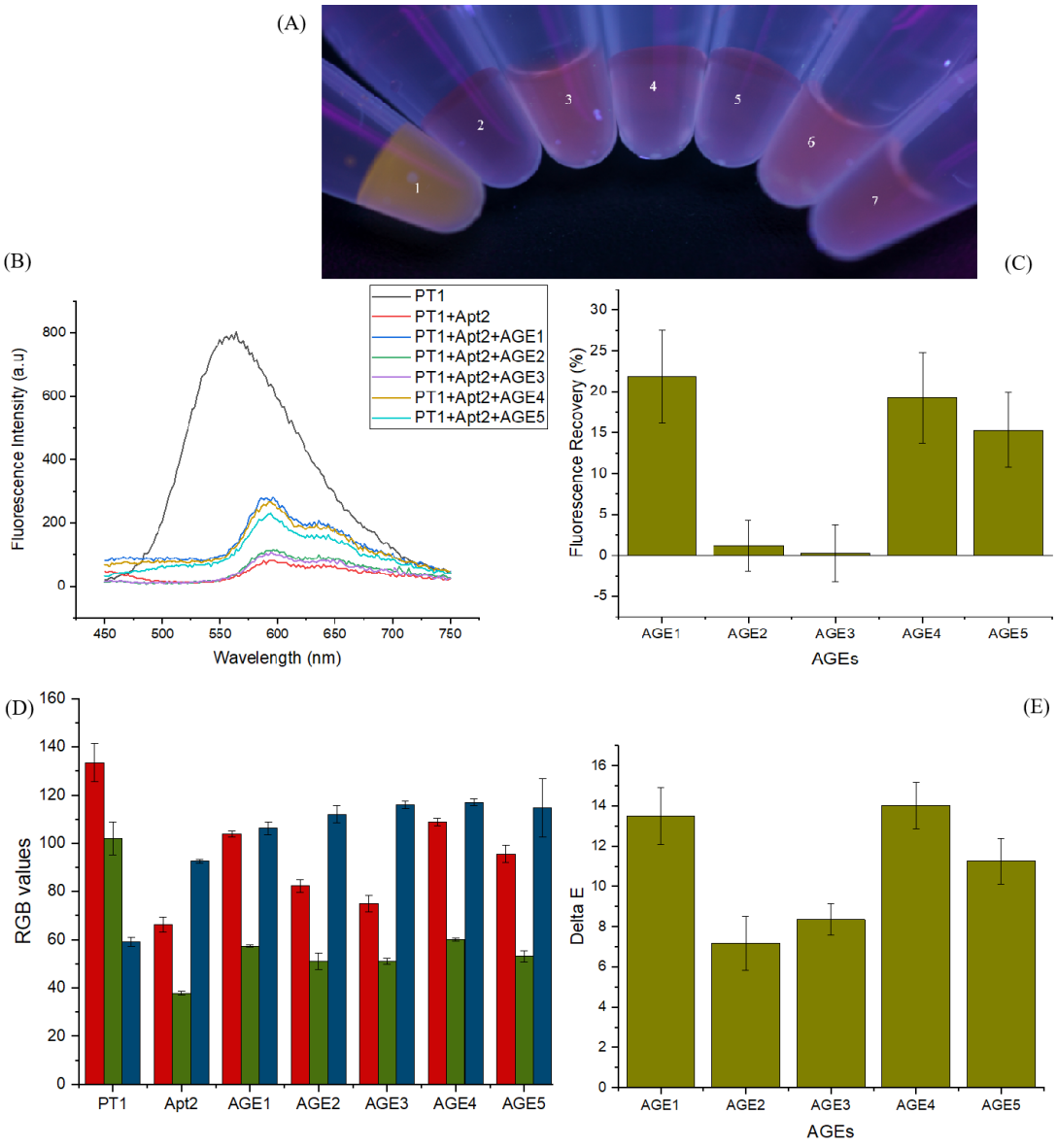

Figure 4.3 - 150µg/ml AGEs detection in 116.67µM PT1 and in presence of 5µM Apt2 (A) Vials (B) Fluorescence Intensity spectra (C) Fluoresce Recovery mean values and standard deviation (D) RGB mean values and standard deviation (E) Delta-E mean values and standard deviation

A similar assay is carried out also for **10µM Apt3** in presence of **116.67µM PT1**. **AGEs** fixed concentration of **150µg/ml** in PBS is the result of an optimization in order to have a clear visual output. To ensure reproducibility, every analysis is repeated in three independent trials; then, every bar graph is a mean of the values and standard deviation of the results is included. Results are shown in Figure 4.4. AGE1, AGE4 and AGE5 are best detected; RGB analysis and Delta-E values are further evidences of this result. In this case AGE1 has intrinsic fluorescence and a high peak at very low wavelengths is detected. However, this peak is not of this project interest.

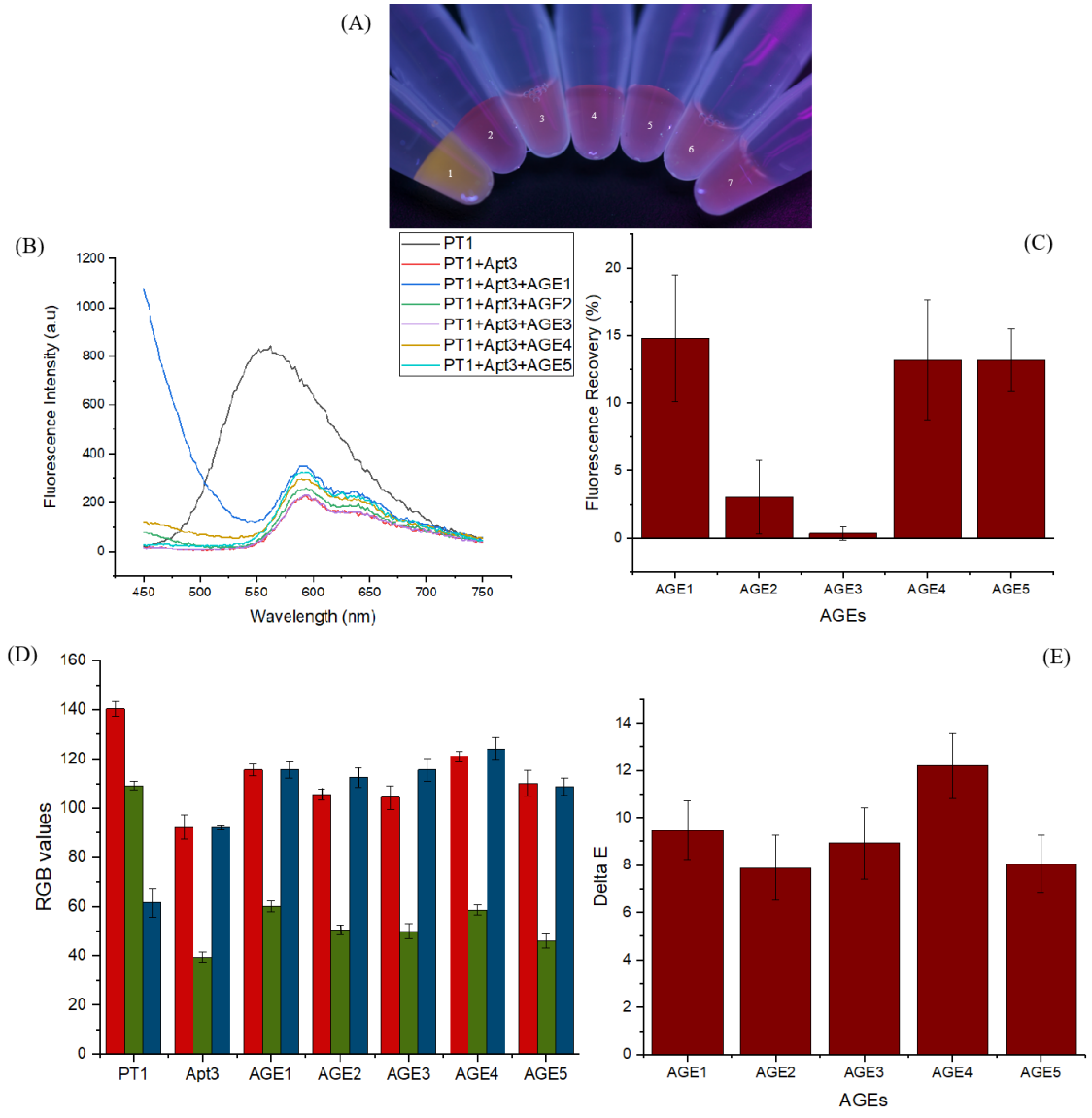

Figure 4.4 - 150µg/ml AGEs detection in 116.67µM PT1 and in presence of 10µM Apt3 (A) Vials (B) Fluorescence Intensity spectra (C) Fluoresce Recovery mean values and standard deviation (D) RGB mean values and standard deviation (E) Delta-E mean values and standard deviation

A similar assay is carried out also for **10µM Apt4** in presence of **116.67µM PT1**. **AGEs** fixed concentration of **150µg/ml** in PBS is the result of an optimization in order to have a clear visual output. To ensure reproducibility, every analysis is repeated in three independent trials; then, every bar graph is a mean of the values and standard deviation of the results is included. Results are shown in Figure 4.5. AGE1 and AGE4 are best detected; RGB analysis and Delta-E values are further evidences of this result.

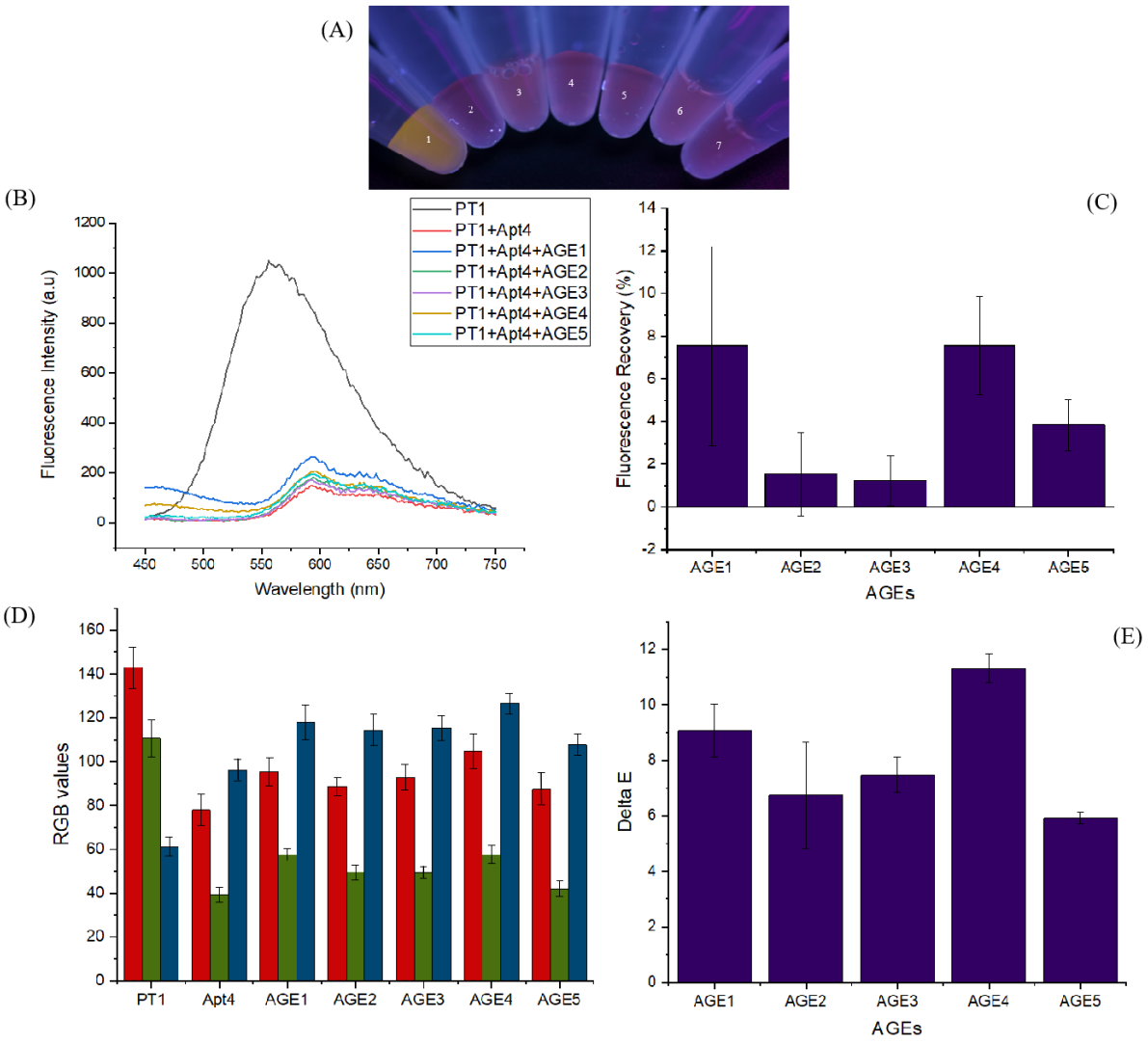

Figure 4.5 - 150µg/ml AGEs detection in 116.67µM PT1 and in presence of 10µM Apt4 (A) Vials (B) Fluorescence Intensity spectra (C) Fluoresce Recovery mean values and standard deviation (D) RGB mean values and standard deviation (E) Delta-E mean values and standard deviation

A similar assay is carried out also for **10µM Apt1** in presence of **300µM (stock) PTsyn**. **AGEs** fixed concentration of **150µg/ml** in DI is the result of an optimization in order to have a clear visual output. To ensure reproducibility, every analysis is repeated in three independent trials; then, every bar graph is a mean of the values and standard deviation of the results is included. Results are shown in Figure 4.6. AGE1, AGE3 and AGE2 are best detected; RGB analysis and Delta-E values are further evidences of this result. In this case the high peak at very low wavelengths is detected in correspondence of Apt1; it is believed to be a measurement error and for this reason is not of this project interest.

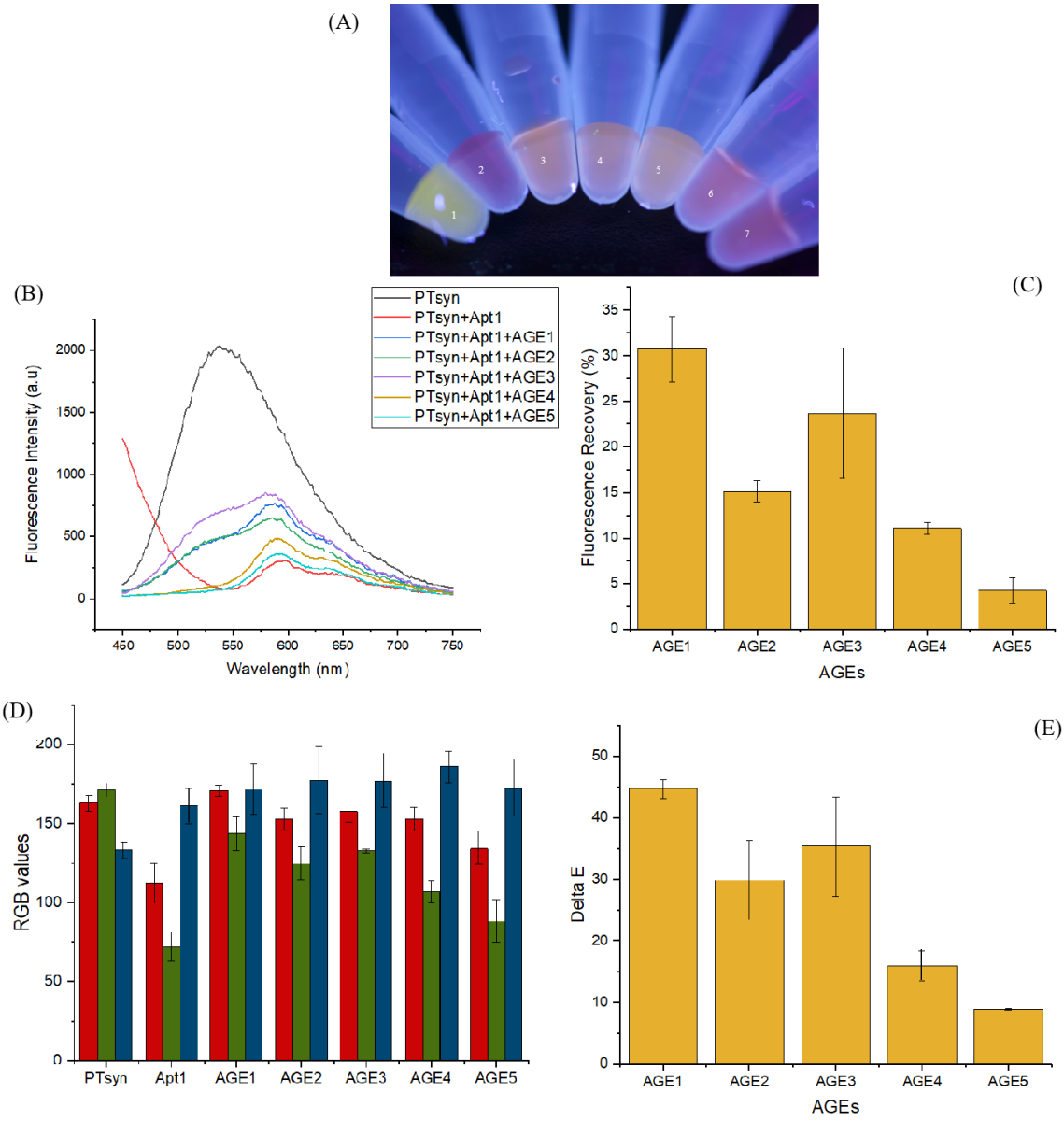

Figure 4.6 - 150µg/ml AGEs detection in 300µM PTsyn and in presence of 10µM Apt1 (A) Vials (B) Fluorescence Intensity spectra (C) Fluoresce Recovery mean values and standard deviation (D) RGB mean values and standard deviation (E) Delta-E mean values and standard deviation

A similar assay is carried out also for **5µM Apt2** in presence of **300µM (stock) PTsyn**. **AGEs** fixed concentration of **150µg/ml** in DI is the result of an optimization in order to have a clear visual output. To ensure reproducibility, every analysis is repeated in three independent trials; then, every bar graph is a mean of the values and standard deviation of the results is included. Results are shown in Figure 4.7. AGE3, AGE1 and AGE2 are best detected; RGB analysis and Delta-E values are further evidences of this result.

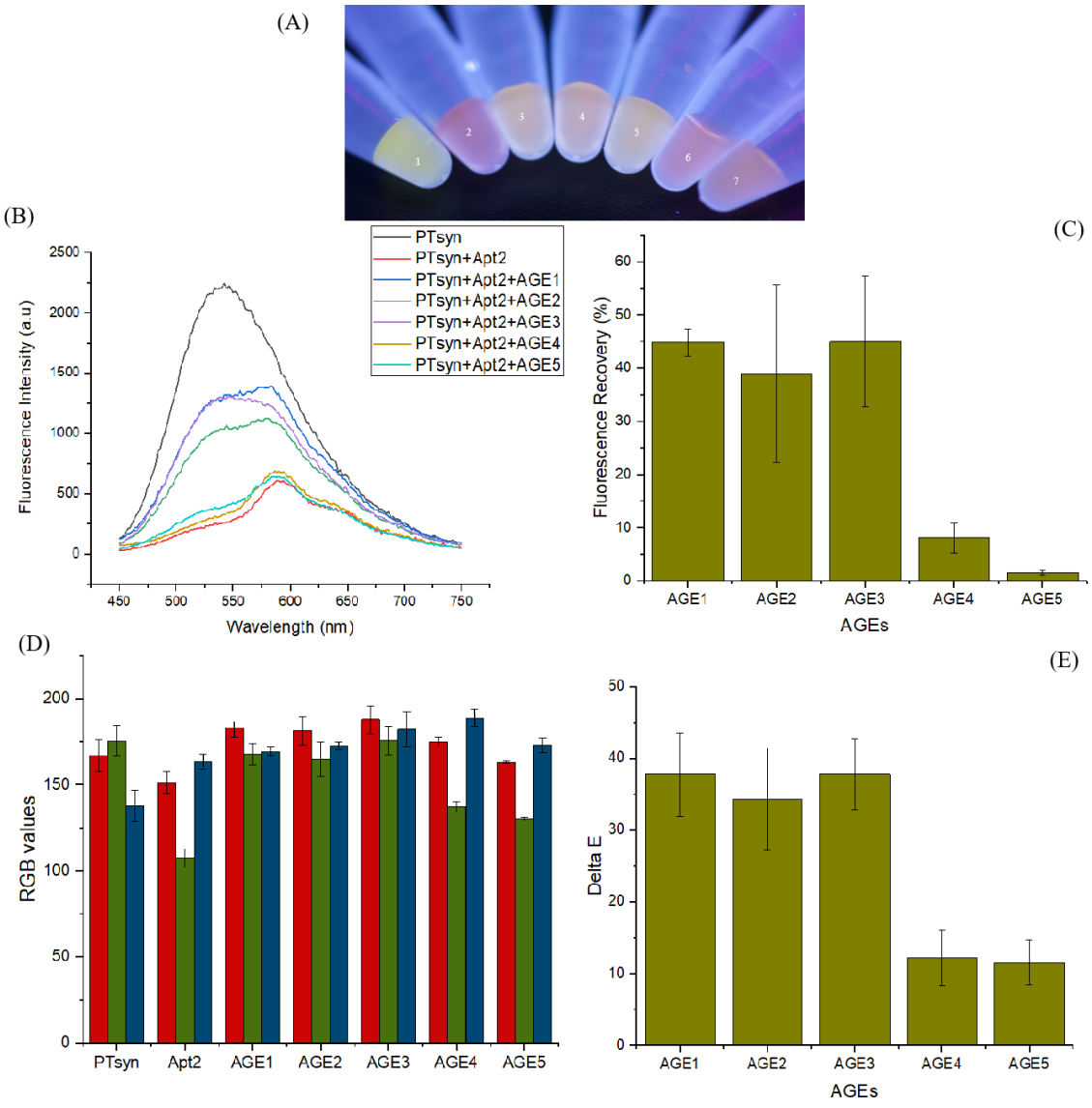

Figure 4.7 - 150µg/ml AGEs detection in 300µM PTsyn and in presence of 5µM Apt2 (A) Vials (B) Fluorescence Intensity spectra (C) Fluoresce Recovery mean values and standard deviation (D) RGB mean values and standard deviation (E) Delta-E mean values and standard deviation

A similar assay is carried out also for **5µM Apt3** in presence of **300µM (stock) PTsyn**. **AGEs** fixed concentration of **150µg/ml** in DI is the result of an optimization in order to have a clear visual output. To ensure reproducibility, every analysis is repeated in three independent trials; then, every bar graph is a mean of the values and standard deviation of the results is included. Results are shown in Figure 4.8. AGE3, AGE2 and AGE1 are best detected; RGB analysis and Delta-E values are further evidences of this result.

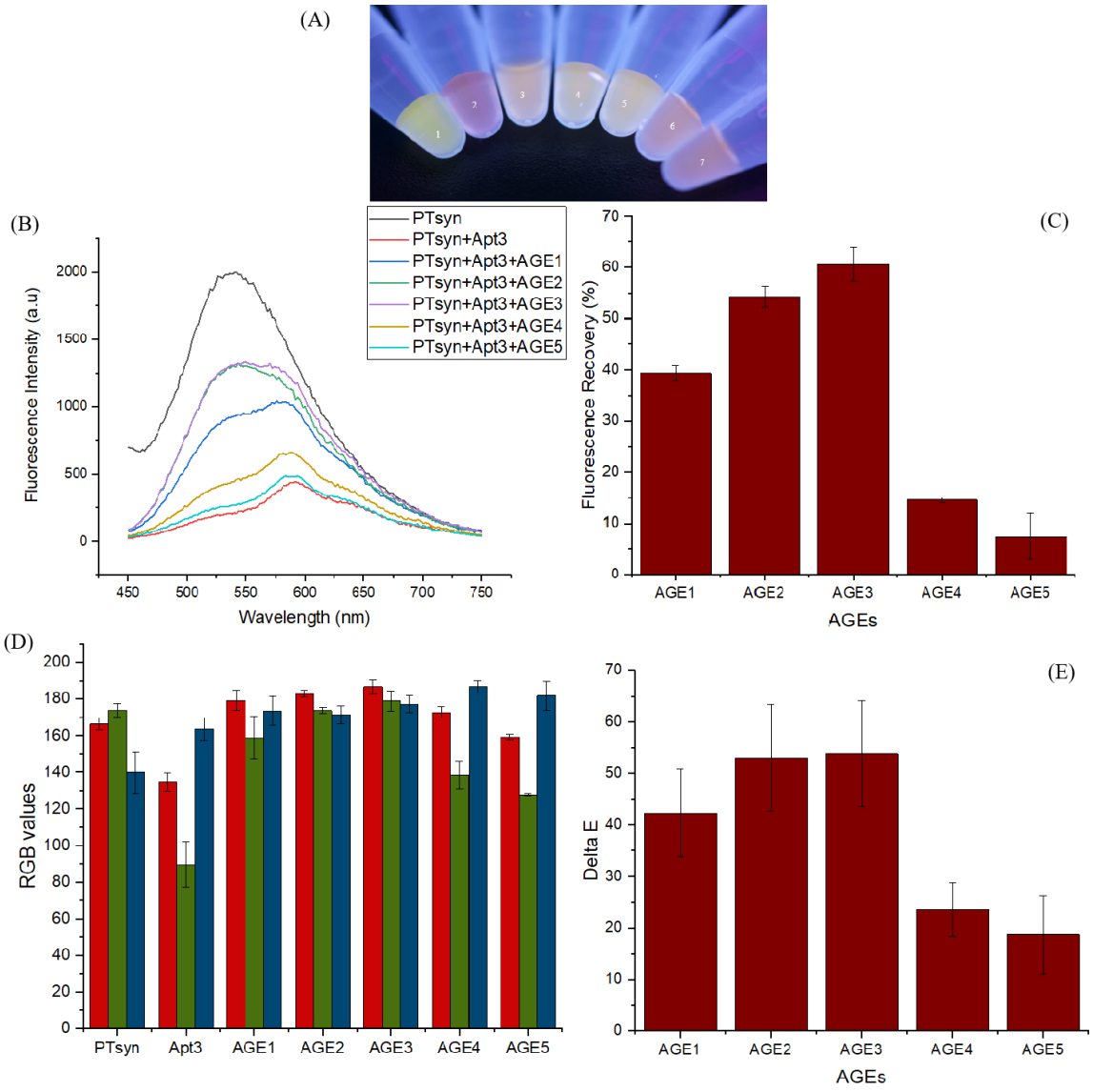

Figure 4.8 - 150µg/ml AGEs detection in 300µM PTsyn and in presence of 5µM Apt3 (A) Vials (B) Fluorescence Intensity spectra (C) Fluoresce Recovery mean values and standard deviation (D) RGB mean values and standard deviation (E) Delta-E mean values and standard deviation

A similar assay is carried out also for **10µM Apt4** in presence of **300µM (stock) PTsyn**. **AGEs** fixed concentration of **150µg/ml** in DI is the result of an optimization in order to have a clear visual output. To ensure reproducibility, every analysis is repeated in three independent trials; then, every bar graph is a mean of the values and standard deviation of the results is included. Results are shown in Figure 4.9. AGE1, AGE2 and AGE3 are best detected; RGB analysis and Delta-E values are further evidences of this result.

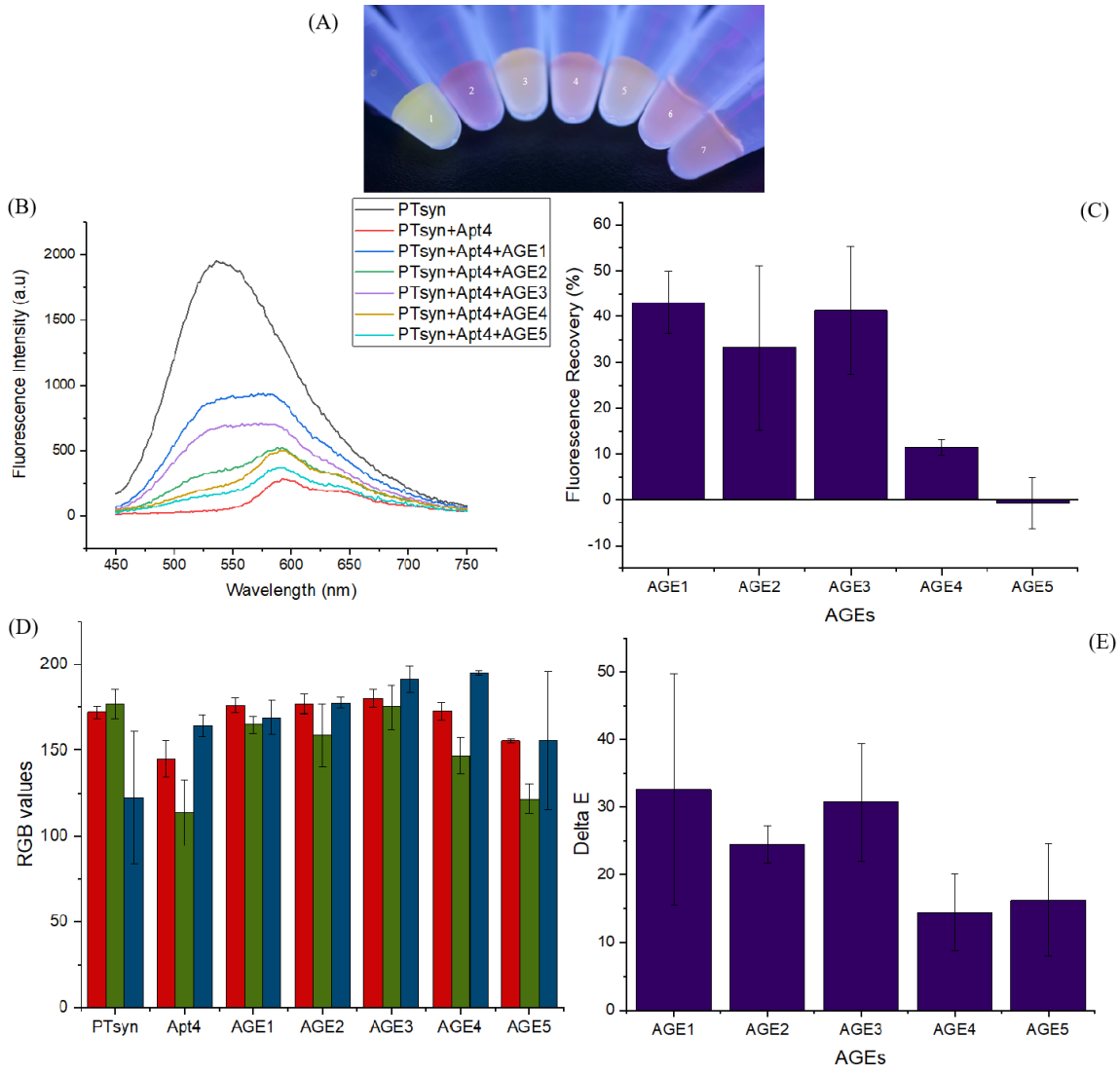

Figure 4.9 - 150µg/ml AGEs detection in 300µM PTsyn and in presence of 10µM Apt4 (A) Vials (B) Fluorescence Intensity spectra (C) Fluoresce Recovery mean values and standard deviation (D) RGB mean values and standard deviation (E) Delta-E mean values and standard deviation

A similar assay is carried out also for **10µM Apt1** in presence of **50µM PTG**. Excitation wavelength for PTG is 420nm. **AGEs** fixed concentration of **150µg/ml** in DI is the result of an optimization in order to have a clear visual output. To ensure reproducibility, every analysis is repeated in two independent trials; then, every bar graph is a mean of the values and standard deviation of the results is included. Results are shown in Figure 4.10. AGE4 is best detected; RGB analysis and Delta-E values are further evidences of this result.

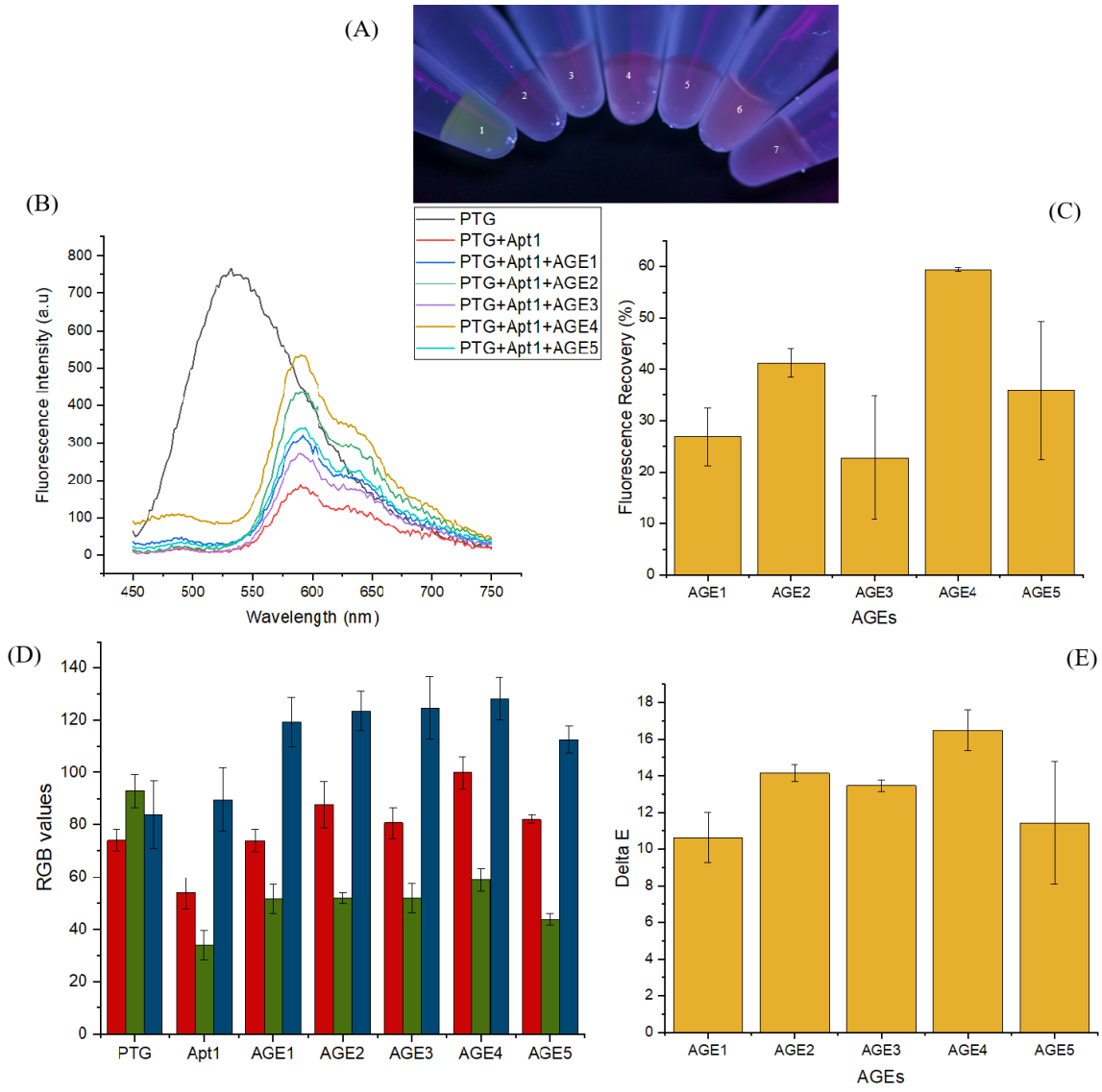

Figure 4.10 - 150µg/ml AGEs detection in 50µM PTG and in presence of 10µM Apt1 (A) Vials (B) Fluorescence Intensity spectra (C) Fluoresce Recovery mean values and standard deviation (D) RGB mean values and standard deviation (E) Delta-E mean values and standard deviation

A similar assay is carried out also for **5µM Apt2** in presence of **50µM PTG**. Excitation wavelength for PTG is 420nm. **AGEs** fixed concentration of **150µg/ml** in DI is the result of an optimization in order to have a clear visual output. To ensure reproducibility, every analysis is repeated in three independent trials; then, every bar graph is a mean of the values and standard deviation of the results is included. Results are shown in Figure 4.11. AGE4 is best detected; RGB analysis and Delta-E values are further evidences of this result.

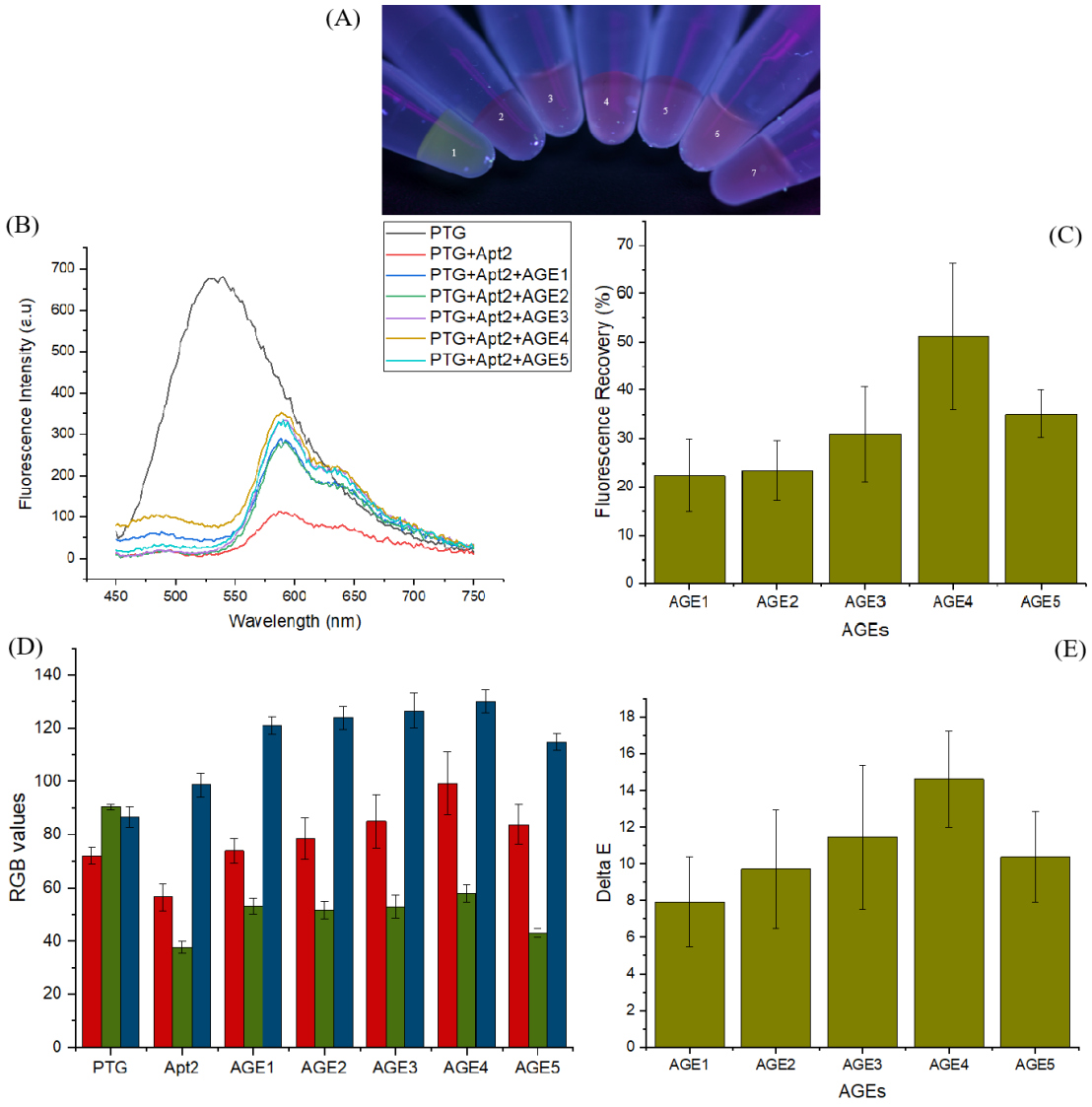

Figure 4.11 - 150µg/ml AGEs detection in 50µM PTG and in presence of 5µM Apt2 (A) Vials (B) Fluorescence Intensity spectra (C) Fluoresce Recovery mean values and standard deviation (D) RGB mean values and standard deviation (E) Delta-E mean values and standard deviation

A similar assay is carried out also for **5µM Apt3** in presence of **50µM PTG**. Excitation wavelength for PTG is 420nm. **AGEs** fixed concentration of **150µg/ml** in DI is the result of an optimization in order to have a clear visual output. To ensure reproducibility, every analysis is repeated in three independent trials; then, every bar graph is a mean of the values and standard deviation of the results is included. Results are shown in Figure 4.12. AGE4 and AGE2 are best detected; RGB analysis and Delta-E values are further evidences of this result.

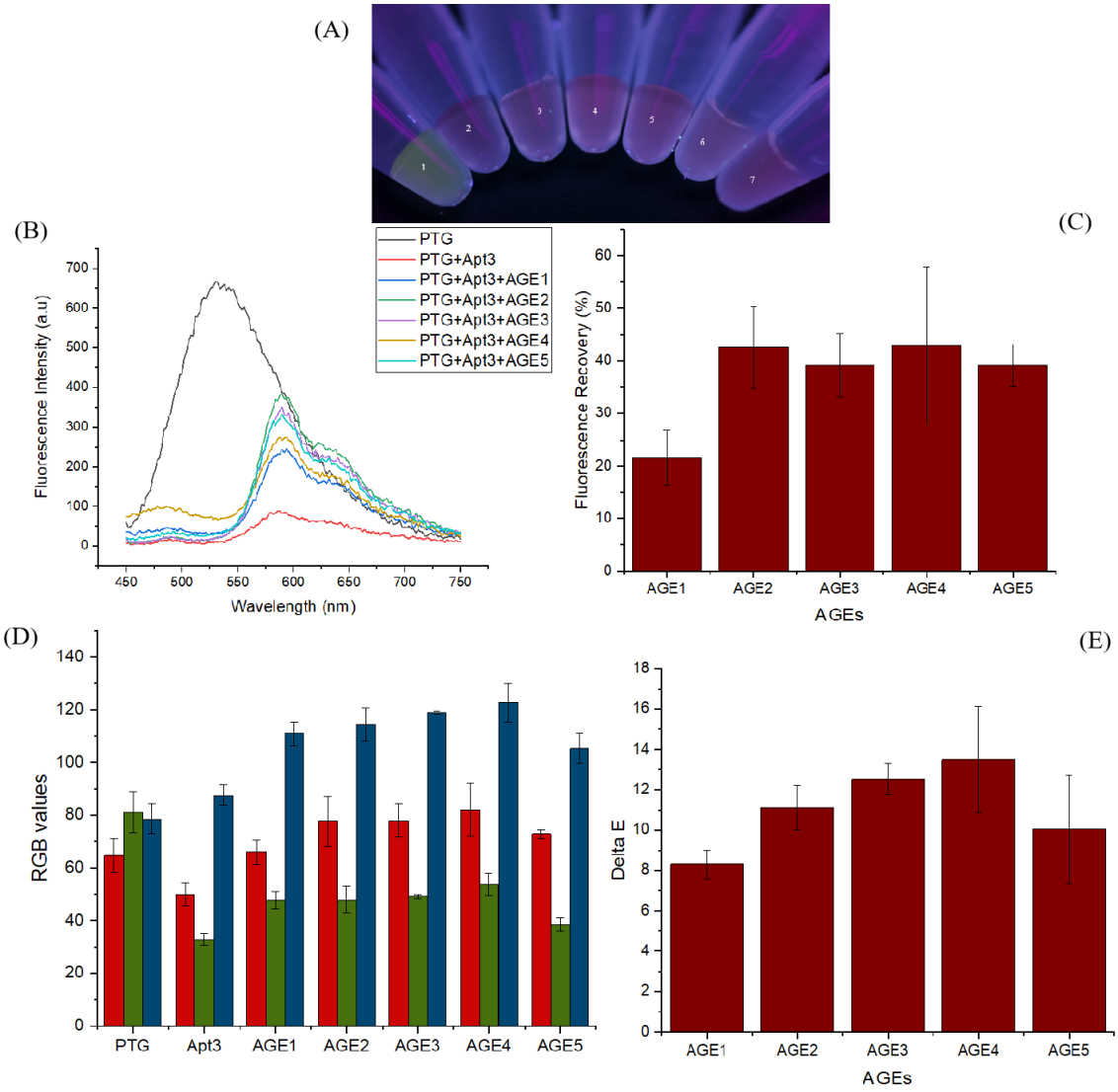

Figure 4.12 - 150µg/ml AGEs detection in 50µM PTG and in presence of 5µM Apt3 (A) Vials (B) Fluorescence Intensity spectra (C) Fluoresce Recovery mean values and standard deviation (D) RGB mean values and standard deviation (E) Delta-E mean values and standard deviation

A similar assay is carried out also for **10µM Apt4** in presence of **50µM PTG**. Excitation wavelength for PTG is 420nm. **AGEs** fixed concentration of **150µg/ml** in DI is the result of an optimization in order to have a clear visual output. To ensure reproducibility, every analysis is repeated in three independent trials; then, every bar graph is a mean of the values and standard deviation of the results is included. Results are shown in Figure 4.13. AGE4 and AGE3 are best detected; RGB analysis and Delta-E values are further evidences of this result.

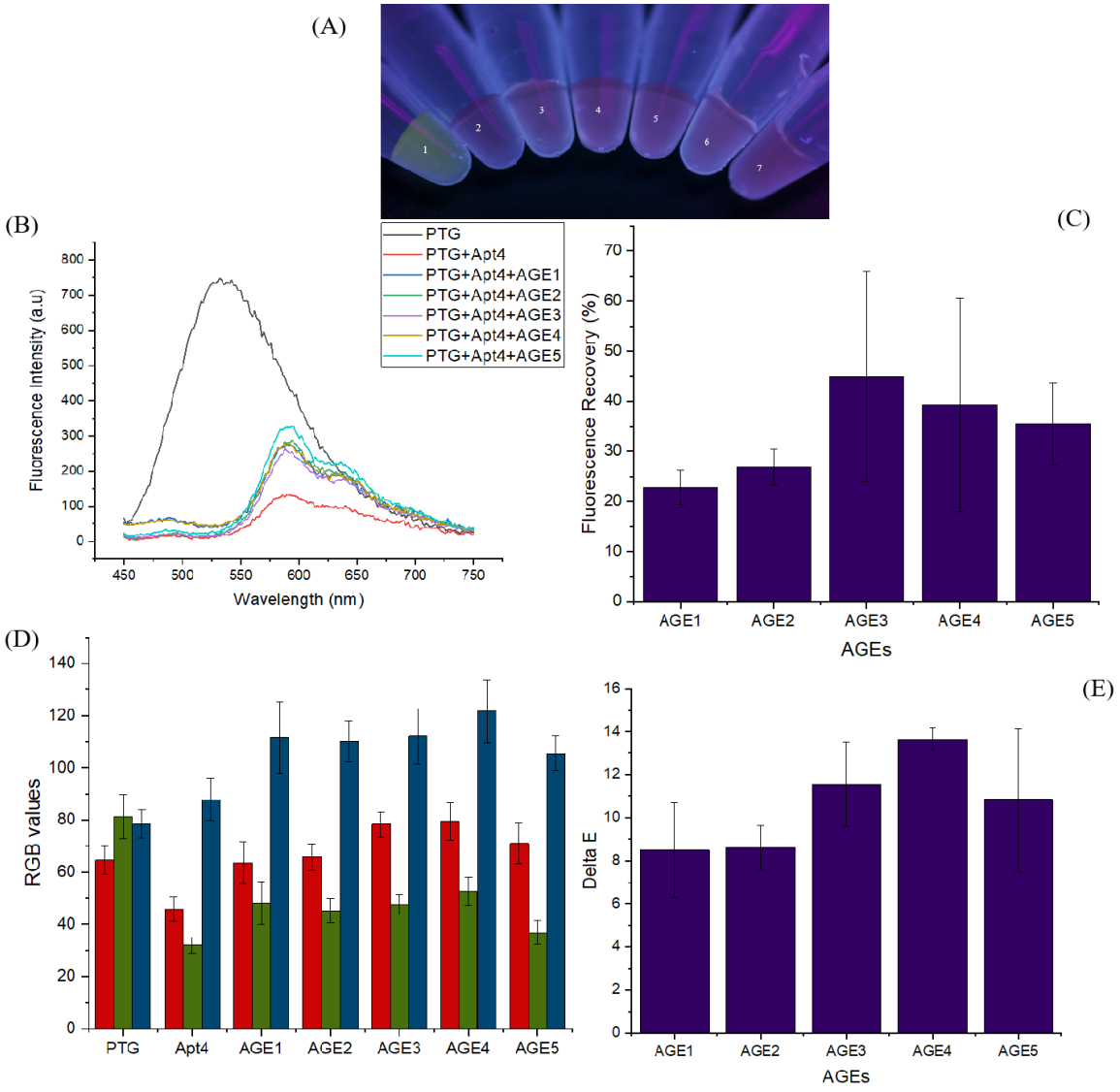

Figure 4.13 - 150µg/ml AGEs detection in 50µM PTG and in presence of 10µM Apt4 (A) Vials (B) Fluorescence Intensity spectra (C) Fluoresce Recovery mean values and standard deviation (D) RGB mean values and standard deviation (E) Delta-E mean values and standard deviation

A similar assay is carried out also for **20µM Apt1** in presence of **300µM PT5**. **AGEs** fixed concentration of **150µg/ml** in DI is the result of an optimization in order to have a clear visual output. To ensure reproducibility, every analysis is repeated in three independent trials; then, every bar graph is a mean of the values and standard deviation of the results is included. Results are shown in Figure 4.14. AGE1 is best detected; RGB analysis and Delta-E values are further evidences of this result.

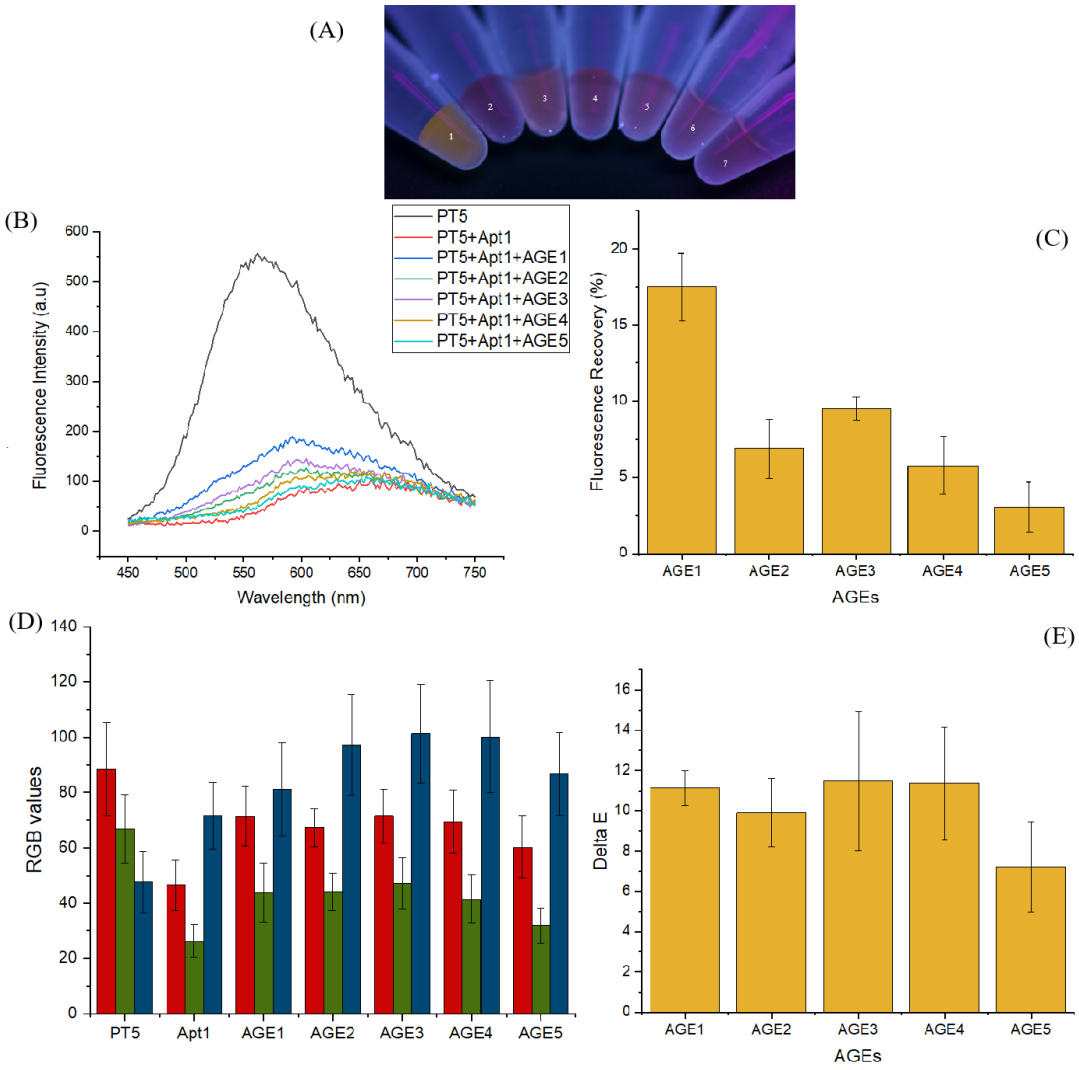

Figure 4.14 - 150µg/ml AGEs detection in 300µM PT5 and in presence of 20µM Apt1 (A) Vials (B) Fluorescence Intensity spectra (C) Fluoresce Recovery mean values and standard deviation (D) RGB mean values and standard deviation (E) Delta-E mean values and standard deviation

A similar assay is carried out also for **15µM Apt2** in presence of **300µM PT5**. **AGEs** fixed concentration of **150µg/ml** in DI is the result of an optimization in order to have a clear visual output. To ensure reproducibility, every analysis is repeated in three independent trials; then, every bar graph is a mean of the values and standard deviation of the results is included. Results are shown in Figure 4.15. AGE1 is best detected; RGB analysis and Delta-E values are further evidences of this result.

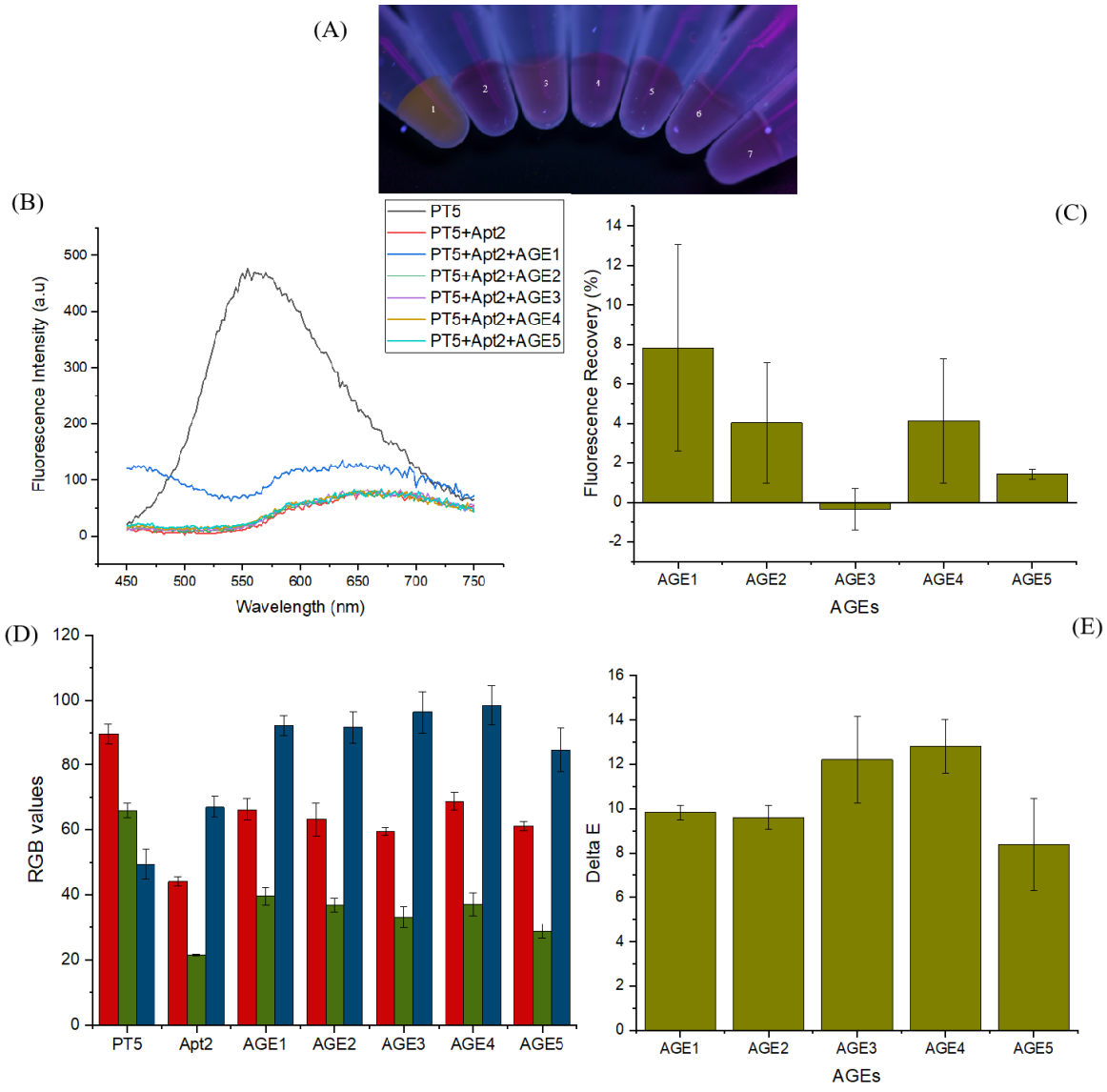

Figure 4.15 - 150µg/ml AGEs detection in 300µM PT5 and in presence of 15µM Apt2 (A) Vials (B) Fluorescence Intensity spectra (C) Fluoresce Recovery mean values and standard deviation (D) RGB mean values and standard deviation (E) Delta-E mean values and standard deviation

A similar assay is carried out also for **15µM Apt3** in presence of **300µM PT5**. **AGEs** fixed concentration of **150µg/ml** in DI is the result of an optimization in order to have a clear visual output. To ensure reproducibility, every analysis is repeated in three independent trials; then, every bar graph is a mean of the values and standard deviation of the results is included. Results are shown in Figure 4.16. AGE1 is best detected; RGB analysis and Delta-E values are further evidences of this result.

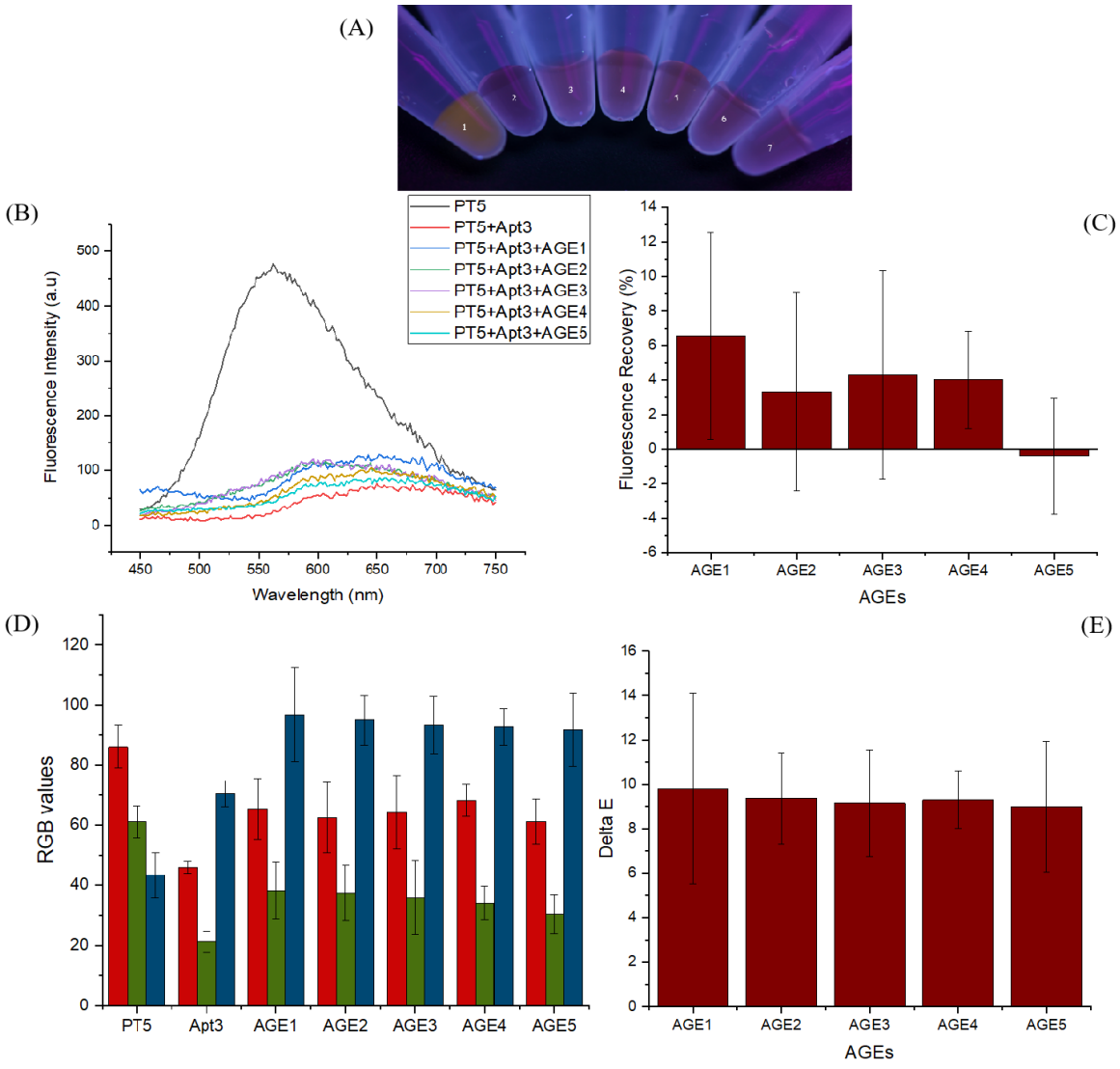

Figure 4.16 - 150µg/ml AGEs detection in 300µM PT5 and in presence of 15µM Apt3 (A) Vials (B) Fluorescence Intensity spectra (C) Fluoresce Recovery mean values and standard deviation (D) RGB mean values and standard deviation (E) Delta-E mean values and standard deviation

A similar assay is carried out also for **20µM Apt4** in presence of **300µM PT5**. **AGEs** fixed concentration of **150µg/ml** in DI is the result of an optimization in order to have a clear visual output. To ensure reproducibility, every analysis is repeated in three independent trials; then, every bar graph is a mean of the values and standard deviation of the results is included. Results are shown in Figure 4.17. AGE1 is best detected; RGB analysis and Delta-E values are further evidences of this result.

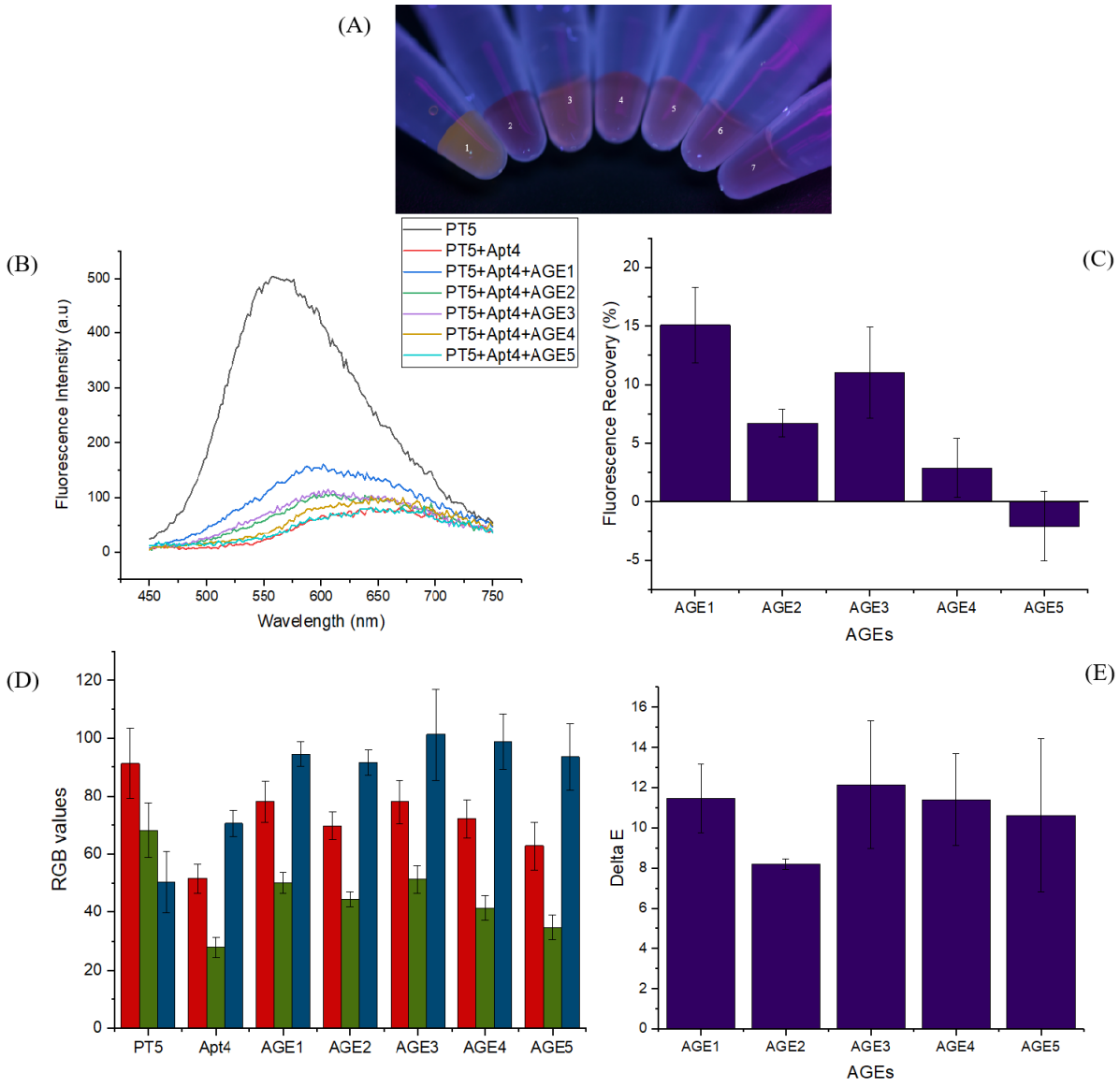

Figure 4.17 - 150µg/ml AGEs detection in 300µM PT5 and in presence of 20µM Apt4 (A) Vials (B) Fluorescence Intensity spectra (C) Fluoresce Recovery mean values and standard deviation (D) RGB mean values and standard deviation (E) Delta-E mean values and standard deviation

4.1.1 SUMMARY

Both numerical and optical results depend on the particular structure of the polythiophenes and their functional groups.

The best detected AGEs are, respectively, in descending order:

- 116.67µM **PT1** + 10µM **Apt1** present best detection of 150µg/ml **AGE1**, **AGE4** and **AGE5**
- 116.67µM **PT1** + 5µM **Apt2** present best detection of 150µg/ml **AGE1**, **AGE4** and **AGE5**
- 116.67µM **PT1** + 10µM **Apt3** present best detection of 150µg/ml **AGE1**, **AGE4** and **AGE5**
- 116.67µM **PT1** + 10µM **Apt4** present best detection of 150µg/ml **AGE1** and **AGE4**

- 300µM **PTsyn** + 10µM **Apt1** present best detection of 150µg/ml **AGE1**, **AGE3** and **AGE2**
- 300µM **PTsyn** + 5µM **Apt2** present best detection of 150µg/ml **AGE3**, **AGE1** and **AGE2**
- 300µM **PTsyn** + 5µM **Apt3** present best detection of 150µg/ml **AGE3**, **AGE2** and **AGE1**
- 300µM **PTsyn** + 10µM **Apt4** present best detection of 150µg/ml **AGE3**, **AGE1** and **AGE2**

- 50µM **PTG** + 10µM **Apt1** present best detection of 150µg/ml **AGE4**
- 50µM **PTG** + 5µM **Apt2** present best detection of 150µg/ml **AGE4**
- 50µM **PTG** + 5µM **Apt3** present best detection of 150µg/ml **AGE4** and **AGE2**
- 50µM **PTG** + 10µM **Apt4** present best detection of 150µg/ml **AGE3** and **AGE4**

- 300µM **PT5** + 20µM **Apt1** present best detection of 150µg/ml **AGE1**
- 300µM **PT5** + 15µM **Apt2** present best detection of 150µg/ml **AGE1**
- 300µM **PT5** + 15µM **Apt3** present best detection of 150µg/ml **AGE1**

- 300µM **PT5** + 20µM **Apt4** present best detection of 150µg/ml **AGE1** and **AGE3**

PTG and **PT5** are highly unstable polymers most probably due to rapid degradation they undergo after UV light exposition; this is the reason why the error bars are significantly wide (i.e. standard deviation values are far from zero). Reproducibility of the results is not guaranteed and for this reason they are not further studied in their limit of detection, in plasma or on PVDF membranes.

PTsyn has not shown any response in plasma and on PVDF membranes, even if showed highly bright (therefore distinguishable) responses due to its particular structure; it is believed that most probably suffered UV light degradation.

4.2 SELECTIVITY STUDIES

Selectivity in this solution-based assay is assessed using other proteins, sugars or other interfering molecules that may be present in human samples. The best detected AGE, in presence of the aptamer, for each polythiophene, in the respective optimized concentrations, is used as the control sample. In order to give a proper comparison between the different polymers at varying AGE detected, it is been chosen to keep the aptamer variable constant, fixing Apt1 as the only one studied. In Chapter 5 it will be proved that in this project there is no differentiation between aptamers for AGEs detection purposes. It is possible to immediately see a difference in colour between the picked-out AGE and the other molecules, meaning that AGE is exclusively detected by the polythiophene in presence of an aptamer, even in a complex system. For each polymer a high fluorescence recovery (more than 5%) is registered in presence of AGE, while small to negligible fluorescence recovery (less than 5%) is observed upon addition of other molecules.
The samples are placed under UV illumination zone and digital images are taken using a SONY camera at a fixed distance; the images are then analysed using ImageJ software, 100x100 pixels are used to carry out RGB and delta E analysis. Apt-AGE mixture is incubated 30 minutes.

The considered interfering molecules are:
A – Hemoglobin from bovine blood – 1mg/ml
B – Glucose – 1mg/ml
C – Glycolaldehyde dimer – 1mg/ml
D – y-Globulins from bovine blood – 1mg/ml
E – DL. Glyceraldehyde – 1mg/ml
F – Fibrinogen from human plasma – 1mg/ml
G – Albumin serum bovine – 1mg/ml
H – Methylglyoxal solution – 1mg/ml

Referring to Figure 4.18, for **PT1 AGE1** is, among other AGEs, the one that shows higher fluorescence recovery and in particular, in presence of **Apt1**.

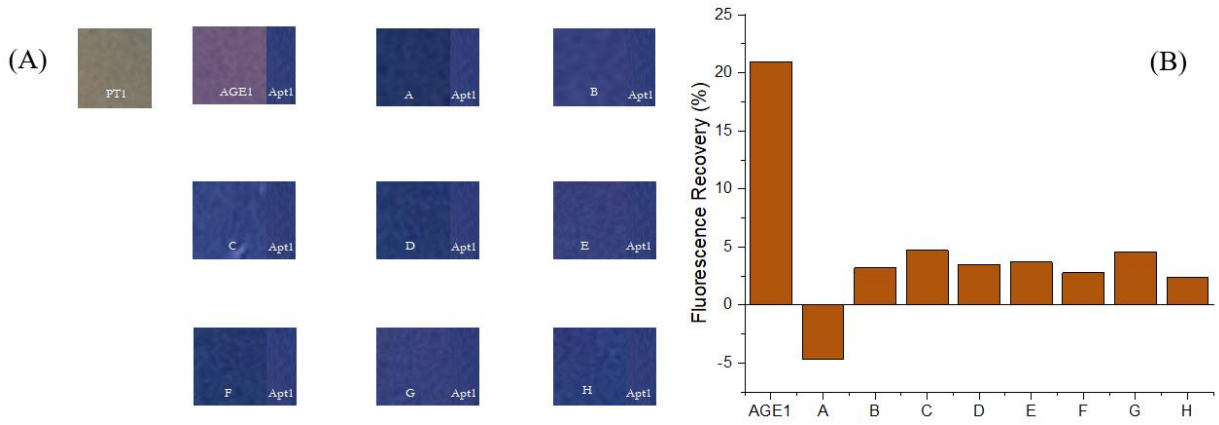

Figure 4.18 - Selectivity for PT1 (A) Colour array of AGE1 and interfering molecules in presence of Apt1 (B) Fluorescence recovery graph

A similar study is carried out also for **PTsyn**; **AGE3** is showing best results in terms of fluorescence recovery. Results are shown in Figure 4.19 in presence of **Apt1**.

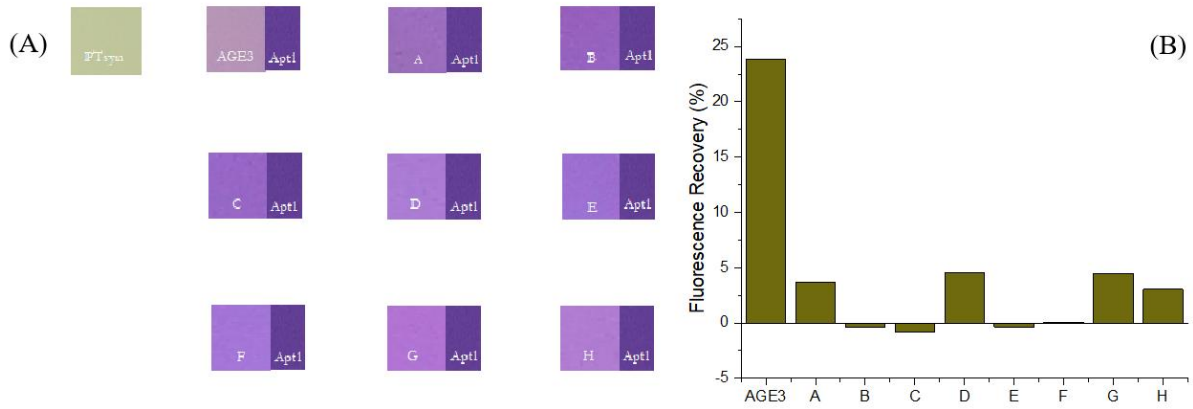

Figure 4.19 - Selectivity for PTsyn (A) Colour array of AGE3 and interfering molecules in presence of Apt1 (B) Fluorescence recovery graph

A similar study is carried out also for **PTG**; **AGE4** is showing best results in terms of fluorescence recovery in presence of **Apt1**. However, PTG has undergone degradation in a small range of time, leading to unreliable outputs: selectivity study failed and the related colorimetric array, indeed, does not show any significant colour change. Results are shown in Figure 4.20.

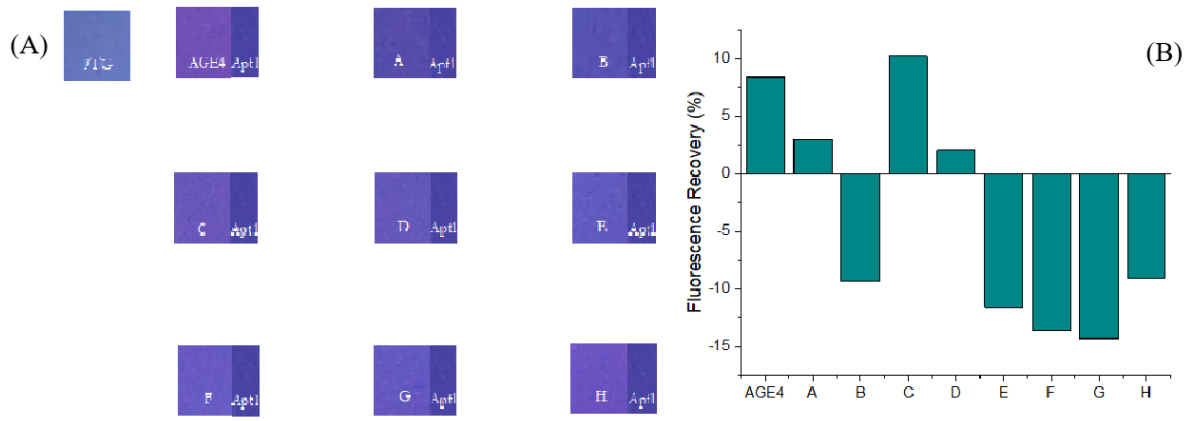

Figure 4.20 - Selectivity for PTG (A) Colour array of AGE4 and interfering molecules in presence of Apt1 (B) Fluorescence recovery graph

A similar study is carried out also for **PT5**; **AGE1** is showing best results in terms of fluorescence recovery in presence of **Apt1**. Results are shown in Figure 4.21.

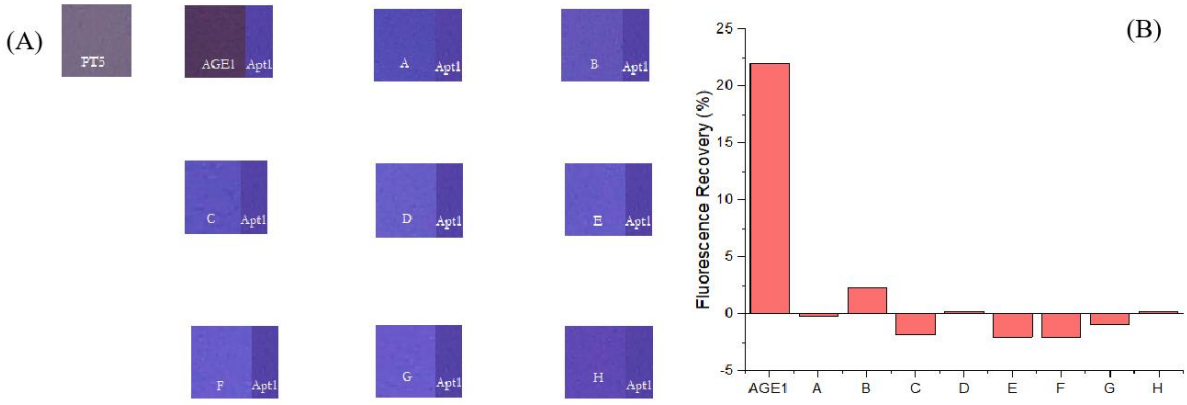

Figure 4.21 - Selectivity for PT5 (A) Colour array of AGE1 and interfering molecules in presence of Apt1 (B) Fluorescence recovery graph

4.3 LIMIT OF DETECTION

For **116.67µM PT1** in presence of **10µM Apt1**, different **AGE1** concentrations both in buffer (PBS) and plasma are analysed. Analysis carried out in PBS corresponds to the optimization of AGEs concentration in the overall assay in such a way that 150µg/ml is the optimal concentration of the biomarker in order to have a significant visual response. In order to ensure reproducibility, the survey is conducted in three independent trials. The samples are placed under UV illumination zone and digital images are taken using a SONY camera at a fixed distance; the images are then analysed using ImageJ software, 100x100 pixels are used to carry out RGB and delta E analysis. Apt1-AGE1 mixture is incubated 30 minutes.

Figure 4.22 (A) shows different colours of the samples due to various concentrations of AGE1 dissolved in PBS. Vial 1 contains only PT1 while vial 2 is the solution of PT1 and Apt1. As expected, the addition of the aptamer to the polymer solution cause the formation of duplex structure resulting in the quenching of the fluorescence intensity and a colour shift from yellow to red (red colour is perceived as purple, due to the blueish tone of the UV lamp) of about 36nm. The subsequent addition, in vial 3, of AGE1 to the PT1-Apt1 solution is responsible for the shift to pink colour. It is possible to notice in Figure 4.22 (B) that decreasing AGE1 concentrations, ranging from 300µg/ml (vial 3) to 1.5 µg/ml (vial 8), cause the colour change from pink to dark purple due to less i-motif structures formation: referring to Figure 4.22 (C), increasing AGE1 concentration, indeed, corresponds to higher possibility of i-motif complexes creation between AGE1 and Apt1 that hinders the planarization of the polymer. So, at increasing AGE1 concentration, higher fluorescence recovery is revealed. Figure 4.22 (D) shows further evidence of complex formation through RGB analysis via ImageJ software: there is a significant change in the R value (from 101.5 to 27.8) and in G value (from 106.5 to 51.3) after the addition of Apt1 to PT1. Subsequent addition of AGE1 to the solution cause reversion back of R value (103.5) and G value (112.3); however, at decreasing AGE1 concentrations, both R and G values decrease. Delta E measure is reported in Figure 4.22 (E): difference in colours can be distinguished among the vials. The correlation between delta E values and AGE1 concentration clearly shows that only from 3µg/ml the colours are visually distinguishable ($\Delta E > 2.3$).

The limit of detection (LOD) in PBS from fluorescence recovery measurements is about 2.43µg/ml, calculated from the linear fit: $y = 28.18145x - 10.86903$.

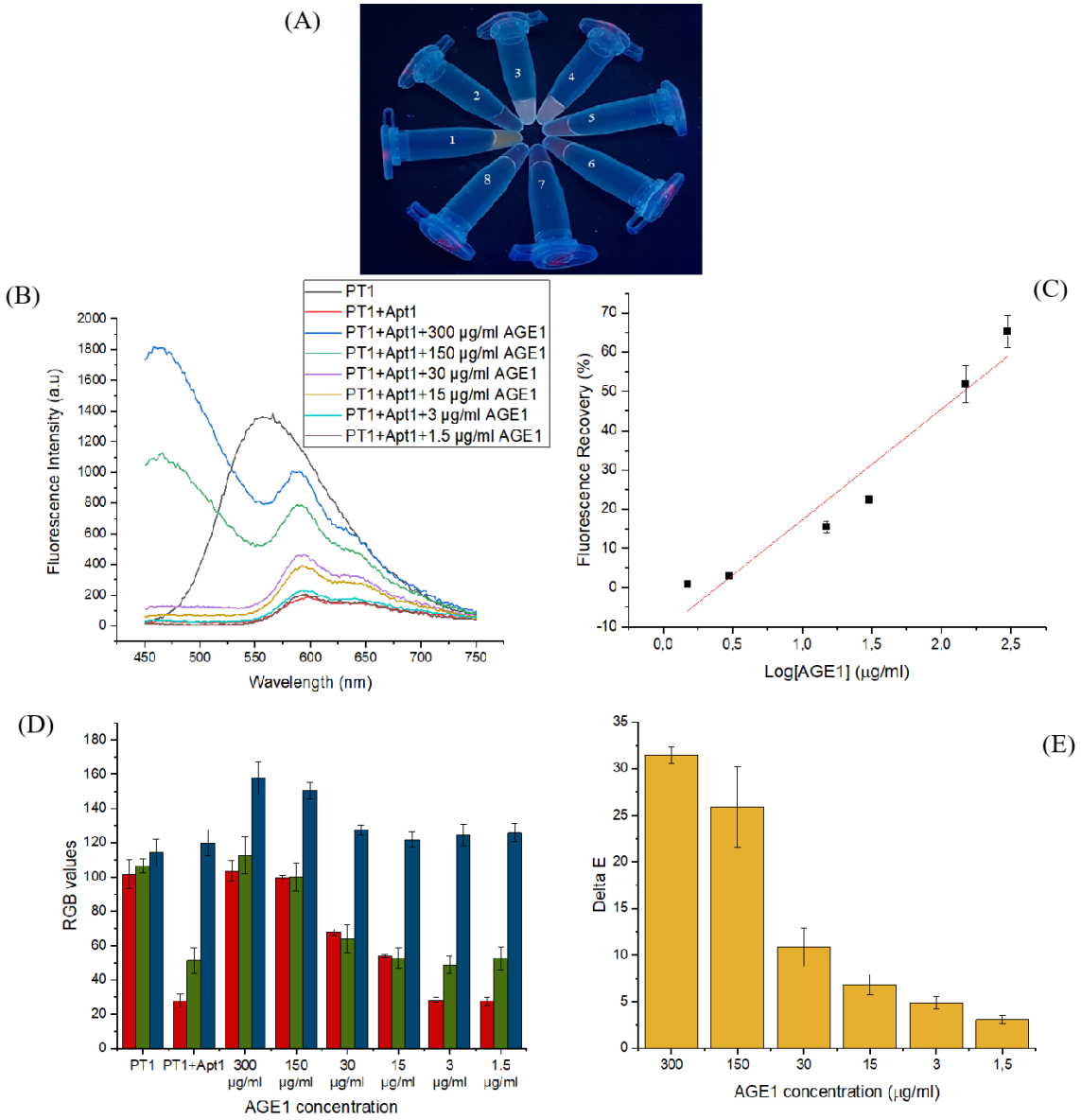

Figure 4.22 - Optical response of PT1 in presence of Apt1 and at different AGE1 concentrations in PBS (A) Vials (B) Fluorescence intensity spectra (C) Fluorescence recovery semi-logarithmic plot (D) RGB mean values and standard deviation (E) Delta E mean values and standard deviation

4.4 ANALYSIS IN PLASMA

The proposed process needs to be validated for clinical applications and, for this reason, different concentrations of **AGE1** in **116.67µM PT1** and **10µM Apt1** are investigated also in plasma, a more complex system with other interfering molecules. In order to ensure reproducibility, the survey is conducted in three independent trials. The samples are placed under UV illumination zone and digital images are taken using a SONY camera at a fixed distance; the images are then analysed using ImageJ software, 100x100 pixels are used to carry out RGB and delta E analysis. Apt1-AGE1 mixture is incubated 30 minutes.

As represented in Figure 4.23 (A) there are different colorimetric responses corresponding to the various concentrations of AGE1 dissolved in plasma. The colour of vial 1 shift, as expected, from yellow, corresponding to the random coil configuration of the polymer, to red, corresponding to the duplex formation between polymer and aptamer, in plasma solution (vial 2). The addition of PT1 to Apt1-AGE1 mixture (vial 3) cause the alteration in pink colour; in particular, a shift from pink to purple is visualized upon decreasing concentrations of AGE1 from 150µg/ml (vial 3) to 1.5 µg/ml (vial 7). Figure 4.23 (B) shows the significant quenching of fluorescence intensity related to the addition of the aptamer to the polymer, and subsequent reverting back upon increasing AGE1 concentration. Even in this case, as depicted in Figure 4.23 (C), increasing AGE1 concentration corresponds to higher possibility of i-motif complexes creation between AGE1 and Apt1 that hinders the planarization of the polymer. So, at increasing AGE1 concentration, higher fluorescence recovery is revealed. Further evidence of Apt1-AGE1 complex formation is given through RGB analysis, Figure 4.23 (D). Corresponding to the addition of the aptamer, there is a significant change of RGB values, that are then re-established upon addition of the AGE1, indicating the reset of the fluorescence recovery. RGB values also undergo variation at varying concentrations of AGE1. Figure 4.23 (E) illustrate delta E values that range from 3 to 22 in the set of concentration from 1.5 µg/ml to 150µg/ml, pointing that the colour difference between PT1-Apt1 complex and PT1-Apt1-AGE1 mixture can be clearly visually distinguished also in a complex system like plasma. However, delta E values are decreasing at decreasing marker concentration and vice versa. Even in this case, colours can be distinguished preferentially at higher biomarker concentrations (from 3µg/ml where $\Delta E > 2.3$) while the limit of detection (LOD) in plasma from fluorescence recovery measurement is around 1.5µg/ml in plasma, calculated from the linear fit:

$y = 17.01265x - 3.11443.$

So, this methodology can be used for the detection of AGEs at clinically relevant concentration ranges in plasma samples. Moreover, the addition of plasma shows an increase in the fluorescence intensity, but this does not interfere with the final outcome.

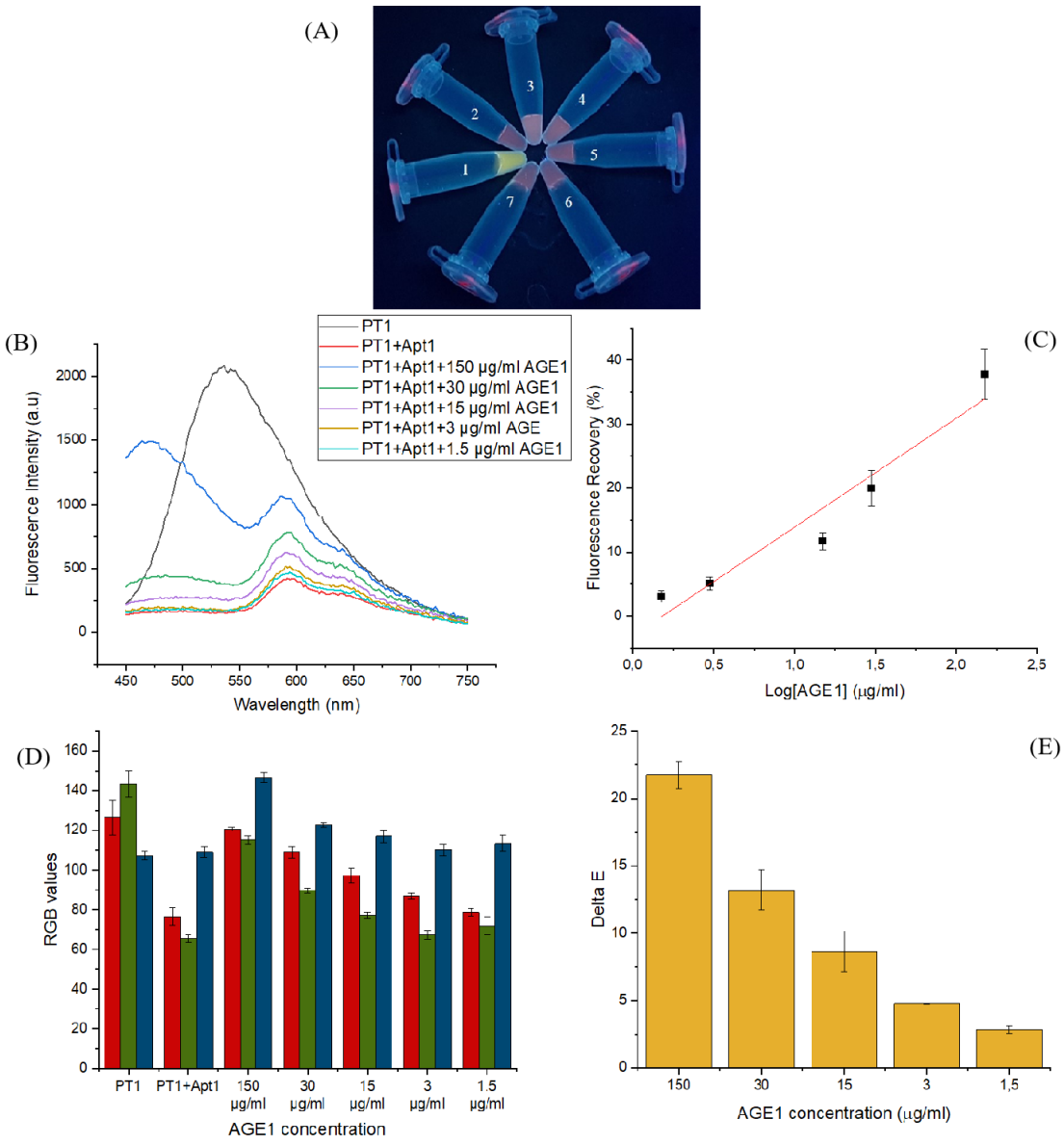

Figure 4.23 - Optical response of PT1 in presence of Apt1 and at different AGE1 concentrations in plasma (A) Vials (B) Fluorescence intensity spectra (C) Fluorescence recovery semi-logarithmic plot (D) RGB mean values and standard deviation (E) Delta E mean values and standard deviation

4.5 ANALYSIS ON PVDF MEMBRANE

Membranes allows various analytes to bound onto the surface by several mechanisms such as electrostatic, van der Waals (dipole induced), hydrogen bonding or hydrophobic interactions. Molecules immobilization requires membranes' small pore size and high porosity: this leads to slow wicking rate that allows the reagent to interact with the membrane in longer range of time [165].

Membranes with polyvinylidene (PVDF) are featured by high chemical strength and temperature resistance thanks to highly electronegative fluorine atoms on the membrane itself; for this reason, PVDF membranes are successfully used for diagnostics [166, 167]. They can be both hydrophilic and hydrophobic: the first has moderate capillary flow rate with low protein binding capacity, while the latter has very low capillary flow rate and high protein binding capacity [168]. **PT1** in presence of **10µM Apt1** is used to detect **150µg/ml** of **AGE4** biomarker on hydrophilic PVDF membranes. This is exclusively a preliminary study, in particular a colour-based study: different colours are detected and measured only through RGB and delta E analysis.

Tubes of 2µM PT1 in 0.01%Tween are centrifuged several times al 8000rpm for 3 minutes in order to optimize homogeneity of PT1 on PVDF membrane, followed by two washing cycles with DI water. Tween is a surfactant added to DI water in order to reduce non-specific binding and it showed, with respect to DI water, better and more coherent optical response, as shown in Figure 4.26. The samples are placed under UV illumination zone and digital images are taken using a SONY camera at a fixed distance; the images are then analysed using ImageJ software, 100x100 pixels are used to carry out RGB and delta E analysis. Apt1-AGE4 mixture is incubated 30 minutes.

The sensing strategy is the same described also in PBS solution and in plasma and is based on the observation of PT1 optical properties: in the random coil configuration the polymer shows high fluorescence intensity and yellow colour (Figure 4.24 a). Upon addition of the aptamer a colour change into red/pink-ish, corresponding to the red shift, is observed meaning that the polymer formed a duplex structure with the aptamer (Figure 4.24 b). The presence of the biomarker, AGE4, is identified in the orange colour of the membrane meaning that the i-motif structure between the aptamer and the biomarker is formed and it hinders the duplex configuration (Figure 4.24 c). Due to the difficulty to perform the fluorescence intensity scan, no information is reported about quenching and/or recovery of

fluorescence. Differences in colours are particularly enhanced in 150µg/ml AGE4 concentration. Further evidences of the validity of the sensing strategy on PVDF membranes are given by the RGB and delta E analysis (Figure 4.25 (A) and (B)): upon addition of the aptamer there is a significant change in the RGB values, then recovered after the addition of the biomarker. Delta E graph confirms that 150µg/ml is the optimized concentration of AGE4 in order to have a notable colour change even at naked eye.
Further optimizations are required for a more detailed concentration-dependent study.

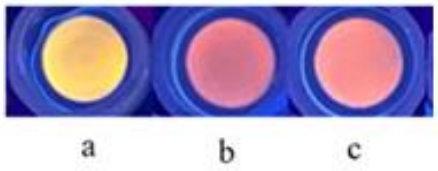

Figure 4.24 - Optical response of PT1 in presence of Apt1 and at 150µg/ml AGE4concentration on PVDF membrane (a): PT1 in Tween (b): PT1+Apt1 solution (c): PT1+Apt1+150µg/ml AGE4;

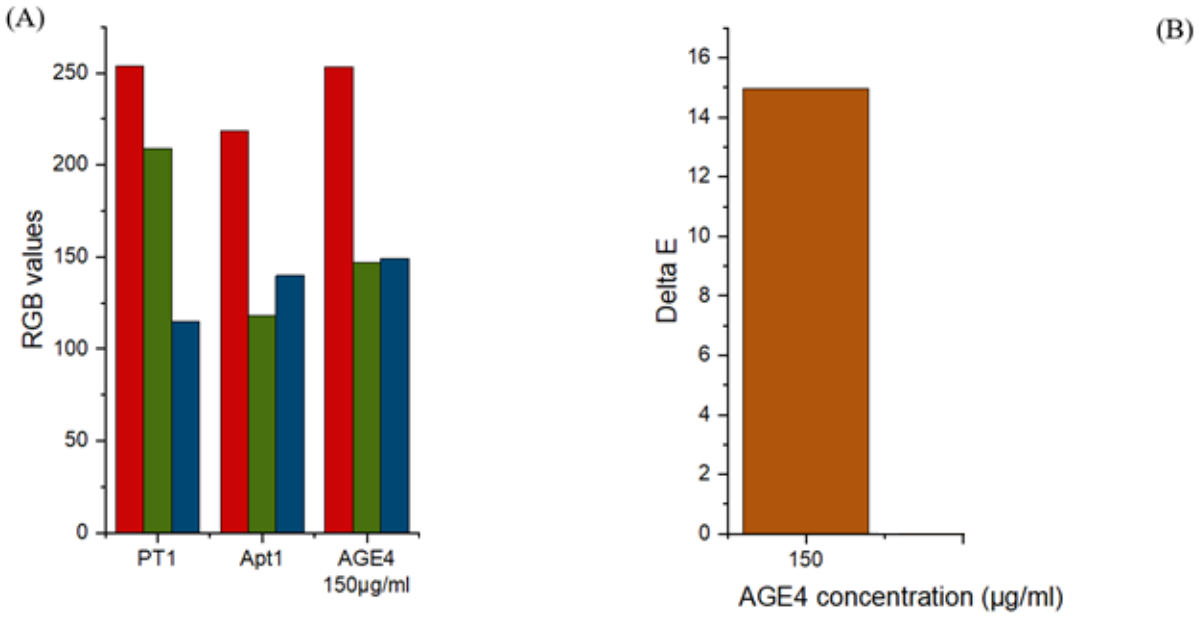

Figure 4.25 - Optical response of PT1 in presence of Apt1 and at 150µg/ml AGE4 concentration on PVDF membrane (A) RGB values (B) Delta E values

In conclusion, a PVDF membrane colorimetric array is also given in Figure 4.26, upon development of the collected data. Colours in pattern (B), in Tween, are clearly more differentiable with respect to pattern (A), in DI water as buffer.

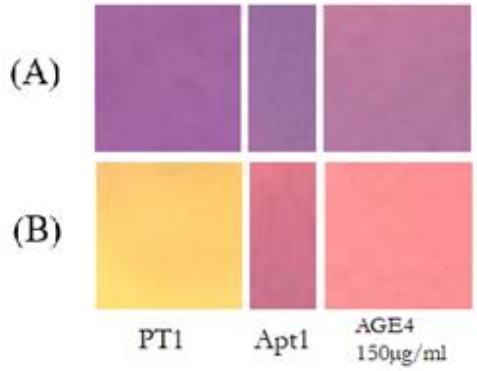

Figure 4.26 - Colorimetric array of PT1 in presence of Apt1 at 150µg/ml AGE4 concentration on PVDF membrane (A) in DI water (B) in Tween

4.6 COMPARISON WITH OTHER SENSING STRATEGIES

The most commonly used methods for AGEs detection and measure are immunochemical mechanisms like immunohistochemistry and enzyme-linked immunosorbent assay antibodies [169, 170] and bioanalytical such as fluorescence spectroscopy, UV-visible spectroscopy, surface plasmon resonance, boronate affinity chromatography, high-performance liquid chromatography (HPLC), liquid chromatography-mass spectroscopy (LC/MS) and fluorescent phenylboronate gel electrophoresis [143, 171]. Currently, no gold standard technique is developed for AGEs investigation. Other methods studied for AGEs detection are biochemical techniques like nitroblue tetrazolium assay and thiobarbituric acid colorimetric method [144-172]. Enzyme-linked immunosorbent assay (ELISA) is today the most common technique used for AGEs measurement but is featured by low reproducibility and low specificity [173].

The majority of these methods are not suitable in developing world because they require sophisticated and bulky laboratory instruments and trained personnel who carry out the

analysis. In Table 4.1 a summary of the major advantages and disadvantages of the methods mentioned above for the detection of AGEs biomarkers.

Table 4.1- Advantages and disadvantages of major techniques used for AGEs measurement [144]

Technique	*Advantages*	*Disadvantages*
Immunohistochemistry	Tissue localization of AGEs can be determined, and its colocalization with RAGEs can also be determined	Lack sensitivity and reproducibility
ELISA	Rapid and currently most frequently used	Specificity of antibodies is often difficult to characterize and due to steric constraints, all epitopes are not accessible to the antibodies
HPLC	Provides very precise quantification of AGEs	Cumbersome chromatographic systems and long retention time
LC/MS	Most accurate technique	Very expensive
UV–Visible spectroscopy	A quick preliminary tool for initial monitoring of glycation reaction	Not appropriate for quantitative estimation of glycation products
Fluorescence spectroscopy	Most valuable, simple and most commonly used methods for the measurement of AGEs	Nonfluorescent AGEs cannot be determined
Boronate affinity chromatography	Simple and efficient	Nonspecific interactions between boronate and nonglycosylated proteins
Fluorescent phenylboronate gel electrophoresis	A simple, cost-effective detection and analysis tool for glycated proteins and provides direct visualization of glycated proteins	Only suitable for the analysis of samples with limited complexity

These methods are not reproducible, are expensive and time consuming; moreover, due to their poor specificity, there is a huge disparity in the measure obtained with different techniques. Therefore, the developed point of care assay for AGEs detection represents an innovation: the analysis is simple, easy to carry out, reproducible and highly sensitive.
This new and highly specific method will assist in the early diagnosis of glycation-associated diseases.

Chapter 5: CONCLUSIONS AND FUTURE OUTLOOK

5.1 CONCLUSIONS

A simple colorimetric and fluorometric assay for carbonyl/oxidative stress biomarkers (AGEs, sugar molecules attached to proteins) detection is successfully developed using, as luminescent reporters, polythiophenes. Even though there are several studies on fluorescent and colorimetric biosensors using conjugated polymers in solution-based sensing, for nucleic acid detection, there are still few hypotheses on how the sensing ability of the polythiophene may vary with the structure and pendant groups. For this reason, four different cationic polythiophenes with varying pendant groups that could improve sensitivity and selectivity through modification and hydrophobicity variation of the whole conjugated polymer, have been designed and synthesized by oxidative polymerization. The pendant groups lead to tuning of the response to polar and non-polar molecules.

The electrostatic interactions among polymers, aptamers and AGEs provide a clear colour difference even at naked eye observation, that is this project primary aim. The limits of detection for the naked eye investigation through fluorescence intensity analysis of AGEs are 2.43µg/ml in PBS solution and 1.5µg/ml in plasma with an incubation time of 30 minutes. The numerical and optical response in plasma prove the use of the proposed methodology in clinical applications for early diagnosis of T2D, since the limit of detection is below the threshold clinical level that induce significant ROS generation, that is about 10µg/ml [35-37].

Besides these aspects, as explained in the selectivity studies in section 4.2, the assay reveals negligible interferences with other interfering molecules present in a complex system, such as high concentration sugar and protein molecules. Further evidence is proved in Figure 5.1, in which no significant difference is reported in delta E values, therefore in the perception of colour difference, between PBS testing conditions and plasma analysis.

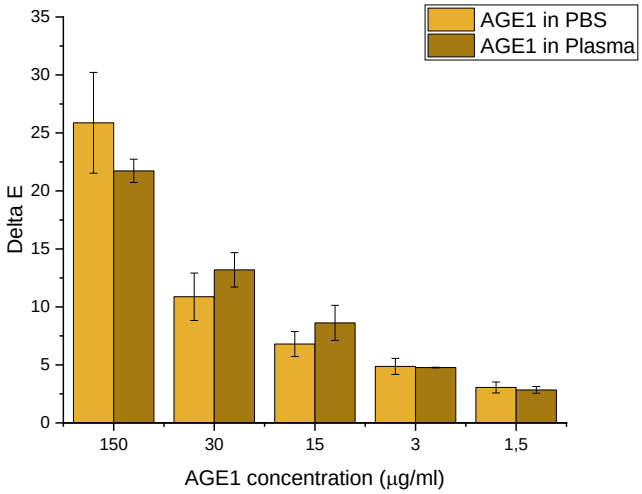

Figure 5.1 - Delta E mean values and standard deviation for different concentrations of AGE1 in presence of Apt1 and PT1 both in PBS and plasma

This point out the relevance of the proposed methodology in point of care applications for selective and sensitive detection of AGEs in analytically relevant concentrations avoiding the use of sophisticated instruments.

The proposed assay is also valid on PVDF membranes in which PT1 is diluted in Tween solution in order to have a better optical response with respect to DI water. However, this is exclusively a preliminary investigation, in particular a colour-based analysis. Further studies are required, in order to get a more complete picture.

As mentioned in Chapter 4, in Figure 5.2 is demonstrated that there is no differentiation among the studied aptamers in PBS. Figure 5.2 a and 5.2 b shows in both fluorescence recovery and delta E that for all four aptamers, the best detected AGEs for **PT1** are AGE1, AGE4 and AGE5. A similar analysis is carried out also for PTsyn, PTG and PT5. Again, in **PTsyn** (Figure 5.2 c and 5.2 d), for all four aptamers taken into account, the best detected AGEs are, respectively, AGE3, AGE1 and AGE2. Figure 5.2 e and 5.2 f shows that in **PTG**, for all four aptamers considered, AGE4 stands out followed by AGE2 and AGE3. Finally, **PT5** can easily detect AGE1 in presence of all four aptamers equally as depicted in Figure 5.2 g and 5.2 h. These outcomes are obviously coherent to the results found in buffer conditions; delta E in this sense is a further evidence of the fluorescence recovery measure. However, PTG and PT5 show high instability due to UV light exposure that cause chemical degradation: for this reason, the carried-out trials are not coherent and, consequently, the

standard deviations are too wide to consider it reliable (i.e. standard deviation values are far from zero). As a consequence, even AGEs differentiation graph at varying aptamers exhibit inconsistency. Polymer degradation is the major limit for the optical output that has been found during the progress of this project.

PTsyn showed very good responses in PBS solution due to its particular structure that yield highly fluorescent and therefore distinguishable outcomes. PTsyn however has not shown any response in plasma and on PVDF membranes; it is believed that most probably suffered UV light degradation.

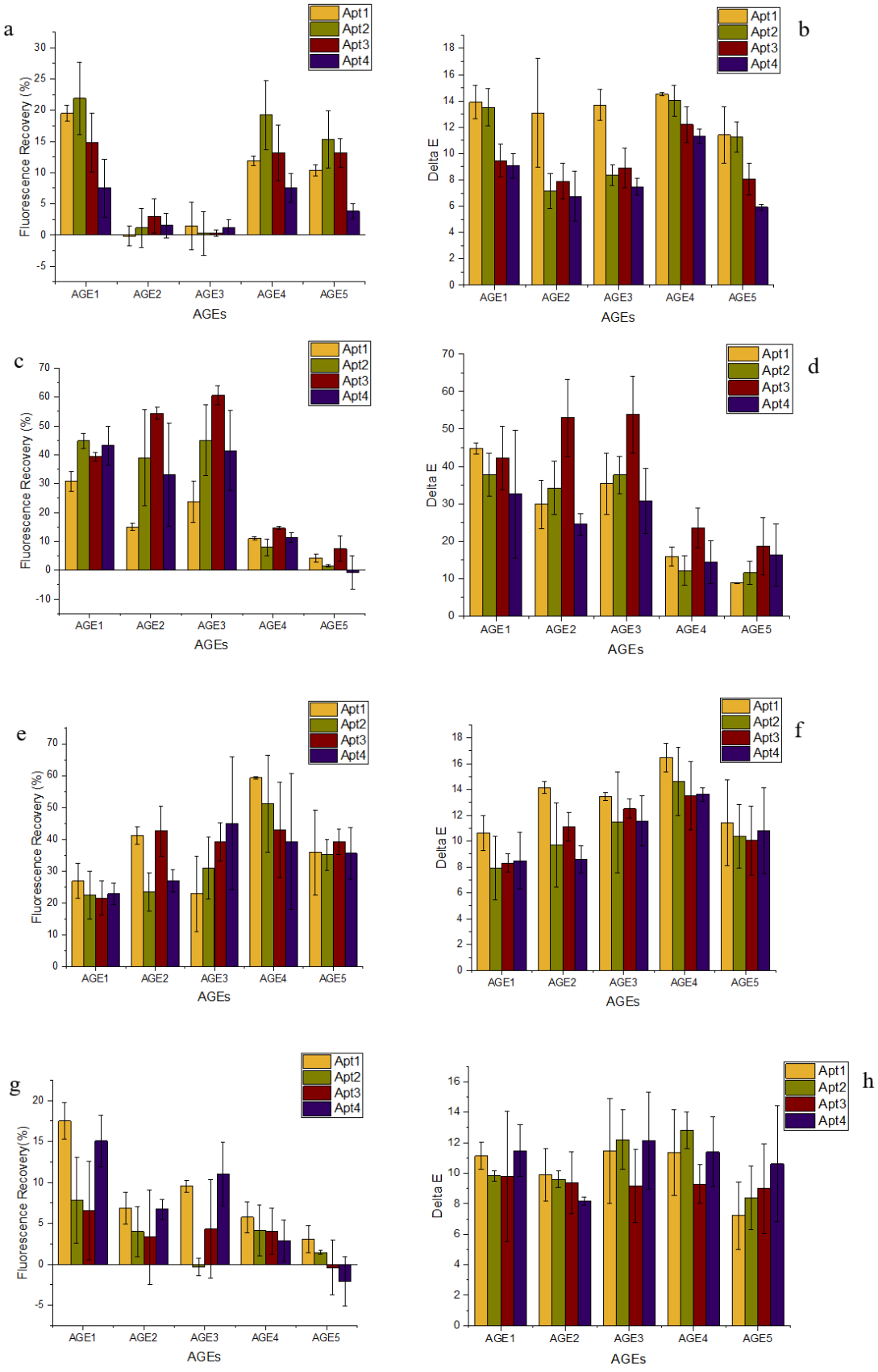

Figure 5.2 - AGEs differentiation at varying aptamer sequence. Fluorescence recovery and Delta E mean values and standard deviations of: (a) and (b): PT1, (c) and (d): PTsyn, (e) and (f): PTG, (g) and (h): PT5

Therefore, it is possible to fix just one aptamer sequence and develop a colorimetric array in PBS conditions. Figure 5.3 shows AGEs differentiation with varying polythiophenes employed, at fixed Apt1 sequence.

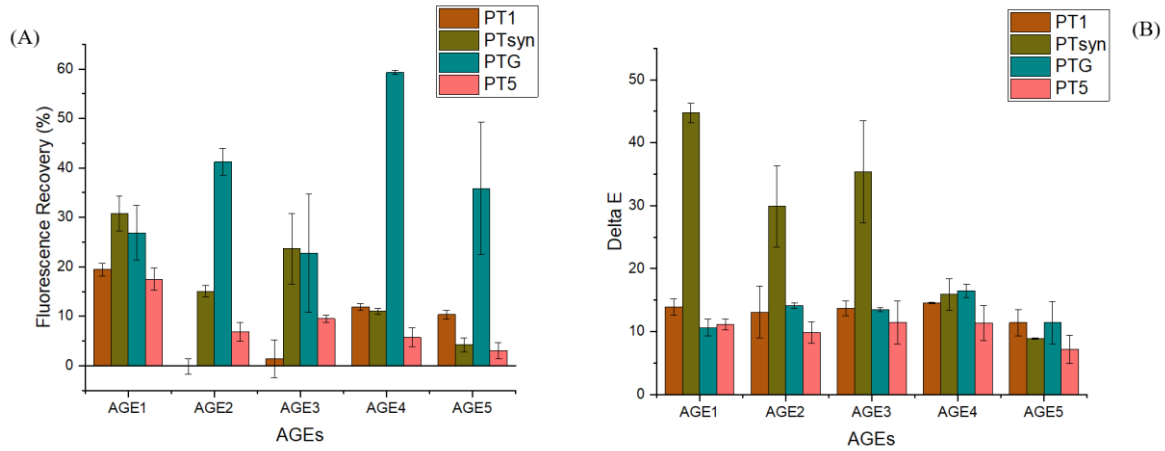

Figure 5.3 - AGEs differentiation at varying PTs in PBS conditions (A) Fluorescence Recovery mean values and standard deviation (B) Delta E mean values and standard deviation

The primary aim of this thesis is to visually differentiate among different AGEs using different optical reporters. A colorimetric array is therefore proposed, at fixed Apt1 (Apt) sequence, as depicted in Figure 5.4.

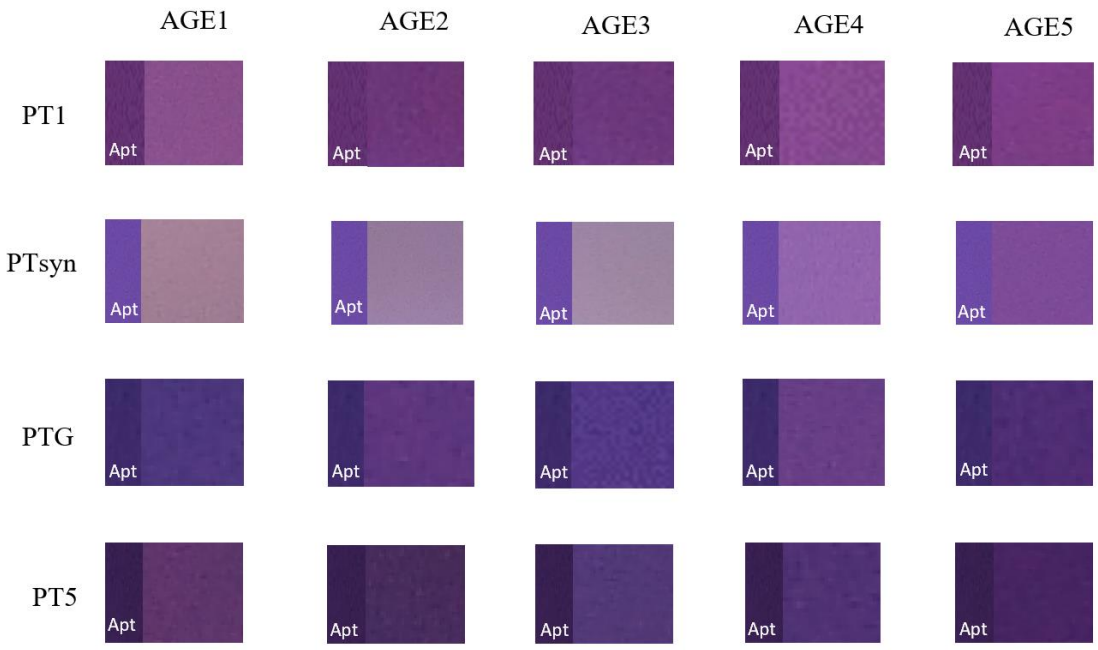

Figure 5.4 - Colorimetric array at fixed Apt1 and varying PTs and AGEs in PBS conditions

As demonstrated either in Figure 5.3 and in the colorimetric array of Figure 5.4, there actually is a differentiation in terms of fluorescence recovery mean values, delta E mean values and colours among AGEs at varying PTs and fixed Apt1 and, in particular, for PT1 AGE1, AGE4 and AGE5 are best detected (pink colour in the colorimetric array); in case of PTsyn, AGE3, AGE1 and AGE2 are best recognized (light pink); PTG shows an evident colour difference in case of AGE4 and AGE2, while PT5 reveals brighter colour corresponding to AGE1. Even in this case PTG and PT5 data lack in reliability due to the already mentioned polymer degradation; as a consequence, colours are less differentiable.
Even though every polymer shows good outcome for AGEs detection in PBS solution, PT1 is demonstrated to yield the best and more reproducible optical responses.
This solution-based assay can be ideal for POC management framework for detection of carbonyl and oxidative stresses and may also be used in nutrition and metabolic fields as a regulator of food intake in people suffering T2D.

5.2 FUTURE PERSPECTIVES

For the evaluation of colorimetric response of AGEs, only four polymers have been considered in this thesis (PT1, PTsyn, PTG and PT5). Even though there are several studies on fluorescent and colorimetric biosensors using conjugated polymers in solution-based sensing, for nucleic acid detection, there are still few hypotheses on how the sensing ability of the polythiophene may vary with the structure and pendant groups. For this reason, future studies will remark old PTs composition and will include to utilize new PTs with varying stoichiometric ratios pendant groups in order to improve the limit of detection and differentiation of varying AGEs for naked eye detection. Moreover, additional aptamers are to be investigated in order to detect new AGEs and determine further evidences of specificity of this assay.

Also, this solution-based assay has to be translated into the flow-through paper-based assay; no electronic tool exploiting vertical flow assay has been indeed developed in this project, so it remains an objective of the future perspectives.

Further studies on plasma for different polythiophenes are required in order to have a more complete picture of the assay. Analysis on PVDF membranes and urine at different concentrations are still to be optimized and left to future laboratory activities. The basic hypotheses related to the sensing mechanism are the same as described in this project; however, urine shows high autofluorescence and it will be necessary to neutralize this feature in order to have a colorimetric and fluorometric response.

Generally, a detailed analysis on patients' clinical samples is required to find out the patient to patient variations.

Moreover, the colorimetric array can also be improved, mostly in the editing process, in order to have a better optical naked-eye differentiation.

Circulating AGEs can be due not only to the biochemical reactions described in the previous chapters, but also through ingestion of high AGEs content foods, such as red meat, certain cheeses, oils, etc.

So, AGEs assay must be elaborated on with food samples due to the varied presence of these biomarkers in daily consumed foods and drinks; it would be interesting to find the various levels and concentrations of AGEs in the above-mentioned specimens. It is indeed pivotal for those suffering type 2 diabetes, the determination of the amount of AGEs in food intake in such a way that a low AGEs diet can be established. The control of food

intake through a dietary intervention is a simple way of prevention against premature aging and diseases such as diabetes.

The development of a flow-through device for multiple and simultaneous detection of various carbonyl/oxidative stress related to diseases such as T2D, could give a holistic approach for the monitoring of diabetes and its possible complications.

Moreover, it is believed that the addition of carbon nanotubes (CNTs) with PTs in this flow-through device would allow dual (optical and electrical) detection of the markers and could further improve the limit of detection.

APPENDIX I – SYNTHESIS OF POLYMERS

Synthesis of Cationic Polythiophenes

All the reagents and solvents are obtained from Sigma Aldrich and used without further purification. PTs are synthesized by oxidative polymerization of their monomers; nuclear magnetic resonance, NMR, spectra are recorded on a Bruker Advance 400 MHz spectrometer.

This procedure is carried out for PT1 as well as for all the mentioned polymers.

Synthesis of precursor 1 (3-methoxy-4-methylthiophene)

To a dry round-bottom flask, 1-methyl-2-pyrrolidinone (6.7 mL, 69.80 mmol) and sodium methoxide/MeOH (25 wt%; 17.8 mL, 78.50 mmol) were added. After heating this mixture to 110 °C, 3-bromo-4-methylthiophene (5 g, 28.20 mmol) and CuBr (2.47 g, 17.20 mmol) were added. The round-bottom flask was then equipped with a water-cooled condenser and refluxed for 1 day at 110 °C (Figure A1(a)). The reaction mixture was cooled to room temperature and then a solution of 1 g of sodium bromide in 40 mL of water was added and stirred vigorously for 1 h. The mixture was then filtered and extracted with 50 mL diethyl ether five times. The combined organic layers were washed with water at least three times and dried over $MgSO_4$. Solvent was then removed by rotary evaporator to yield a light-yellow oil. This light-yellow oil was further purified with column chromatography to yield 3-methoxy-4-methylthiophene (2.28 g (63%)). ^{1}H NMR (400 MHz, $CDCl_3$) δ (ppm): 6.84 (1H, d), 6.18 (1H, d), 3.84 (3H, s), 2.11 (3H, s) (Figure A1(b)).

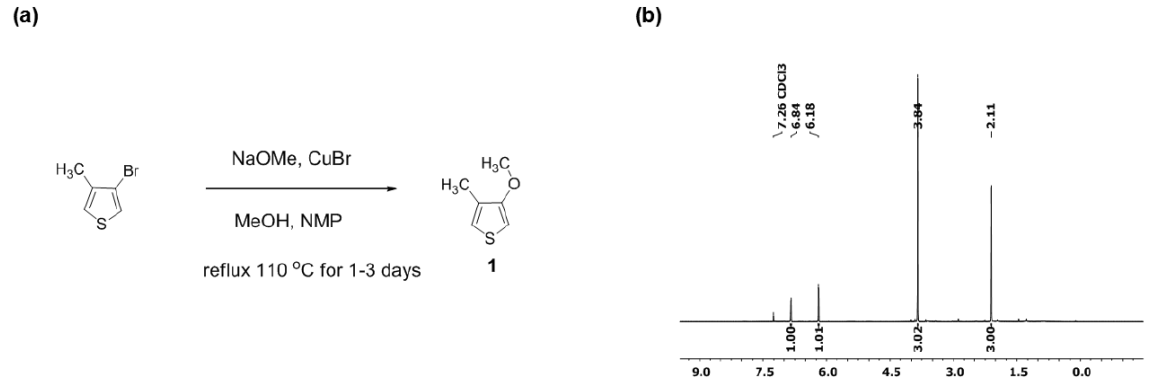

Figure A1 - (a) Synthetic route to 3-methoxy-4-methylthiophene (b) ^{1}H NMR spectrum of 3-methoxy-4-methylthiophene (400 MHz, $CDCl_3$).

Synthesis of precursor 2 (3-(3-Bromo) propoxy-4-methylthiophene)

A mixture of 3-methoxy-4-methylthiophene (precursor 1) (0.84 g, 6.60 mmol), 3-bromo-1-propanol (2.00 g, 14.4 mmol), and $NaHSO_4$ (123 mg, 0.900 mmol) in 15 mL of toluene was added to a two neck round bottom flask. This reaction mixture was heated at 100 °C for 24 hours under nitrogen atmosphere (Figure A2(a)); meanwhile the produced methanol was distilled off from the reaction flask. The reaction mixture was allowed to cool to room temperature. Toluene was removed by rotary evaporator and the remaining reaction mixture was extracted five times with diethyl ether, subsequently washed with water and dried over magnesium sulphate. Diethyl ether was removed by rotary evaporator. The crude product was purified with column chromatography (silica gel, hexane) to give 1.0 g (65%) 2 as colourless oil. ^{1}H NMR (400 MHz, $CDCl_3$) δ (ppm): 6.83 (1H, d), 6.19 (1H, d), 4.08 (2H, m), 3.59 (2H, m), 2.34 (2H, m), 2.09 (3H, s) (Figure A2(b)).

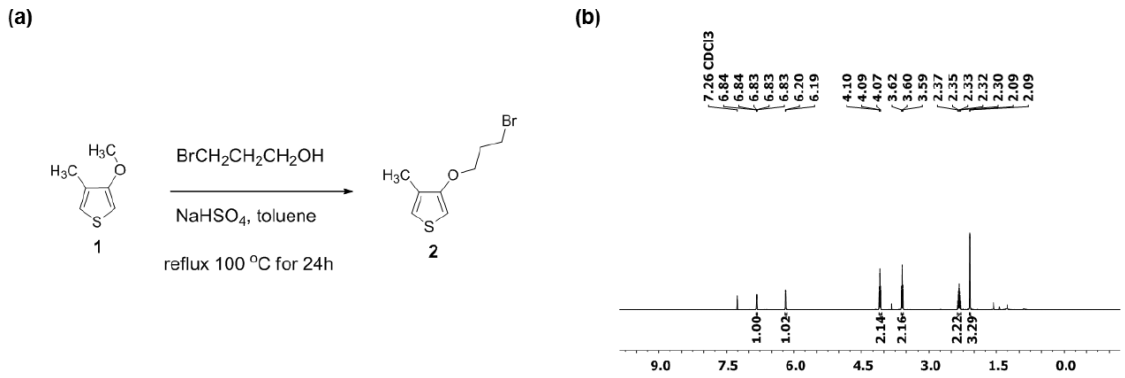

Figure A2 - (a) Synthetic route to 3-methoxy-4-methylthiophene (b) ^{1}H NMR spectrum of 3-(3-Bromo) propoxy-4-methylthiophene (400 MHz, $CDCl_3$).

Synthesis of monomer 1

To a round bottom flask 3-(3-Bromo) propoxy-4-methylthiophene (0.27 g, 1.15 mmol), triethylamine (26.45 mmol, 3.7 ml) and THF (30 mL) were added. The mixture was stirred at 72 °C for two days (Figure A3(a)). The crude product was washed with THF to give 0.30 g (77%) monomer 1. ^{1}H NMR (400 MHz, DMSO-d6) δ (ppm): 7.09 (d, 1H), 6.53 (d, 1H), 4.02 (t, 2H), 3.29 (m, 8H), 2.08 (m, 2H), 2.03 (s, 3H), 1.20 (t, 9H). ^{13}C NMR (100 MHz, DMSO-d6) δ (ppm): 155.41, 128.56, 121.09, 97.85, 66.61, 53.60, 52.52, 21.88, 12.92, 7.53 (Figure A3(b)).

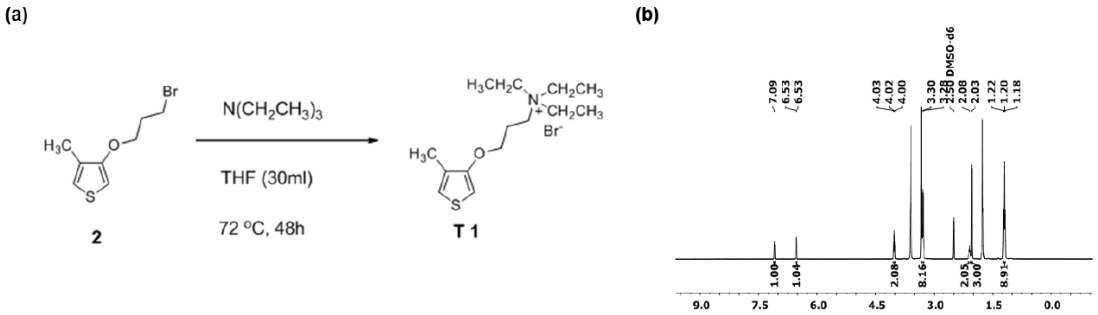

Figure A3 - (a) Synthetic route to monomer 1 (b) ^{1}H NMR spectrum of monomer 1 (400 MHz, DMSO-d6).

Synthesis of PT1

A solution of 3-(4-Methyl-3'-thienyloxy)propyl triethylammonium bromide (monomer 1) (270 mg, 0.910 mmol) of in 5 mL dry $CHCl_3$ was added dropwise to a solution of anhydrous $FeCl_3$ (590 mg, 3.640 mmol) in 25 mL of dry $CHCl_3$, and stirred for 24 h at room temperature under N_2 atmosphere, then evaporated to dryness (Figure 111 A5(a)). The crude product was washed with $CHCl_3$ and diethyl ether subsequently many times to get rid of $FeCl_3$ and starting material. The collected polymer was dried in vacuum for 24 h. ^{1}H NMR is shown in Figure A5(b).

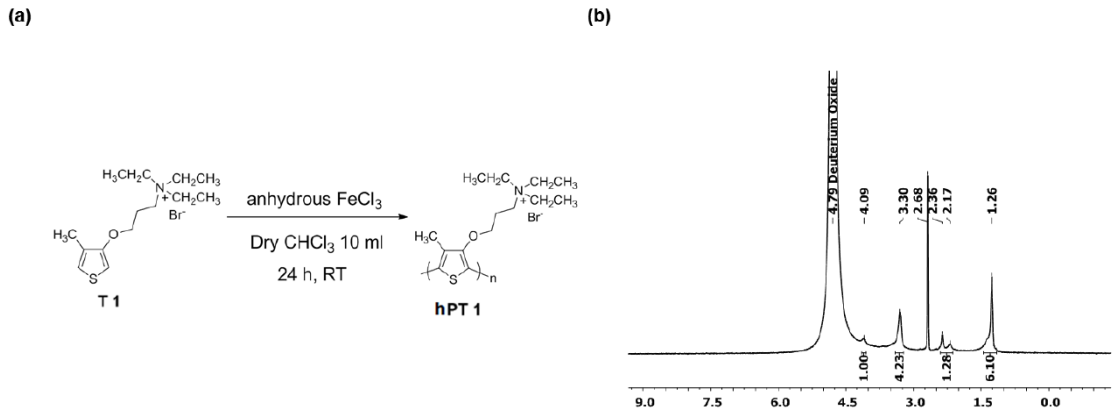

Figure A4 - (a) Synthetic route to PT1 by oxidative polymerization of monomer 1 (b) ^{1}H NMR spectrum of PT1 (400 MHz, D2O - DMSO).

APPENDIX II – MAILLARD REACTION

Maillard reaction in foods

Maillard reaction is described for the first time by Louis-Camille Maillard in 1912. They are extremely complex reactions leading to a multiplicity of products [174].

Typically, the Maillard reaction results in the formation of a Schiff base followed by a rearrangement process into an Amadori product (or Heyns product).

It is possible to summarize and simplify the stages of the Maillard reactions into three steps:

1. Initial stage (Early Maillard Reaction): the product remains colourless upon UV absorption. Two reactions occur at this stage: sugar-amine condensation (reaction A) and Amadori rearrangement (reaction B).
2. Intermediate stage (Advanced Maillard Reaction): the product's colour can shift into yellow if UV absorption occurs. This stage involves sugar degradation (reaction C) and fragmentation (reaction D), as well as degradation of amino acids (reaction E).
3. Final stage (Final Maillard Reaction): the product assumes a highly pigmented colour upon condensation of aldols (reaction F), condensation of aldehyde-amine and formation of heterocyclic nitrogen compounds (reaction G).

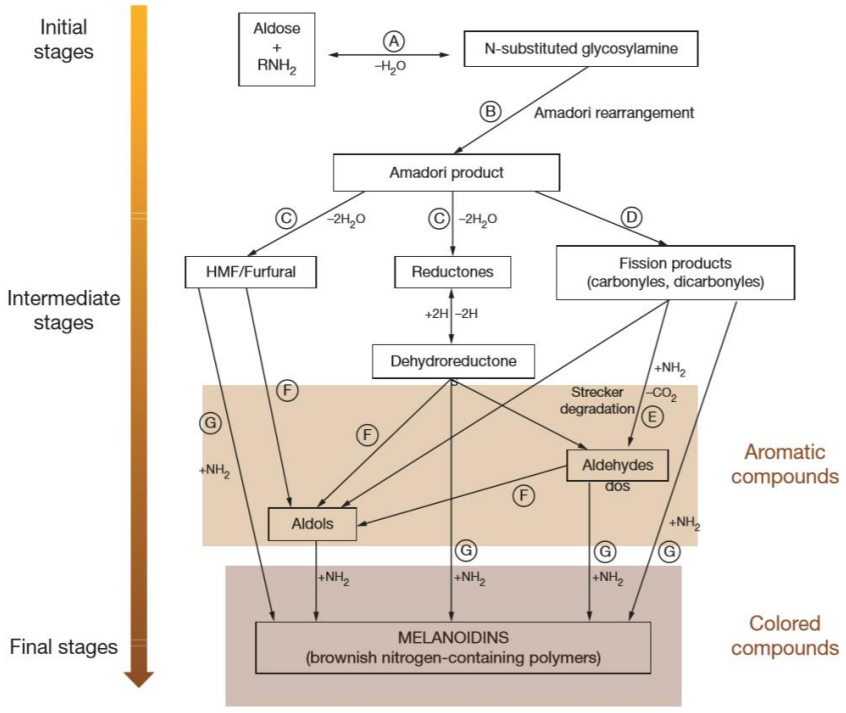

Reactions from A to G are described in the figure below [174].

The final products (melanoidins) result dark brown in colour and are formed by enzymatic and non-enzymatic reactions, which are extremely complex to differentiate, and their chemical analysis is difficult since they are relatively intractable. Maillard reactions occur typically when the products are stored for long periods at room temperature or during transportation overseas where temperature can easily increase up to 70°C.

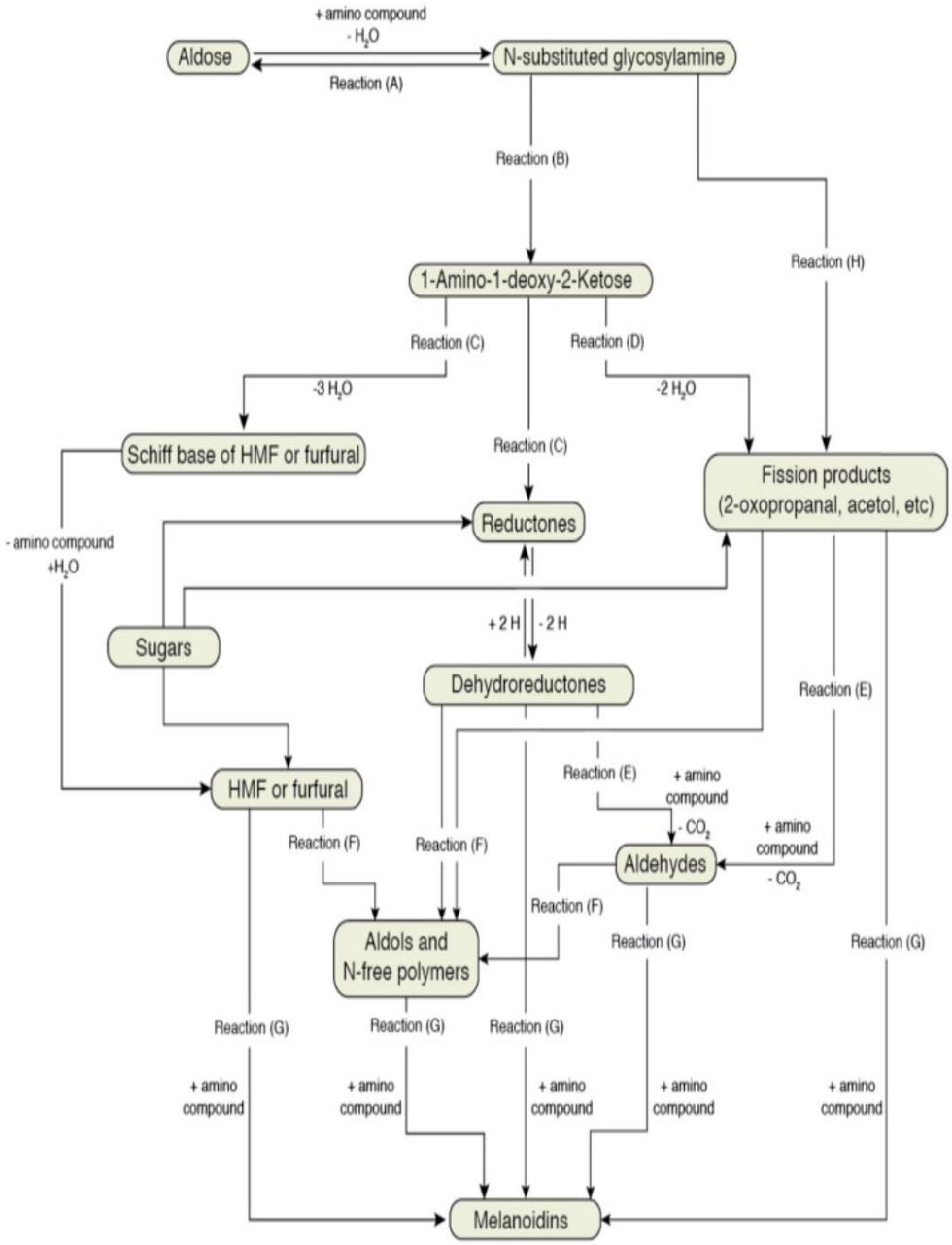

REFERENCES

1. Rani, V., et al., *Oxidative stress and metabolic disorders: Pathogenesis and therapeutic strategies.* Life sciences, 2016. **148**: p. 183-193.
2. Yadav, U., et al., *Oxidative stress in metabolic disorders: pathogenesis, prevention, and therapeutics.* Oxidative medicine and cellular longevity, 2016. **2016**.
3. Tierney LM Jr, S.S., Whooley MA, *Current Essentials of Medicine*. 4 ed. 2011: New York: McGraw-Hill.
4. Mulholland, P.G., June; Wallace, James *Introduction to paediatric pharmaceutical care*. Scottish Neonatal and Paediatric Pharmacists Group. 16.
5. https://www.who.int/
6. De Luca, C. and J.M. Olefsky, *Inflammation and insulin resistance.* FEBS letters, 2008. **582**(1): p. 97-105.
7. Shoelson, S.E., J. Lee, and A.B. Goldfine, *Inflammation and insulin resistance.* The Journal of clinical investigation, 2006. **116**(7): p. 1793-1801.
8. Hurrle, S. and W.H. Hsu, *The etiology of oxidative stress in insulin resistance.* Biomedical journal, 2017. **40**(5): p. 257-262.
9. Muller, G., *Microvesicles/exosomes as potential novel biomarkers of metabolic diseases.* Diabetes Metab Syndr Obes, 2012. **5**: p. 247-82.
10. Semchyshyn, H.M. and V.I. Lushchak, *Interplay Between Oxidative and Carbonyl Stresses: Molecular Mechanisms, Biological Effects and Therapeutic Strategies of Protection, Oxidative Stress - Molecular Mechanisms and Biological Effects*, D.V. Lushchak, Editor. 2012: InTech. p. 33.
11. Kivatinitz, S.C., *Relationship Between Protein Oxidation Markers and Oxidative Stress Biomarkers, Inflammatory Diseases - Immunopathology, Clinical and Pharmacological Bases*. 2012: InTech.
12. Dalle-Donne, I., et al., *Protein carbonylation in human diseases.* Trends Mol Med, 2003. **9**(4): p. 169-76.
13. Niedworok, J. and P. Fijałkowski, *Effect of Long-Term Aluminium Chloride Intoxication on Selected Biochemical Parameters and Oxidative--Antioxidative Balance in Experimental Animals.* Polish Journal of Environmental Studies, 2004. **13**(1): p. 41-43.

14. Lowe, F., *Biomarkers of Oxidative Stress.* Systems Biology of Free Radicals and Antioxidants, 2014.
15. Dalle-Donne, I., et al., *Biomarkers of oxidative damage in human disease.* Clin Chem, 2006. **52**(4): p. 601-23.
16. Ahmed, N., *Advanced glycation endproducts--role in pathology of diabetic complications.* Diabetes Res Clin Pract, 2005. **67**(1): p. 3-21.
17. Sher, M., et al., *Paper-based analytical devices for clinical diagnosis: recent advances in the fabrication techniques and sensing mechanisms.* Mol Diagn. 2017 April, 17(4): 351-366
18. Cooke, J., et al., *Narrative review of primary care point-of-care testing (POCT) and antibacterial use in respiratory tract infection (RTI).* BMJ open respiratory research, 2015. **2**(1): p. e000086.
19. St John, A. and C.P. Price, *Existing and emerging technologies for point-of-care testing.* The Clinical Biochemist Reviews, 2014. **35**(3): p. 155.
20. Gutierres, S.L. and T.E. Welty, *Point-of-care testing: an introduction.* Annals of Pharmacotherapy, 2004. **38**(1): p. 119-125.
21. Posthuma-Trumpie, G.A., J. Korf, and A. van Amerongen, *Lateral flow (immuno) assay: its strengths, weaknesses, opportunities and threats. A literature survey.* Analytical and bioanalytical chemistry, 2009. **393**(2): p. 569-582.
22. Ye, X., et al., *Iodide-responsive Cu–Au nanoparticle-based colorimetric platform for ultrasensitive detection of target cancer cells.* Analytical chemistry, 2015. **87**(14): p. 7141-7147.
23. Zhao, W., M.A. Brook, and Y. Li, *Design of gold nanoparticle-based colorimetric biosensing assays.* ChemBioChem, 2008. **9**(15): p. 2363-2371.
24. Jelinek, R. and S. Kolusheva, *Biomolecular sensing with colorimetric vesicles*, in *Creative Chemical Sensor Systems*. 2007, Springer. p. 155-180.
25. Song, Y., W. Wei, and X. Qu, *Colorimetric biosensing using smart materials.* Advanced Materials, 2011. **23**(37): p. 4215-4236.
26. Rajwar, D., et al., *Tailoring Conformation-Induced Chromism of Polythiophene Copolymers for Nucleic Acid Assay at Resource Limited Settings.* ACS applied materials & interfaces, 2016. **8**(13): p. 8349-8357.
27. Ahmad, K.M., et al., *Probing the limits of aptamer affinity with a microfluidic SELEX platform.* PloS one, 2011. **6**(11): p. e27051.

28. Wang, G., et al., *Selection and characterization of DNA aptamer against glucagon receptor by cell-SELEX.* Scientific reports, 2017. **7**(1): p. 7179.

29. Miyachi, Y., et al., *Selection of a DNA aptamer that binds 8-OHdG using GMP-agarose.* Bioorganic & medicinal chemistry letters, 2009. **19**(13): p. 3619-3622.

30. Higashimoto, Y., et al., *Blockade by phosphorothioate aptamers of advanced glycation end products-induced damage in cultured pericytes and endothelial cells.* Microvascular research, 2013. **90**: p. 64-70.

31. Byrnes, S., G. Thiessen, and E. Fu, *Progress in the development of paper-based diagnostics for low-resource point-of-care settings.* Bioanalysis, 2013. **5**(22): p. 2821-2836.

32. Xu, H., et al., *Aptamer-functionalized gold nanoparticles as probes in a dry-reagent strip biosensor for protein analysis.* Analytical Chemistry, 2008. **81**(2): p. 669-675.

33. Liu, G., et al., *Aptamer− nanoparticle strip biosensor for sensitive detection of cancer cells.* Analytical chemistry, 2009. **81**(24): p. 10013-10018.

34. Jauset-Rubio, M., et al., *Advances in aptamers-based lateral flow assays.* TrAC Trends in Analytical Chemistry, 2017.

35. Tahara, N., et al., *Positive association between serum level of glyceraldehyde-derived advanced glycation end products and vascular inflammation evaluated by [18F] fluorodeoxyglucose positron emission tomography.* Diabetes care, 2012: p. DC_120087.

36. Soboleva, A., et al., *Probing protein glycation by chromatography and mass spectrometry: analysis of glycation adducts.* International journal of molecular sciences, 2017. **18**(12): p. 2557.

37. Hammad, L.A., et al., *Multiple-reaction monitoring liquid chromatography mass spectrometry for monosaccharide compositional analysis of glycoproteins.* Journal of the American Society for Mass Spectrometry, 2009. **20**(6): p. 1224-1234.

38. "Causes of Diabetes". *National Institute of Diabetes and Digestive and Kidney Diseases. June 2014.* Archived *from the original on 2 February 2016. Retrieved* 10 February *2016.*

39. Melmed, Shlomo; Polonsky, Kenneth S.; Larsen, P. Reed; Kronenberg, Henry M., eds. (2011). *Williams textbook of endocrinology* (12th ed.). Philadelphia: Elsevier/Saunders. pp. 1371–1435.

40. Ganguly S, Tan HC, Lee PC, Tham KW (April 2015). *"Metabolic bariatric surgery and type 2 diabetes mellitus: an endocrinologist's perspective"*. Journal of Biomedical Research. **29** (2): 105–11.
41. Smyth S, Heron A (January 2006). "*Diabetes and obesity: the twin epidemics*". *Nature Medicine*. **12** (1): 75–80.
42. Ripsin CM, Kang H, Urban RJ (January 2009). *"Management of blood glucose in type 2 diabetes mellitus". American Family Physician. **79** (1): 29–36.*
43. Risérus U, Willett WC, Hu FB (January 2009). "*Dietary fats and prevention of type 2 diabetes*". *Progress in Lipid Research*. **48** (1): 44–51.
44. Gardner, David G.; Shoback, Dolores, eds. (2011). *"Chapter 17: Pancreatic hormones & diabetes mellitus". Greenspan's basic & clinical endocrinology (9th ed.). New York: McGraw-Hill Medical.*
45. Diabetes mellitus a guide to patient care. *Philadelphia: Lippincott Williams & Wilkins. 2007. p.* 15.
46. Melmed, Shlomo; Polonsky, Kenneth S.; Larsen, P. Reed; Kronenberg, Henry M., eds. (2011). *Williams textbook of endocrinology* (12th ed.). Philadelphia: Elsevier/Saunders. pp. 1371–1435.
47. Vos T, Allen C, Arora M, Barber RM, Bhutta ZA, Brown A, et al. (GBD 2015 Disease and Injury Incidence and Prevalence Collaborators) (October 2016). "*Global, regional, and national incidence, prevalence, and years lived with disability for 310 diseases and injuries, 1990-2015: a systematic analysis for the Global Burden of Disease Study 2015*". *Lancet*. **388** (10053): 1545–1602.
48. Smyth S, Heron A (January 2006). "Diabetes and obesity: the twin epidemics". *Nature Medicine*. **12** (1): 75–80.
49. Wild S, Roglic G, Green A, Sicree R, King H (May 2004). "*Global prevalence of diabetes: estimates for the year 2000 and projections for 2030*". *Diabetes Care*. **27** (5): 1047–53.
50. Wild S, Roglic G, Green A, Sicree R, King H (May 2004). *"Global prevalence of diabetes: estimates for the year 2000 and projections for 2030". Diabetes Care. **27** (5): 1047–53.*
51. Rahman, T., et al., *Oxidative stress and human health.* Advances in bioscience and biotechnology, 2012. **3**(07): p. 997.

52. Li, R., Z. Jia, and M.A. Trush, *Defining ROS in biology and medicine.* Reactive oxygen species (Apex, NC), 2016. **1**(1): p. 9.

53. Kirkham, P.A. and P.J. Barnes, *Oxidative stress in COPD.* Chest, 2013. **144**(1): p. 266-273.

54. Nam, J.S. and C.W. Ahn, *Oxidative stress, point-of-care test, and metabolic syndrome.* The Korean journal of internal medicine, 2014. **29**(1): p. 20.

55. de Vos, L.C., et al., *Advanced glycation end products: An emerging biomarker for adverse outcome in patients with peripheral artery disease.* Atherosclerosis, 2016. **254**: p. 291-299.

56. A. Goldin, J.A. Beckman, A.M. Schmidt, M.A. Creager, *Advanced glycation end products: sparking the development of diabetic vascular injury,* Circulation 114 (6) (2006).

57. V.M. Monnier, D.R. Sell, *Prevention and repair of protein damage by the Maillard reaction in vivo,* Rejuvenation Res. 9 (2) (2006).

58. S. Jaisson, P. Gillery, *Evaluation of nonenzymatic posttranslational modification-derived products as biomarkers of molecular aging of proteins,* Clin. Chem. 56 (9) (2010).

59. C. Cerami, H. Founds, I. Nicholl, T. Mitsuhashi, D. Giordano, S. Vanpatten, et al., *Tobacco smoke is a source of toxic reactive glycation products,* Proc. Natl. Acad. Sci. U. S. A. 94 (25) (1997).

60. T. Goldberg, W. Cai, M. Peppa, V. Dardaine, B.S. Baliga, J. Uribarri, et al., *Advanced glycoxidation end products in commonly consumed foods,* J. Am. Diet. Assoc. 104 (8) (2004).

61. T. Miyata, Y. Ueda, A. Yoshida, S. Sugiyama, Y. Iida, M. Jadoul, et al., *Clearance of pentosidine, an advanced glycation end product, by different modalities of renal replacement therapy,* Kidney Int. 51 (3) (1997).

62. E. Yagmur, F. Tacke, C. Weiss, B. Lahme, M.P. Manns, P. Kiefer, et al., *Elevation of Nepsilon-(carboxymethyl)lysine-modified advanced glycation end products in chronic liver disease is an indicator of liver cirrhosis,* Clin. Biochem. 39 (1) (2006).

63. Won, K.-B., et al., *High serum advanced glycation end-products predict coronary artery disease irrespective of arterial stiffness in diabetic patients.* Korean circulation journal, 2012. **42**(5): p. 335-340.

64. Meerwaldt, R., et al., *The clinical relevance of assessing advanced glycation endproducts accumulation in diabetes.* Cardiovascular Diabetology, 2008. **7**(1): p. 29.

65. Uribarri, J., et al., *Advanced glycation end products in foods and a practical guide to their reduction in the diet.* Journal of the American Dietetic Association, 2010. **110**(6): p. 911-916. e12.

66. Kitahara, Y., et al., *Glyceraldehyde-derived advanced glycation end products (AGEs). A novel biomarker of postprandial hyperglycaemia in diabetic rats.* Clinical and experimental medicine, 2008. **8**(3): p. 175-177.

67. Dalle-Donne, I., et al., *Protein carbonyl groups as biomarkers of oxidative stress.* Clinica chimica acta, 2003. **329**(1): p. 23-38.

68. Purdel, N.C., D. Margina, and M. Ilie, *Current methods used in the protein carbonyl assay.* Annual Research & Review in Biology, 2014. **4**(12): p. 2015-2026.

69. Levine RL, Garland D, Oliver CN, Amici A, Climent I, Lenz A, et al. *Determination of carbonyl content in oxidatively modified proteins*. Methods Enzymol 1990.

70. Lyras L, Evans PJ, Shaw PJ, Ince PG, Halliwell B. *Oxidative damage and motor neurone disease difficulties in the measurement of protein carbonyls in human brain tissue*. Free Radic Res 1996.

71. Reznick AZ, Packer L. *Oxidative damage to proteins: spectrophotometric method for carbonyl assay*. Methods Enzymol 1994.

72. Kupiec, T., *Quality-control analytical methods: High-performance liquid chromatography.* International journal of pharmaceutical compounding, 2004. **8**: p. 223-227.

73. Zhu, X., et al., *A paper electrode integrated lateral flow immunosensor for quantitative analysis of oxidative stress induced DNA damage.* Analyst, 2014. **139**(11): p. 2850-2857.

74. Hawkins, C.L., P.E. Morgan, and M.J. Davies, *Quantification of protein modification by oxidants.* Free Radical Biology and Medicine, 2009. **46**(8): p. 965-988.

75. Yan, L.-J. and R.S. Sohal, *Gel electrophoretic quantitation of protein carbonyls derivatized with tritiated sodium borohydride.* Analytical biochemistry, 1998. **265**(1): p. 176-182.

76. Cox, K., et al., *Immunoassay Methods.* 2004.

77. *Biocell protein carbonyl ELISA kit* (ALX-850-312-KI01). Enzo Life Sciences, Version: March 22; 2011.

78. Wehr NB, Levine RL. *Quantitation of Protein Carbonylation by Dot Blot*. Anal Biochem. 2012;423(2):241–245.

79. Yager, P., G.J. Domingo, and J. Gerdes, *Point-of-care diagnostics for global health.* Annu. Rev. Biomed. Eng., 2008. **10**: p. 107-144.

80. Abram, T.J., *A PDMS Sample Pretreatment Device for the Optimization of Electrokinetic Manipulations of Blood Serum*. 2009, California Polytechnic State University, San Luis Obispo.

81. Gervais, L. and E. Delamarche, *Toward one-step point-of-care immunodiagnostics using capillary-driven microfluidics and PDMS substrates.* Lab on a Chip, 2009. **9**(23): p. 3330-3337.

82. Chin, C.D., V. Linder, and S.K. Sia, *Commercialization of microfluidic point-of-care diagnostic devices.* Lab on a Chip, 2012. **12**(12): p. 2118-2134.

83. Chan, C.P.Y., et al., *Evidence-based point-of-care diagnostics: current status and emerging technologies.* Annual Review of Analytical Chemistry, 2013. **6**: p. 191-211.

84. Dhawan, A., et al., *Current and Future Challenges in Point-of-Care Technologies: A Paradigm-Shift in Affordable Global Healthcare with Personalized and Preventive Medicine.*

85. Mace, C.R. and R.N. Deraney, *Manufacturing prototypes for paper-based diagnostic devices.* Microfluidics and nanofluidics, 2014. **16**(5): p. 801-809.

86. Gervais, L., N. De Rooij, and E. Delamarche, *Microfluidic Chips for Point-of-Care Immunodiagnostics.* Advanced Materials, 2011. **23**(24): p. H151-H176.

87. Hu, J., et al., *Advances in paper-based point-of-care diagnostics.* Biosensors and Bioelectronics, 2014. **54**: p. 585-597.

88. Arugula, M.A. and A. Simonian, *Novel trends in affinity biosensors: current challenges and perspectives.* Measurement Science and Technology, 2014. **25**(3): p. 032001.

89. Sanjay, S.T., et al., *Biomarker detection for disease diagnosis using cost-effective microfluidic platforms.* Analyst, 2015.

90. Radzicka, A. and R. Wolfenden, *A proficient enzyme.* Science, 1995. **267**(5194): p. 90-93.

91. Cate, D.M., et al., *Recent Developments in Paper-Based Microfluidic Devices.* Analytical chemistry, 2014. **87**(1): p. 19-41.
92. Aldewachi, H., et al., *Gold nanoparticle-based colorimetric biosensors*. Nanoscale, 2018, 10, 18.
93. Liu, X., et al., *Peptide functionalized gold nanoparticles with optimized particle size and concentration for colorimetric assay development: Detection of cardiac troponin I.* Acs Sensors, 2016. **1**(12): p. 1416-1422.
94. Ornatska, M., et al., *Paper bioassay based on ceria nanoparticles as colorimetric probes.* Analytical chemistry, 2011. **83**(11): p. 4273-4280.
95. Laromaine, A., et al., *Protease-triggered dispersion of nanoparticle assemblies.* Journal of the American Chemical Society, 2007. **129**(14): p. 4156-4157.
96. JI, E., *CONJUGATED POLYELECTROLYTES: SYNTHESIS, PHOTOPHYSICAL STUDIES AND APPLICATIONS TO SENSORS AND BIOCIDAL ACTIVITY*. 2009, UNIVERSITY OF FLORIDA
97. Patil, A.O., A.J. Heeger, and F. Wudl, *Optical properties of conducting polymers.* Chemical Reviews, 1988. **88**(1): p. 183-200.
98. Scherf, U. and E.J.W. List, *Semiconducting Polyfluorenes—Towards Reliable Structure–Property Relationships.* Advanced Materials, 2002. **14**(7): p. 477-487.
99. YU, Z.R., *Water-Soluble p-Conjugated Polymer for Biosensor Applications*. 2012.
100. McQuade, D.T., A.E. Pullen, and T.M. Swager, *Conjugated polymer-based chemical sensors.* Chem Rev, 2000. **100**(7): p. 2537-74.
101. Gunes, S., H. Neugebauer, and N.S. Sariciftci, *Conjugated polymer-based organic solar cells.* Chem Rev, 2007. **107**(4): p. 1324-38.
102. Kraft, A., A.C. Grimsdale, and A.B. Holmes, *Electroluminescent Conjugated Polymers—Seeing Polymers in a New Light.* Angewandte Chemie International Edition, 1998. **37**(4): p. 402-428.
103. Sirringhaus, H., *Device Physics of Solution-Processed Organic Field-Effect Transistors.* Advanced Materials, 2005. **17**(20): p. 2411-2425.
104. Shiraki, T., et al., *Unexpected chiral induction from achiral cationic polythiophene aggregates and its application to the sugar pattern recognition.* Chem Commun (Camb), 2012. **48**(56): p. 7091-3.

105. Zhan, R., Z. Fang, and B. Liu, *Naked-Eye Detection and Quantification of Heparin in Serum with a Cationic Polythiophene.* Analytical Chemistry, 2009. **82**(4): p. 1326-1333.

106. Nilsson, K.P.R. and O. Inganas, *Chip and solution detection of DNA hybridization using a luminescent zwitterionic polythiophene derivative.* Nat Mater, 2003. **2**(6): p. 419-424.

107. Lee, K., *Functionalized Conjugated Polymers for Signal Amplifying Biosensors and Sensor Arrays.* 2008.

108. Kim, J. and T. Swager, *Control of conformational and interpolymer effects in conjugated polymers.* Nature, 2001. **411**(6841): p. 1030.

109. Lee, K., L.K. Povlich, and J. Kim, *Recent advances in fluorescent and colorimetric conjugated polymer-based biosensors.* Analyst, 2010. **135**(9): p. 2179-2189.

110. Tuncel, D. and H.V. Demir, *Conjugated polymer nanoparticles.* Nanoscale, 2010. **2**(4): p. 484-494.

111. Ho, H.A., A. Najari, and M. Leclerc, *Optical detection of DNA and proteins with cationic polythiophenes.* Acc Chem Res, 2008. **41**(2): p. 168-78.

112. Jiang, H., et al., *Conjugated polyelectrolytes: synthesis, photophysics, and applications.* Angew Chem Int Ed Engl, 2009. **48**(24): p. 4300-16.

113. Lee, K., L.K. Povlich, and J. Kim, *Recent advances in fluorescent and colorimetric conjugated polymer-based biosensors.* Analyst, 2010. **135**(9): p. 2179-89.

114. Ho, H.A., et al., *Colorimetric and fluorometric detection of nucleic acids using cationic polythiophene derivatives.* Angewandte Chemie, 2002. **114**(9): p. 1618-1621.

115. Tang, Y., et al., *Direct visualization of enzymatic cleavage and oxidative damage by hydroxyl radicals of single-stranded DNA with a cationic polythiophene derivative.* Journal of the American Chemical Society, 2006. **128**(46): p. 14972-14976.

116. Ho, H.-A. and M. Leclerc, *Optical sensors based on hybrid aptamer/conjugated polymer complexes.* Journal of the American Chemical Society, 2004. **126**(5): p. 1384-1387.

117. Cheng, D., et al., *Fluorescence and colorimetric detection of ATP based on a strategy of self-promoting aggregation of a water-soluble polythiophene derivative.* Chemical Communications, 2015. **51**(40): p. 8544-8546.

118. Plante, M.-P., et al., *Polythiophene biosensor for rapid detection of microbial particles in water.* ACS applied materials & interfaces, 2013. **5**(11): p. 4544-4548.
119. Béra Abérem, M., et al., *Protein Detecting Arrays Based on Cationic Polythiophene–DNA-Aptamer Complexes.* Advanced materials, 2006. **18**(20): p. 2703-2707.
120. Yildiz, U.H., P. Alagappan, and B. Liedberg, *Naked eye detection of lung cancer associated miRNA by paper based biosensing platform.* Analytical chemistry, 2012. **85**(2): p. 820-824.
121. Mascini, M., I. Palchetti, and S. Tombelli, *Nucleic acid and peptide aptamers: fundamentals and bioanalytical aspects.* Angewandte Chemie International Edition, 2012. **51**(6): p. 1316-1332.
122. Ni, X., et al., *Nucleic acid aptamers: clinical applications and promising new horizons.* Current medicinal chemistry, 2011. **18**(27): p. 4206-4214.
123. Ku, T.-H., et al., *Nucleic acid aptamers: an emerging tool for biotechnology and biomedical sensing.* Sensors, 2015. **15**(7): p. 16281-16313.
124. Hidding, J., *A therapeutic battle: Antibodies vs. Aptamers.*
125. Radom, F., et al., *Aptamers: molecules of great potential.* Biotechnology advances, 2013. **31**(8): p. 1260-1274.
126. Jayasena, S.D., *Aptamers: an emerging class of molecules that rival antibodies in diagnostics.* Clinical chemistry, 1999. **45**(9): p. 1628-1650.
127. Ha, N.-R., et al., *Paper chip-based colorimetric sensing assay for ultra-sensitive detection of residual kanamycin.* Process Biochemistry, 2017. **62**: p. 161-168.
128. Schüling, T., et al., *Aptamer-based lateral flow assays.* AIMS BIOENGINEERING, 2018. **5**(2): p. 78-102.
129. Wang, L., et al., *An aptamer-based chromatographic strip assay for sensitive toxin semi-quantitative detection.* Biosensors and Bioelectronics, 2011. **26**(6): p. 3059-3062.
130. Liu, J., D. Mazumdar, and Y. Lu, *A simple and sensitive "dipstick" test in serum based on lateral flow separation of aptamer-linked nanostructures.* Angewandte Chemie, 2006. **118**(47): p. 8123-8127.
131. Raston, N.H.A., V.-T. Nguyen, and M.B. Gu, *A new lateral flow strip assay (LFSA) using a pair of aptamers for the detection of Vaspin.* Biosensors and Bioelectronics, 2017. **93**: p. 21-25.

132. Zhou, W., et al., *An aptamer based lateral flow strip for on-site rapid detection of ochratoxin A in Astragalus membranaceus.* Journal of Chromatography B, 2016. **1022**: p. 102-108.

133. Wu, W., et al., *A sensitive lateral flow biosensor for Escherichia coli O157: H7 detection based on aptamer mediated strand displacement amplification.* Analytica chimica acta, 2015. **861**: p. 62-68.

134. Qin, C., et al., *Visual detection of thrombin using a strip biosensor through aptamer-cleavage reaction with enzyme catalytic amplification.* Analyst, 2015. **140**(22): p. 7710-7717.

135. Wang, C., L. Zhang, and X. Shen, *Development of a nucleic acid lateral flow strip for detection of hepatitis C virus (HCV) core antigen.* Nucleosides, Nucleotides and Nucleic Acids, 2013. **32**(2): p. 59-68.

136. Jauset-Rubio, M., et al., *Aptamer lateral flow assays for ultrasensitive detection of β-conglutin combining recombinase polymerase amplification and tailed primers.* Analytical chemistry, 2016. **88**(21): p. 10701-10709.

137. Zhu, C., et al., *Dual-competitive lateral flow aptasensor for detection of aflatoxin B1 in food and feedstuffs.* Journal of hazardous materials, 2018. **344**: p. 249-257.

138. Zhang, G., et al., *A lateral flow strip based aptasensor for detection of Ochratoxin a in corn samples.* Molecules, 2018. **23**(2): p. 291.

139. Woo, M.-A., et al., *Based Colorimetric Sensor Utilizing Peroxidase-Mimicking Magnetic Nanoparticles Conjugated with Aptamers.* World Academy of Science, Engineering and Technology, International Journal of Chemical, Molecular, Nuclear, Materials and Metallurgical Engineering, 2016. **10**(10): p. 1340-1344.

140. Liang, L., et al., *Aptamer-based fluorescent and visual biosensor for multiplexed monitoring of cancer cells in microfluidic paper-based analytical devices.* Sensors and Actuators B: Chemical, 2016. **229**: p. 347-354.

141. Zhang, Y., et al., *Naked-eye quantitative aptamer-based assay on paper device.* Biosensors and Bioelectronics, 2016. **78**: p. 538-546.

142. Wei, X., et al., *Target-responsive DNA hydrogel mediated "stop-flow" microfluidic paper-based analytic device for rapid, portable and visual detection of multiple targets.* Analytical chemistry, 2015. **87**(8): p. 4275-4282.

143. Ahmed, N., et al., *Assay of advanced glycation endproducts (AGEs): surveying AGEs by chromatographic assay with derivatization by 6-aminoquinolyl-N-hydroxysuccinimidyl-carbamate and application to Nε-carboxymethyl-lysine-and Nε-(1-carboxyethyl) lysine-modified albumin.* Biochemical Journal, 2002. **364**(1): p. 1-14.

144. Ashraf, J.M., et al., *Recent advances in detection of AGEs: Immunochemical, bioanalytical and biochemical approaches.* IUBMB life, 2015. **67**(12): p. 897-913.

145. Nagai, R., et al., *Glycolaldehyde, a reactive intermediate for advanced glycation end products, plays an important role in the generation of an active ligand for the macrophage scavenger receptor*, Diabetes, vol. 49, 2000. P. 1714-1723.

146. Deng, R., et al., *Glucose-derived AGEs promote migration and invasion of colorectal cancer by up-regulating Sp1 expression*. Elsevir, 2017.

147. Ahmed, N., et al., *Methylglyoxal-derived hydroimidazolone advanced glycation end-products of human lens proteins*, Investigative ophthalmology and visual science, 2003. P. 5287.

148. Reddy, S., et al., *N-(Carboxymethyl) lysine is a dominant advanced glycation end product (AGE) antigen in tissue proteins*, Department of Chemistry and Biochemistry and School of Medicine, University of South Carolina, Columbia, South Carolina, 1995.

149. Matsui, T., et al., *Glyceraldehyde-derived pyridinium (GLAP) evokes oxidative stress and inflammatory and thrombogenic reactions in endothelial cells via the interaction with RAGE.* Cardiovascular diabetology, 2015. **14**(1): p. 1.

150. Higashimoto, Y., et al., *In vitro selection of DNA aptamers that block toxic effects of AGE on cultured retinal pericytes.* Microvascular research, 2007. **74**(1): p. 65-69.

151. Li, E., et al., *Synthesis of a new cationic polythiophene derivative and its application for colorimetric and fluorometric detection of iodide ion and anionic surfactants in water.* Macromolecular Chemistry and Physics, 2012. **213**(9): p. 887-892.

152. Tu, M.-C., et al., *Vapor phase solvatochromic responses of polydiacetylene embedded matrix polymers.* Journal of Materials Chemistry C, 2017. **5**(7): p. 1803-1809.

153. Levine, M. and T.M. Swager, *Conjugated Polymer Sensors: Design, Principles, and Biological Applications.* Functional Supramolecular Architectures, 2011: p. 79-134.

154. Persaud, K.C., *Polymers for chemical sensing.* Materials Today, 2005. **8**(4): p. 38-44.
155. Tu, M.-C., et al., *Tuning pendant groups of polythiophene on carbon nanotubes for vapour classification.* Sensors and Actuators B: Chemical, 2017. **247**: p. 916-922.
156. Gonçalves, V., et al., *Detection of volatile organic compounds using a polythiophene derivative.* physica status solidi (a), 2010. **207**(7): p. 1756-1759.
157. Gonçalves, V. and D.T. Balogh, *Optical chemical sensors using polythiophene derivatives as active layer for detection of volatile organic compounds.* Sensors and Actuators B: Chemical, 2012. **162**(1): p. 307-312.
158. Chayer, M., K. Faid, and M. Leclerc, *Highly conducting water-soluble polythiophene derivatives.* Chemistry of Materials, 1997. **9**(12): p. 2902-2905.
159. Ho, H.A. and M. Leclerc, *New colorimetric and fluorometric chemosensor based on a cationic polythiophene derivative for iodide-specific detection.* Journal of the American Chemical Society, 2003. **125**(15): p. 4412-4413.
160. Fichou, D., *Handbook of oligo-and polythiophenes*. 2008: John Wiley & Sons.
161. Hill, B., T. Roger, and F.W. Vorhagen, *Comparative analysis of the quantization of color spaces on the basis of the CIELAB color-difference formula.* ACM Transactions on Graphics (TOG), 1997. **16**(2): p. 109-154.
162. *ColorMine*. [cited 2018; Available from: http://colormine.org/delta-e-calculator.
163. Byun, K., et al., *Advanced glycation end-products produced systemically and by macrophages: A common contributor to inflammation and degenerative diseases.* Pharmacology & therapeutics, 2017. **177**: p. 44-55.
164. Singh, V.P., et al., *Advanced glycation end products and diabetic complications.* The Korean Journal of Physiology & Pharmacology, 2014. **18**(1): p. 1-14.
165. Baker, R.W. and U.b. Staff, *Membrane technology*. Kirk-Othmer Encyclopedia of Chemical Technology, 2000.
166. Li, H., et al., *Flow reproducibility of whole blood and other bodily fluids in simplified no reaction lateral flow assay devices.* Biomicrofluidics, 2017. **11**(2): p. 024116.
167. Liu, F., et al., *Progress in the production and modification of PVDF membranes.* Journal of membrane science, 2011. **375**(1-2): p. 1-27.
168. Behnke, U., *TD Brock: Membrane Filtration. A User's Guide and Reference Manual. 381 Seiten, 115 Abb., 27 Tab. Springer-Verlag, Berlin, Heidelberg, New York, Tokyo 1983, Preis: 87, -DM.* Food/Nahrung, 1983. **27**(10): p. 1025-1025.

169. Stitt, A.W., et al., *Advanced glycation end products (AGEs) co-localize with AGE receptors in the retinal vasculature of diabetic and of AGE-infused rats.* The American journal of pathology, 1997. **150**(2): p. 523.

170. Ansari, N.A., et al., *Immuno-chemistry of hydroxyl radical modified GAD-65: A possible role in experimental and human diabetes mellitus.* IUBMB life, 2015. **67**(10): p. 746-756.

171. Uribarri, J., et al., *Dietary glycotoxins correlate with circulating advanced glycation end product levels in renal failure patients.* American journal of kidney diseases, 2003. **42**(3): p. 532-538.

172. Ansari, N.A., K. Alam, and A. Ali, *Preferential recognition of Amadori-rich lysine residues by serum antibodies in diabetes mellitus: role of protein glycation in the disease process.* Human immunology, 2009. **70**(6): p. 417-424.

173. Méndez, J.D., et al., *Trends in advanced glycation end products research in diabetes mellitus and its complications.* Molecular and cellular biochemistry, 2010. **341**(1-2): p. 33-41.

174. Rufian-Henares, J.A., Pastoriza, S., *Maillard Reaction*, Encyclopedia of Food and Health, 2016. **593**

ACKNOWLEDGEMENTS

Having come to the end of this course of study, I would like to thank my Professor at Politecnico di Milano, Guglielmo Lanzani, for giving me the opportunity to do the experience in Singapore, and Bo Liedberg, professor at the Nanyang Technological University of Singapore who has allowed me to expand my knowledge of biosensors. I would like to thank the whole CBSS group, where I felt in a multicultural family: they welcomed me into their laboratory with affection and sympathy. In particular, thanks to Gopal who followed me with infinite patience and professionalism from the first to the last day. Thanks to his contribution in the development and implementation of this project. Thanks also to all the people in the laboratory, who have always been kind and helpful to me: Garima, Sushanth, James, Alps, Gaurav, Antareep, Nevena, Iuna, Neha, Eve and Aarti. A special thought goes to Komal: I found a sincere friend in her. Thanks to all the professors who contributed to my training both in Chemical Engineering and in Materials Engineering and Nanotechnology and more generally thanks to my University, Politecnico di Milano, where I spent the best and worse years. Thanks to everyone and to the events that made this path overwhelming because they spurred me to do better and better and to reach important goals. Thanks to all the people who were next to me, followed and cheered me even during the worst exams: Stefano, Laura, Federica, Francesco and Nicholas. Thanks also to my lifelong friends, Maria Luisa, Carolina, Rossana, Daniela and all the high school friends: without them I wouldn't be who I am today. A special thought goes to Delinda and Stefania, my closest friends and sincere sisters. Thanks to my sister Marta, my life partner and to our special brothers, Camillo and Nino. Thanks especially to Grandma who gave me the right energy to deal with everything and who understood things that I didn't even know how to explain. Thanks to Ludovico, who fills a special place in my heart: these years have been a professional path for us but also the first of a long life together. Finally, my most important thanks go to my parents Rossana and Giuseppe, who have not only made all this and millions of other opportunities possible, but have accompanied me on every adventure and misadventure, always encouraging me to give my best with the firmness and rigor that distinguishes them but also with infinite sweetness, love and esteem. I want to thank them especially for the person I am today and who I will become. I would like to dedicate a thank you to myself, because I never gave up, even when the challenges were bigger than me, even when I doubted my abilities, even when I was deeply disappointed. Without even one of these factors I wouldn't be here, thanks because I made it thanks to you.

RINGRAZIAMENTI

Giunta al termine di questo percorso di studi vorrei ringraziare il mio Relatore al Politecnico di Milano, Prof. Guglielmo Lanzani, per avermi dato la possibilità di fare l'esperienza a Singapore, e Bo Liedberg, Professore alla Nanyang Technological University di Singapore che ha permesso di ampliare le mie conoscenze nell'ambito dei biosensori. Ringrazio tutto il gruppo CBSS, in cui mi sono sentita in una famiglia multiculturale: mi hanno accolto nel loro laboratorio con affetto e simpatia. In particolare, ringrazio Gopal che mi ha seguito con infinita pazienza e professionalità dal primo all'ultimo giorno. Grazie al suo contributo nello sviluppo e nella realizzazione di questo progetto. Grazie anche alle persone che in laboratorio si sono sempre mostrate gentili e disponibili nei miei confronti: Garima, Sushanth, James, Alps, Gaurav, Antareep, Nevena, Iuna, Neha, Eve e Aarti. Un pensiero speciale va a Komal: in lei ho trovato un'amica sincera. Grazie a tutti i professori che hanno contribuito alla mia formazione sia in Ingegneria Chimica che in Ingegneria dei Materiali e Nanotecnologie e più in generale alla mia Università, il Politecnico di Milano, in cui ho trascorso gli anni più belli e più brutti. Grazie a tutti coloro e agli eventi che hanno reso davvero difficile questo percorso perché mi hanno spronato a fare sempre meglio e a raggiungere traguardi importanti. Grazie a tutte le persone che mi hanno accompagnato, seguito e rallegrato anche gli esami più pesanti: Stefano, Laura, Federica, Francesco e Nicholas. Grazie anche alle amiche di una vita, Maria Luisa, Carolina, Rossana, Daniela e tutti gli amici del liceo: senza di loro non sarei quella che sono oggi. Un pensiero speciale va a Delinda e Stefania, due amiche del cuore e due sorelle. Grazie a mia sorella Marta, da sempre mia compagna di vita e ai nostri fratelli a quattro zampe, Camillo e Nino. Grazie specialmente alla Nonna che mi ha dato l'energia giusta per affrontare tutto e che ha capito cose che nemmeno sapevo spiegare. Grazie a Ludovico, che occupa un posto speciale nel mio cuore: questi anni sono stati per noi un percorso professionale ma anche i primi di una lunga vita insieme. Infine, il mio ringraziamento più importante va ai miei genitori, Rossana e Giuseppe, che non solo hanno reso tutto questo e milioni di altre opportunità possibili, ma mi hanno accompagnato in ogni avventura e disavventura, incoraggiandomi sempre a dare il meglio di me con la fermezza e il rigore che li contraddistingue ma anche con infinita dolcezza, amore e stima. Li voglio ringraziare soprattutto per la persona che sono oggi e che diventerò, sperando di seguire il loro esempio di responsabilità e determinazione. Un grazie lo vorrei dedicare a me stessa, perché non ho mai mollato, neanche quando le sfide erano più grandi di me, o quando ho dubitato delle mie capacità, neanche quando ero profondamente delusa. Senza anche solo uno di questi fattori non sarei qui, grazie perché ce l'ho fatta anche grazie al vostro sostegno.